Development of Novel Energy Systems for LNG Locomotives

By

Mohammed Al Ali

A Thesis Submitted in Partial Fulfillment

of the Requirements for the Degree of

Master of Applied Science

in

Mechanical Engineering

Faculty of Engineering and Applied Science

University of Ontario Institute of Technology

Oshawa, Ontario, Canada

Abstract

The use of diesel in the railway sector brings challenges to the engineers to meet the current emissions standards set by governments. This thesis addresses potential solutions to overcome the emissions problems in the current diesel fueled locomotives with economic benefits using liquefied natural gas (LNG) locomotives. Six novel energy systems for LNG locomotives are developed with different prime movers and fuel combinations. The systems are analyzed energetically and exergetically, and their performances are compared for evaluation purposes. The environmental impact and the fuel cost for each system are considered in the comparison. The current study investigates the use of the fuel combinations including LNG-ULSD, LNG-LPG, LNG-H_2 and LNG only to run the locomotive using different prime movers like internal combustion engines, solid oxide fuel cell (SOFC) and gas turbine.

System 1 is the baseline system, which uses ULSD only as fuel in a compression ignition engine. System 2 uses LNG-ULSD with the compression ignition engine in addition to small spark ignition engine that uses the boil-off gas from the LNG tank, this system can run on ULSD only. System 3 runs with LNG-ULSD and is similar to system 2, but with an additional high pressure direct injection pump for the natural gas and exhaust gas recirculation, this system cannot run with ULSD only. The fourth system uses spark ignition engine as prime mover to operate with LNG-LPG fuels, the system can run on propane only mode. System 5 uses LNG with compressed hydrogen in spark ignition engine. System 6 uses LNG only as fuel and SOFC with internal reforming as prime mover with a gas turbine to run the locomotive auxiliaries. System 7 uses LNG only as fuel and gas turbine as prime mover with organic Rankine cycle for heat recovery.

System 6, which uses the SOFC system, has the highest energy and exergy efficiencies with 48.2% and 45.2% with significant savings in the fuel cost. All proposed systems have environmental benefit of GHG reduction where System 5 has the lowest CO_2 emissions, because it uses compressed hydrogen as fuel with LNG. The systems exhibit a considerable reduction in the NOx, HC, CO, and PM emissions depending on the fuel combinations, where some of the systems meet the emissions standards. The systems were compared with the baseline system ,which uses diesel only, in terms of the freight duty cycle to show the reduction in emissions and fuel cost savings.

Acknowledgment

I would like to acknowledge my supervisor Professor Dr. Ibrahim Dincer for his support, guidance and patience to help me overcome the challenges that I came across during my thesis study.

In addition, I would like to acknowledge the help of various colleagues at UOIT, namely, Dr. Calin Zamfirescu for his useful comments and feedbacks, Miss Janette Hogerwaard for her great help in providing useful sources and explanations. Finally, I appreciate the help and support from my colleagues in ACE 3030B, especially Monu Malik and Vishvadeep Singh.

Furthermore, I would like to express my gratitude to my parents for their unlimited support and inspiration through my life. My loving wife's help, support and motivation are highly appreciated. This thesis is then dedicated to my parents and my wife.

Last but not least, the scholarships and support from the Ministry of Higher Education in the Kingdom of Saudi Arabia through the Saudi Culture Bureau in Canada are greatly acknowledged.

Table of Contents

List of Figures

List of Tables

Nomenclature

A_{ac} Active area (m^2)

AF Mass based air-fuel ratio

b Cylinder bore (m)

$B1$ Resistivity constant 1 (S/m)

$B2$ Resistivity constant 2 (K)

$BMEP$ Break mean effective pressure (kPa)

Cf Cost of fuel ($)

c_p Specific heat at constant pressure (kJ/kg K)

c_v Specific heat at constant volume (kJ/kg K)

D   Gaseous diffusivity (m^2/s)

E Cell voltage (V)

Em Emissions in one duty cycl

ex Specific exergy (kJ/kg)

$\dot{E}x$ Exergy rate (kW)

F Faraday constant (C/mol)

FE Fuel ratio

g Gravitational acceleration (m/s^2)

h Specific enthalpy (kJ/kg)

HHV   Higher heating value (kJ/kg)

I   Electrical current (A)

j Current density (A/m^2)

j_{Oa} Exchange current density of the anode (A/m^2)

j_{Oc} Exchange current density of the cathode (A/m^2)

k Heat transfer coefficient (W/m^{2}K)

L Thickness (m)

LHV   Lower heating value (kJ/kg)

M	Molar mass (kg/kmol)
$\dot{m}$	Mass flow rate (kg/s)
N	Engine speed (rpm)
$\dot{n}$	Molal flow rate (mol/s)
N_c	Number of cylinders in the engine
P	Pressure (kPa)
$\dot{Q}$	Heat rate (kW)
r	Compression ratio
R	Gas constant (kJ/kg K)
s	Specific entropy (kJ/kg K)
$\dot{S}$	Entropy rate (kW/K)
SFC	Specific fuel consumption (kg/kWh)
T	Temperature (°C or K)
v	Velocity (m/s)
V	Volume (m^3 or L)
$\dot{V}$	Volume flow rate (m^3/s)
$\dot{W}$	Power (kW)
w	Weighting factor
X_1	Number of moles of air
X_2	Number of moles of carbon dioxide
X_3	Number of moles of water vapour
X_4	Number of moles of nitrogen
y	Molar fraction

Greek Letters

α	Number of atoms of carbon
β	Number of atoms of hydrogen
γ	Fuel cell losses, (V)

δ   electrical resistivity (Ω)

Δ Difference

η Energy efficiency

ρ Density (kg/m^3)

Σ Sum

ψ Exergy efficiency

Subscripts

$1,2,\ldots i$ state points

a Anode

act Activation polarization

$AdFT$ Adiabatic flame temperature

Aux   Auxiliary

c Cathode

$chem$ Chemical

CI Compression ignition engine

$comb$ Combustion

$conc$ Concentration polarization

d Displacement

$Dest$ Destruction

Duty   One duty cycle

e Exit

el Electrolyte

eq Equivalent

f Formation

FC Fuel cell

gen Generation

i Inlet

int	Inter connecter
k	Heat transfer location
m	Main
ohm	Ohm losses
p	Product
$phys$	Physical
u	Universal
r	Reactant
sys	System
rev	Reversible
SI	Spark ignition engine
TP	Traction power
v	Volumetric

Superscript

$chem$	Chemical
eff	Effective
$phys$	Physical

Acronyms

$ASTM$	American Society for Testing and Materials
$BNSF$	Burlington Northern Santa Fe Corporation
CC	Combustion chamber
CI	Compression ignition engine
CNG	Compressed natural gas
EGR	Exhaust gas recirculation
EMD	Electro-Motive Diesel
FC	Fuel cell

GE   General Electric

GHG   Greenhouse gas

GT   Gas turbine

HPDI High pressure direct injection

ICE   Internal combustion engine

LNG   Liquefied natural gas

LPG   Liquefied petroleum gas

MOU   Memorandum of understanding

ORC   Organic Rankine cycle

SOFC Solid oxide fuel cell

ULSD Ultra low sulfur diesel

Chapter 1 : Introduction

1.1 Energy and Fuel Aspects

World energy resources are under severe pressure due to exorbitant rise in energy consumptions. This energy consumption is attributed to high economic growth, change in lifestyle, an increase in the population etc., especially in the developing countries. Energy is a vital component of the growth of a country. Due to this exponential increase in demand and environmental implications, efforts have been put to shift this energy spectrum towards relatively clean and efficient options. The transportation sector has the highest stakes in fossil fuel based energy scenario; this sector is one of the largest contributors to GHG's and other environmental pollution. This enormous challenge presents a huge opportunity for substantial reduction in environmental impact by replacing conventional fuels with cleaner alternatives.

1.1.1 Railway Sector

The manufacturing of energy efficient, clean and economic engines has always been a challenge for researchers. Energy is one of the essential commodities for maintaining the standard of life. Therefore the energy resources, its supply chain and usage have both political and economic implications. Policy makers draw different policies to push for cleaner, more efficient and cost effective products and processes. The rail sector is a recognizable contributor to this challenge due to the nature and size of its energy systems. Even today railways use a vast number of diesel based locomotives. As diesel has a considerable amount of emissions to the environment, governments set regulations and standards to limit the emissions from locomotives.

The Canadian rail network is one of the largest rail networks in the world with 48,000 kilometers in track. By operating 3043 locomotives and 59,395 freight cars, the rail freight services are the major part of the rail transportation sector which account for 90% of the total operating revenues. However the passenger account for only 5% of the revenue and the remaining of the revenues come from the services provided for passengers, commuter companies, switching, demurrage, and miscellaneous rentals [1]. In the rail sector, roughly there are eleven commodity groups that contribute to carloads as shown in Figure 1.1, where the average number of cars per freight train

is 99. However, there are only 552 passenger cars in service with total passenger trains of 226 [1].
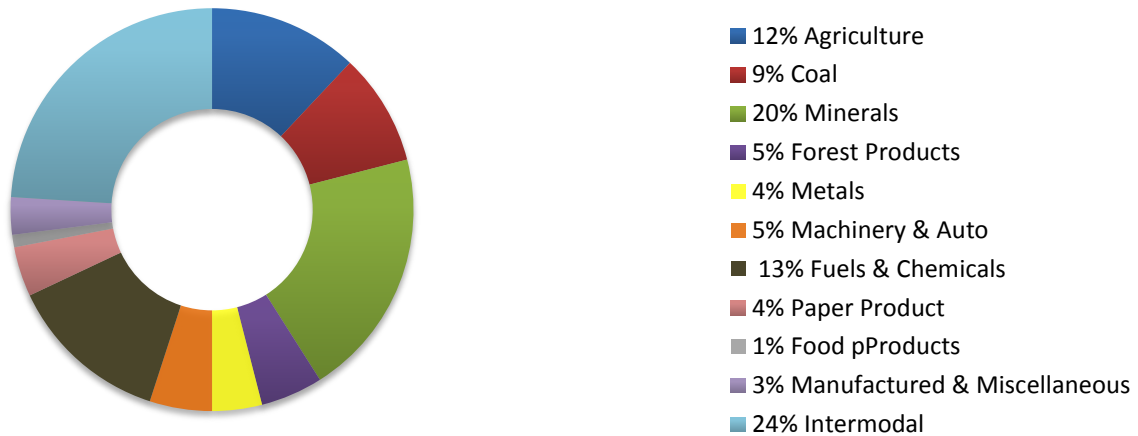
Figure 1.1: Carload originated by commodity grouping (adapted from [1]).

Most of the locomotives are fueled with diesel, where a significant increase in the fuel consumption is noticed between 2011 and 2013. In 2011, 1.98 billion liters of fuel were consumed for freight rail operation, while in 2013, 2.11 billion liters were consumed which show an increase of 6.6%. The greenhouse gas (GHG) emissions from the rail sector are expressed as $CO_{2,eq}$, and in 2012 it was 6,441.98 kt. Due to the environmental effects and considerations, the 2011-2015 Memorandum of Understanding (MOU) has set the targeted amounts and reductions of GHG emissions for 2015 as showed in Table 1.1.

Table 1.1: MOU targeted GHG emissions for 2015.

Railway operation	% Reduction[a]	2010	2011	2012	2015 target	Unit[b]
Class 1 Freight	6%	16.43	16.17	15.8	15.45	kg /1,000 RTK
Intercity Passenger	6%	0.12	0.12	0.11	0.11	kg /PK
Regional & Short lines	3%	15.21	14.88	13.44	14.75	kg /1,000 RTK

a: The reduction from 2010.
b: The units are in kg $CO_{2,eq}$; RTK: revenue tonne kilometer , PK: passenger kilometer.
Source: [2]

There are several alternatives to reduce the emissions varying from making better engine designs to smart energy systems and fuel selection. Alternative fuels can reduce the environmental

impact significantly. One solution to solve this problem is to use cleaner fuel like natural gas. Natural gas is the cleanest fossil fuel with least greenhouse gas (GHG) and other emissions. Additionally, natural gas has an economic advantage over diesel. In transportation, natural gas is used in two forms, either compressed natural gas or liquefied natural gas. The compressed natural gas is not practical for locomotive use due to the high volume needed to carry the natural gas on board, and the gas is compressed all the time. On the other hand, liquefied natural gas (LNG) does not have the volume problem, it also carries more natural gas content that allow for more driving range.

However, there are several challenges that limit the use of natural gas as locomotive fuel. The unitary infrastructure in North America railroad is designed for diesel locomotive where any new alternative fuel should considered the operation with the current infrastructure or with reasonable changes. Another challenge is the need for a technical way to manage the boil-off gas from the cryogenic tank especially in large volume quantity.

1.2 Motivation and Objectives

The increase in the environmental degradation from conventional fueling systems and the improvement of the technologies which allow for cleaner fuels to replace the old fuels drive me to find solutions to this problem in more environmental and economic way. Natural gas is a potential solution to this problem, but several challenges need to be addressed and solved when this solution is applied to locomotives. In the literature, there is a lack of the energy systems that use LNG considering its applications in locomotives. Thus, this research investigates the feasibility of using liquefied natural gas as potential fuel alternative for locomotives.

The specific objectives of this thesis are listed as follow:

- To develop conceptual LNG energy systems for locomotive applications.
- To perform energy and exergy analyses for the proposed systems.
- To determine the exergy destruction locations for the developed systems.
- To conduct parametric study for the proposed systems by varying the important parameters in the systems.
- To study the environmental impact of the newly developed systems.

- To perform a comparative assessment of the proposed systems in terms of their emissions, fuel cost and performance.
- To investigate and compare the proposed systems with the baseline system in one duty cycle.
- To perform a comparison of the NOx, CO, HC and PM emissions of the newly developed systems with the emissions standards.

Chapter 2 : Background

2.1 LNG as Transportation Fuel

Natural gas is used as transportation fuel in the form of compressed natural gas in several countries. A better way of using the natural gas for heavy duty applications is by liquefies it to reduce its volume 600 times to be able to carry more energy content onboard to accomplish more traveling distance. LNG is a cryogenic fuel that needs specific requirements to be used as fuel, such as cryogenic fueling system and tank. There are several ways to use LNG as fuel in transportation depending on the load, prime mover and other requirements. In the current study, LNG is used in internal combustion engines, fuel cells and gas turbine to run the locomotive. Liquefied natural gas has several environmental and economic advantages compared to diesel, which is the primary fuel used for locomotives [3]. These make LNG a potential fuel for locomotives to meet the future emissions requirements with lower cost.

2.1.1 LNG Properties

The natural gas reservoir and its processing play a critical role to shape the composition of the LNG, which specifies its properties. The methane percentage in LNG can vary between 84% to 99% and the other compositions change based on the reservoir and plant as shown in Table 2.1. LNG is a cryogenic fluid that is nontoxic and noncorrosive substance. The boiling point of LNG is -160 ℃ and can be stored at atmospheric pressure; also the density ranges from 430 to 470 kg/m^3 depends on the composition [4]. In their work, the natural gas is assumed to be methane where some of the thermophysical properties of methane are listed in Table 2.2.

Table 2.1: LNG composition from various plants in different countries.

Plant name	Location	Methane[a]	Ethane[a]	Propane[a]	Butane[a]	Nitrogen[a]
Marsa El Braga	Libya	83.68	11.73	3.51	0.28	0.8
GL4Z	Algeria	87.16	8.78	2.1	0.7	1.26
NW Shelf	Australia	89	7.3	2.5	1	0.2
MLNG	Malaysia	91.35	4.3	2.95	1.4	0
Atlantic LNG	Trinidad	95	4.6	0.38	0	0.02
Kenai LNG	Alaska	99.8	0.1	0	0	0.1

a: units are in mole %.
Source: [5]

Table 2.2: Thermophysical properties of methane.

Property	Methane
Chemical formula	CH4
Molar mass (kg/kmol)	16.043
Critical temperature (K)	191.1
Critical pressure (kPa)	4.64
Density (kg/m^3)	432
Latent heat of vaporization (kJ/kg)	510.4
Latent heat of fusion (kJ/kg)	58.4
Enthalpy of formation (kJ/kmol) at (T=25℃ and P=101.3 kPa)	-74,850
Absolute entropy (kJ/kmol ·K) at (T=25℃ and P=101.3 kPa)	186.16

Source: [6]

2.1.2 LNG Safety

LNG is like any other fuel that contains energy and needs special care for safe operation. By knowing the properties of the LNG, the safety regulations and designs can be applied. During the last 40 years, LNG industry had achieved excellent safety record. However, there are several hazards associated with the liquefied natural gas. Most of the literature studies the safety of using LNG in the ships for transporting the LNG and in the terminal plants, although the conditions in the locomotive are different, but there are some similarities to some extent. The main hazards that need to be handled are the vapor cloud, cryogenic effects, fire, explosion, and rollover [7].

When the LNG spills and leaves the cryogenic tank, it gains heat from the surrounding air and converts into gas. Due to the exchange of heat between the natural gas and the air, the water content of the air starts to freeze and the mixture of the natural gas and air creates a vapor cloud. Cryogenic effects are another serious problem that occurs from direct contact between the LNG and the human body that cause a severe damage to the skin or eyes. Also, the cryogenic fluid contact with some of the metals, plastic or rubber causes an embrittlement and fracture. For that reason, the cryogenic tanks are designed to avoid direct contact between human body and other equipment with the LNG. In addition, a special care is needed at the venting valve and relief valves because that is a possible way for the exposure [8].

The fire problem is considered with the vapor cloud because the natural gas in its liquid form cannot burn. For the fire to start, the flammability range of the natural gas and the amount of air

required should be met in addition to an ignition source. The fire occurs in the gas mixer and depends on its local to that mixer, but if the burning rate is higher than the spill rate from the tank then the fire will spread to the source of the natural gas which is the tank. In the tank, fire will evaporate more natural gas to be burned, and generate pressure in the tank that might damage it or make an explosion [9]. However, the LNG is not an explosive substance, but the explosion may occur due to the vapor cloud ignition. Due to the change in the density in the cryogenic tank between the lower layer of the LNG and the upper layer, which can be caused by some heat transfer or leakage in the lower layer, a rollover phenomenon occurs. The stratified layer within the LNG breaks down to allow the hot gas at the lower layer to move up, which is referred to as rollover. The primary consideration in the case of rollover is when there is a large amount of gas that moves from the lower layer to the upper layer that causes a significant pressure increase in the tank. If the venting system is not designed for the rollover, then a possible crack or damage might be in the tank.

Several safety features and actions are practiced in the LNG industry to minimize the risk [4]. The formation of fire from the vapor cloud is not that simple due to the amount of condensate water in the gas-air mixer and high auto-ignition of the natural gas. For LNG fire, dry chemical powder is the only way to extinguish it, where water cannot stop the LNG fire but it can intensify the fire if it is used in the cryogenic tank that accelerates the boil-off gas rate. However extinguish the fire does not stop the boil-off gas and more fuel is combusted, for that reason it is safer to control the fire than extinguish it. To avoid the cryogenic effects, workers are advised to wear special insulated clothes and gloves before entering an expected exposed area. LNG tenders are designed to hold the cryogenic fluid without harming the environment around it. The rollover problem is not a significant issue in a well maintain locomotive due to the prevention procedure and the rollover protection system. The procedures are highlighted by [8] as follow: installing a monitoring system in the cryogenic tank along the liquid column for the pressure, density and temperature; sufficient mixing of the fuel; avoid the formation of the stratification by installing multiple loading points in the tank.

2.2 Cryogenic System

For cryogenic fuels, special equipment are needed to run the cryogenic system. The primary consideration in the cryogenics is the heat transferred to it. Also, the material of these equipment's is carefully selected and designed since these materials can contract due to the low temperature that may cause stress in that equipment. For the locomotives, the cryogenic system consists mainly of the cryogenic tank, cryogenic pump and low-temperature heat exchanger or vaporizer.

2.2.1 Cryogenic Storage Tank

The main purpose of the cryogenic tank, known as Dewar, is to store the fuel and work as an insulator to control the rate of evaporation of the fuel. Venting connections are integrated with the tank to overcome the boil-off gas problems in addition to the fill connections. A pressure management system is included to maintain the required pressure in the tank because some of the fueling systems depend on the tank pressure to deliver the fuel to the engine instead of using cryogenic pump. Some systems provide a heater to heat the cryogenic fuel in case there is no enough pressure in the tank to run the fuel to the engine. The cryogenic tank, venting and filling connections and the pressure management systems are provided by most of the LNG system suppliers [10]. The Westport is an example of one of these suppliers where it produces cryogenic tenders for LNG locomotives. The size and shape of the tank significantly affect the rate of boil-off gas and pressure in the tank. The dewar consists of two layers or double walls where there is a vacuum in between. In some cases, the vacuum is filled with chemical powder to enhance the heat transfer rate [11]. The most widely used material for the cryogenic tanks is the stainless steel, where in some cases the carbon steel is used for the outer wall [12].

2.2.2 Cryogenic Pump

Cryogenic pumps, known as cryopumps, are used to deliver the fuel from the tank to the engine. It is more convenient to include a pump in the fueling system to avoid the shortage of fuel that can affect the operation of the locomotive. The trouble in dealing with cryogenic fluid is that, while pumping when the pressure drops and the liquid is already at the boiling temperature, the liquid will start to evaporate. This vapor, which is 600 times the liquid volume, can be carried along with the liquid that can cause a cavitation problem. That is one reason to design a

particular kind of pump that can deliver the cryogenic fluid without any problem. The cryopumps are vacuum pumps, where they can deliver high pressure fluid to the engine [11]. The positive displacement pumps, for example, are used to deliver high pressure and low flow rate fluid. A pressure relief valve is integrated in the cryogenic pump to avoid a dangerous high-pressure increase due to heat transfer to the pump, for example, during the power failure [13].

Table 2.3: Materials for cryogenic applications.

Material	Specification[a]	Approximated lowest temperature (℃)
Low carbon steel	A 442, A 516	-46
	A 537	-59
Alloy steel	A517	-59
	A203, Gr. A and B, 2.25% Ni	-68
	A203, Gr. D, E, and F, 3.50% Ni	-101
	A553, Type II 8% Ni	-170
	A645, 5.0% Ni ; A353 ; A553, Type I 9% Ni ; A844 (9% Ni)	-195
Stainless steel	304, 304L, 316, 316L, 347	-269
Aluminum	1100, 2014 to 2024, 2219-T87, 3003, 5083-0, 5456, 6061-Tb, 7005	-269
Copper	C10200, C12200 (DHP), C17200, C22000,C26000,C51000,C70600, C71500	-198
Nickel	Monel-K, Hastelloy B, Hastelloy C, Inconel Alloy 600,706, Inconel Alloy 718, Invar-36, Inconel alloy X-700	-269
Titanium	Ti–5Al–2.5Sn, Ti–6Al–4V (ELI)	-196
	Ti–5Al–2.5Sn (ELI)	-253

a: Refer to ASTM standards.
Source: [15]

2.2.3 Low Temperature Heat Exchanger

Low temperature heat exchangers are used to handle the cryogenic fuel, where the effectiveness of the heat exchanger is one of the most important aspects in the cryogenics. The selection of the heat exchanger depends on the application. For small size applications, the concentric tube geometries, perforated plate heat exchanger and regenerators are preferred as the primary

options. However, the coil wound and plate fin geometries dominate the large size applications, since minimizing the cost is targeted. A review of the heat exchangers models for cryogenic use is covered by [14]. Since the selection of the material for the cryogenic system is needed, the suitable materials for cryogenic applications with their approximated lowest temperature are presented in Table 2.3.

2.3 ICE Fuel Injection

In the current investigation, the internal combustion engines are the prime movers for five systems. Depending on the fuels and system design, the injection method is chosen. In some systems, the fuel is mixed with air and then introduced into the intake manifold, where for other systems the fuel is injected into the cylinder directly. In case of a dual fueling system, the natural gas is used with diesel where the diesel is used as a pilot for the natural gas combustion because of the high auto ignition temperature of the natural gas. For up to 60% of the fuel can be replaced with natural gas to supply the locomotive needs and the remaining of the fuel is diesel, natural gas or CNG is premixed with the air before entering the cylinder [16]. When the piston is at the end of the compression stork, the diesel is injected directly to start the combustion, as there is no need for a spark plug, as showed in Figure 2.1. In this case, the engine is capable of operating in diesel mode since the engine is a modified diesel engine.
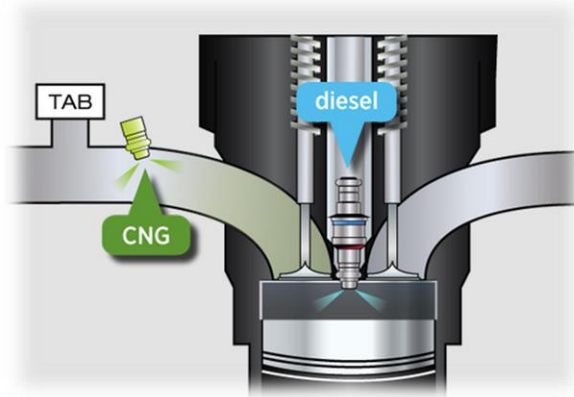
Figure 2.1: Duel fuel with natural gas early injection [16].

Another alternative injection system is the High Pressure Direct Injection (HPDI) which was invented by Westport Power Inc. The HPDI uses a dual concentric needle injector to inject the high pressure natural gas and diesel for piloted purpose only, which is shown in Figure 2.2. The

amount of the diesel used is small, and the natural gas pressure reaches 30MPa at which both fuels are introduced into the cylinder at the end of the compression stroke. This system allows approximately 92% of the fuel to be natural gas, and the remaining is diesel. The HPDI technology is capable of delivering equal horsepower, torque and efficiency characteristics of a diesel only engine [17]. In addition, direct injection system can be used in the spark ignition engines that use natural gas or a combination of gases fuel and spark plug for the combustion. The spark ignition engines are not as efficient as diesel engines, but by using natural gas only as fuel the engine emissions are lower than diesel only or dual fuel engine.
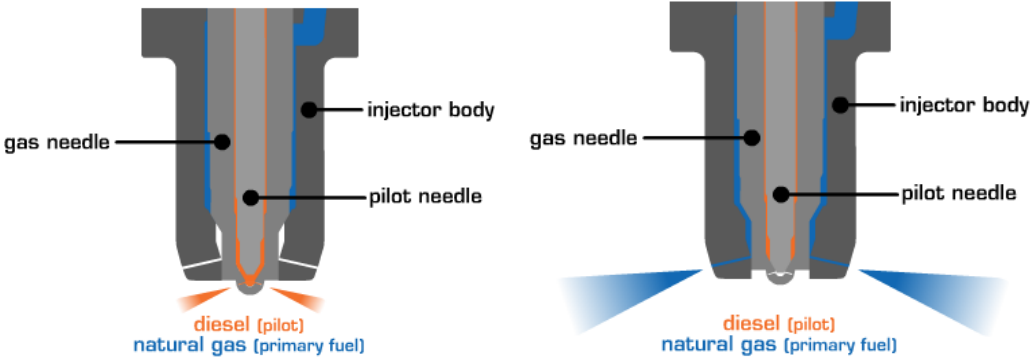
Figure 2.2: HPDI technology [17].

Chapter 3 : Literature Review

3.1 Natural Gas Locomotives (CNG and LNG)

3.1.1 Demonstration Projects

Canadian National Railway Company (CN) had successfully demonstrated the viability of LNG as a locomotive fuel. In 2012, CN tested two main line LNG locomotives that uses LNG tender between two locomotives. The test was for 480 km that used 90% LNG and 10% diesel [18]. Two sets of LNG fuelled locomotives were manufactured by GE and Electro-Motive Diesel (EMD) and tested by BNSF in 2013. Both sets used low pressure and the EMD locomotives employed 60%-40% and GE locomotives 80%-20% LNG-diesel mix for compression ignition. The intensive test had been completed in two months with testing equipment that simulates a train hauling 100 cars of coal on the Facility for Accelerated Service Testing [19, 20].

Three technologies for burning LNG in locomotive diesel engine had been developed by EMD and Caterpillar. These technologies are; Spark Ignited which uses 100% LNG , Dynamic Gas Blending for dual fuelling mode that uses up to 60% LNG, and High Pressure Direct Injection which uses up to 95% LNG[18,21]. CSX had an agreement with GE Transportation for the pilot-scale tests of LNG locomotives in 2014 [22]. In 2013, GE signed a deal with Gasfin for LNG truck fueling stations in Europe. Each of these stations is fully equipped with a high-speed reciprocating compressor, gas pre-treatment system, electric motor, cold box assembly and boil-off gas compressor as well as a GE's turboexpander compressor, driver and control system [23]. Westport Innovations has delivered the first four LNG tenders ordered by CN to EMD. These tenders can fuel either single or dual locomotives, in the EMD project the LNG will be used in a ratio of 60%-80% and have the capability to work with 100% diesel [24]. Indian Railway announced in 2014 about the planning to issue LNG tender for a test program that will be launched in 2016 [25, 26].

Russian oil and gas major Gazprom teamed with Russian Railways to test the conversion of diesel locomotives to natural gas turbine locomotives, in 2013 [27]. The first gas reciprocating locomotive, TEM19, was developed by Russian Institute of Research, Design and Technological

Studies (VNIKTI) and Transmashholding (TNH). This *Tem19 locomotive* has LNG capacity of 3900kg with a gas engine output of 880kW [28]. In mid-2013, Chicago Metropolitan Agency for Planning (CMAP) granted US$34.25 million for Indiana Harbor Belt Railroad to convert 31 locomotives to run on compressed natural gas instead of diesel [29, 30]. The Norfolk Southern Region is constructing CNG locomotives that use an engine running on natural gas only, where the dual mode is not possible [31]. In 2001, Napa Valley Railroad and the Napa Valley Wine Train converted one locomotive to CNG-powered locomotive using 60% natural gas and 40% diesel. By 2008, the conversion reached 100% CNG [32].

3.1.2 LNG Locomotive Patents

In the recent years, several patents related to LNG, cryonic and gases fuels for locomotives were filed. In patent [33], Westport Power Inc. fields their version of two engine system with a gaseous fuel stored in liquefied form on March 29, 2013. The patent integrated a fumigated internal combustion engine where the boil-off gas from the cryogenic tank is used in this engine. The fumigated engine used to run the power of the cryogenic pump or another fuel system. This cryogenic pump supplies the HPDI engine with the required fuel. The efficiency of the fumigated engine is lower than the main engine; because of that further system simplification can be achieved with little maintenance. 90% of the total power that is needed by the system is provided by the first engine that is the HPDI combustion engine. However, the second engine which the fumigated provides no more than 10% of the total power of the system. The patent is suitable for large vehicles applicable such as a locomotive, ship, or a large truck.

In patent [34], Electro-Motive Diesel Inc. filed their version of cryogenic pump system for converting the fuel in December 14, 2012. This patent is directly related to converting liquid fuel to gaseous fuel using cryogenic pump. The system consists of a compressor, combustor, turbine, pump, and heat exchanger. The method how the system work is explained as follow, the first amount of the liquid fuel is pumped to the combustor and mixed with air. Then, combustion takes place in the combustion chamber where the hot exhaust will flow to the turbine to generate work which part of is used to run the pumps and compressor. The exhaust gases are used to heat the second amount of the LNG, which is pumped by the cryogenic pump.

In patent [35], combined cycle powered railway locomotive was filed on August 15, 2012. The patent indicated the idea of using two different prime movers to supply the electricity required. The first prime mover uses the natural gas combustion turbine and the exhaust from that turbine used as the heat source by the second prime mover. The second prime mover considered to be steam turbine that is linked to with the gas turbine shaft to provide the required work for the load. The steam turbine system consist of a once-through steam generator, an air cooled condenser and boiler feed pump. The system made an improvement in the efficiency of the locomotive energy system. It also has lower emissions and fuel economy than the conventional one.

The problem of fuelling more than one locomotive using one tender had a solution that proposed by patent [36] which was filed on July 31, 2012. The patent solved this problem by claiming the new way to fuelling distribution system. The fuel distribution system may include a first locomotive, a second locomotive, and a tender car. At least one pump located onboard the tender car, and at least one fluid conduit attached to the at least one pump which may be configured to deliver gaseous fuel from the tender car to the first and second locomotives. This patent focused mainly on the liquefied gas fuels such as LNG.

Patent [37] related directly to LNG locomotive natural gas turbine. The patent shows significant fuel saving and reduction in the emissions and cost. The patent is about the arrangement of the gas turbine in the locomotive where three pressure shafts are turbine is used with compressors. The high pressure shaft is located above the low and medium pressure shafts and for each shaft there is a compressor that is associated with the pressure. A regenerative heat exchanger is arranged between the high pressure compressor and high pressure turbine that is used to heat the fuel.

Patent [38] proposed a method to convert the diesel engine into natural gas engine. The modifications take place in several parts like installing a throttle body on the diesel engine; inserting a spark plug into a diesel fuel injector opening in the cylinder head; installing a throttle body on the diesel engine; installing a throttle body adaptor between a throttle body and an intake manifold of said diesel engine; and modifying a piston. The compression ratio of the

engine is decreased during the engine operation. In addition, a waste gate and waste gate adaptor and timing mask are installed and included in the conversion method.

3.1.3 Research Work for LNG

Peredel'skii et al. [39] analysed the desirability of replacing petroleum-based vehicle fuel with liquefied natural gas. For the locomotives to move toward the dual operational mode, which uses natural gas- diesel, become possible and more reliable because the LNG solves the natural gas fuelling problem. The authors indicated that LNG is more economic and sustainable than CNG where the LNG can reduce the cost per kilometer 1.5 times and run 2-2.5 times compared with CNG. In addition, the cryogenic tank can carry two to three times more gas per unit volume as compared to CNG cylinders. For the vehicles that run on CNG, LNG provides a practical solution for the CNG filling stations. The study suggests the conversion of the current filling stations to combined filling stations that can supply LNG in addition to gasoline and diesel.

Arteconi et al. [40] carried comparative life cycle GHG emissions analysis for LNG and diesel as heavy vehicle fuels in Europe. In this study, two possibilities for the LNG were considered: purchasing the LNG from the regasification terminal (LNG-TER) or producing it at the service station with small-scale plants (LNG-SSL). The authors found that the GHG of the LNG-TER was 10% less than diesel, but LNG-SSL has almost the same GHG as the diesel. In all cases, the combustion stage was the highest and major GHG in the life cycle analysis. Kumar et al. [41] presented an overview of the LNG characteristics, its worldwide technologies, sources and use in transportation and production. The study compared the GHG of LNG, oil and coal using life cycle analysis.

Two novel LNG –base and gas turbine cogeneration systems were presented by Morosuk et al. [42]. In their study, an advance exergy analysis was applied to one of these systems. The systems studies considered the LNG regasification and generation of electricity as the main output of the system. The base case system consists of three subsystems; LNG sub-system, N_2 sub-system and open gas turbine subsystem. The overall system efficiency is found to be 52.6%, and the highest exergy destruction occurs in expander 2.

Arteconi et al. [43] analysed the potential of the LNG as a vehicle fuel in Italy. The study focuses mainly on the onsite liquefaction that required liquefaction efficiency of 70% and low natural gas price. The liquefaction technologies analysed in this study were Linde cycle and Claude cycle with and without pre-cooling. The results show that the Linde cycle with a pre-cooling stage and Claude cycle have shown a high energy efficiency, the LNG cost is comparable with the purchase cost at the terminal. The onsite regasification is more attractive and economic when distance between the terminal and the fuelling station is large. On the other hand, the analysis indicated that, purchasing LNG at the regasification terminal is useful only if the refuelling station is 2000 km away from the terminal.

Imran et al. [44] investigated the performance and emissions of the direct injection compression ignition engine that uses natural gas, diesel and REM as piloted fuels. The authors compared and assessed the performance of pilot. Tests were conducted for each piloted fuel to perform 48 different operating conditions that consist of six different speeds and eight different power outputs for each speed. The two fuels pilot data were conducted for 36 different operations with six different speeds and six different power output conditions for each speed and compared with the base case which is for single fuel pilot for diesel and REM. The study used four stroke single cylinders for the experiment. The authors concluded that the single fuelling pilot case was more efficient than the duel one due to the low air to fuel ratio obtained in the dual fuelling. In addition, HC emissions in dual fuelling are much higher than the single fuelling base cases. However, the natural gas duel fuelling NOx emission results shows a significant reduction compared to the single fuel base cases, at low power outputs across all speeds.

Cheenkachorn et al. [45] examined experimentally the performance and emissions of heavy – duty diesel engine using natural gas as fuel and piloted with diesel. The tests were carried with the variation of the engine speed between 1100 and 1900 rpm. In the experiment, six cylinders engine were used with the direct injection fuelling system. The diesel only mode was used as the base case to compare it with the dual fuelling. The authors concluded that the duel fuel operation has lower thermal and volumetric efficiencies than the single fuel operation. However, for the speed of 1700 rpm and less, the duel fuel operation shows lower specific fuel consumption

compared to the single operation. For diesel only operation THC and CO emissions were higher than the duel fuel operation while NOx and CO_2 were higher.

A review was carried out by Gómez et al.[46] to illustrate the current state of the thermodynamic cycles that exploit the LNG exergy released in the regasification process. The study covered the Rankine, Brayton and Kalina cycles, as well as combined cycles and cycles with CO_2 capture. They also established fluid selection criteria for the cycles depending on the heat source of that cycle with low and high temperature. The authors concluded that when the heat source is small, Rankine cycle is the best choice where ethane and ethylene are the best suited fluids for this cycle. On the other hand, when intermediate or high temperature source is available, Brayton cycle is the most appropriate with Helium and Nitrogen as the best suit for this case. However, if the high temperature source is available, another more favourable choice can be selected which is the combination of the Rankine and Brayton cycles, and direct expansion.

Sun et al. [47] presented a novel Rankine power cycle used a mixed working fluid to recover the cold energy from liquefied natural gas. The study conducted an exergy analysis for the system where the mixed fluid consists of methane, ethane or ethylene, and propane. The authors studies and analysed the system with and without LNG expansion and found that the cycle without the LNG expansion produce 1.023 kWh where the cycle with the LNG expansion provide 1.346 kWh for one kmol of LNG. By varying the re-warming temperature and Appling different schemes, the exergy efficiency of the cycle ranges between 29.58% and 49.98%. The results showed that for both cases with and without direct LNG expansion ethylene is more favourable to be included in the fluid mixer than ethane.

Kim et al. [48] analysed thermodynamically the performance of a combined power cycle that uses LNG cold energy and low grade heat source. The system consists of an ammonia-water Rankine cycle with and without regeneration and LNG Rankine cycle. The study performed the exergy analysis and parametric study to show the performance of the system and how it is affected by the critical parameters. The simulation results indicate that the most significant

parameter that affects the performance of the system is the ammonia mass fraction. The thermal and exergy efficiencies of the system are 37.7% and 17.2%, respectively.

Three different systems were investigated by Szargut et al. [49] to utilize the cryogenic exergy of LNG for the production of electricity. The analysis was done to produce electricity without any combustion of the natural gas. The first and second systems were using cascaded systems where the first system uses only Ethane as the working fluid, but the second one uses both Ethane and krypton in the system. The third system is not cascaded and uses only Ethane as the working fluid; this is the only system that had been analysed in detail in this study. The main findings for the third system are that the nominal flow rate of the LNG is 6.2 kmol/s and the annual production of the electricity is 31×10^6 kWh.

Dong et al. [50] proposed basic Stirling cryogenic cycle for LNG cold energy recovery where the system consists of Nitrogen Stirling cycle and LNG regasification process. The authors found that the largest exergy losses occur in the seawater heat exchanger, and all heat exchangers exergy loss counts for 92.65% of the system exergy loss. The exergy efficiency of the system found to be 24.26% when the LNG mass flow rate is 1 kg/s, and the pressure is 3 MPa. The study also mentioned the feasibility of the improvement in the basic system where an additional air liquefaction process is integrated into the basic system.

Poompipatpong et al. [51] tested the performance and emissions of a modified diesel engine for natural gas operation experimentally. The engine was four cylinders and four strokes engine where the indirect injection fuelling system was used. Initially, the diesel engine was tested using diesel only to have reference information for the natural gas test. In this case, the engine speed was varying between 1600rpm and 2600rpm and the compression ratio selected to be 22:1. Then the system was modified for the natural gas by replacing the fuel injectors with spark plugs and install new sets of pistons. To utilize the engine performance and emissions the compression ratio was varied to include 9.0:1, 9.5:1, 10.0:1 and 10.5:1 with the engine speed variation between 1000 rpm and 4000 rpm. The authors concluded that natural gas had higher performance than diesel engine with an improvement of 5.67% to 13.07%. For the compression ratios 9.0:1, 9.5:1 and 10.5:1, the highest thermal efficiency was achieved with the engine speed

range between 1500rpm and 2500 rpm. THC and NOx emissions were directly proportional to the compression ratio.

Gómez et al.[52] presented a novel power plant that combine closed Brayton cycle with steam Rankine cycle in series while exploiting the LNG cold exergy in the regasification process. The results were for 1 kg/s of LNG where the system energy and exergy efficiencies found to be 65.61% and 55.09%, respectively. Also, in case of the maximum efficiency the exergy available in the LNG accounts for 20.34% of the fuel exergy, but only 7.98% is exploited to increase the exergy efficiency. The maximum exergy destruction occurs in the combustion chamber that counts for 37.45%.

A review for the spark ignition natural gas engines has been done by Cho et al. [53]. The authors highlighted in this work the operating envelope, fuel economy, emissions, cycle-to-cycle variations in indicated mean effective pressure and strategies to achieve stable combustion of lean burn natural gas engines. The study concluded that the Lean burning is an effective solution to reduce NOx emissions and improve the fuel efficiency. The primary factor that limits the lean burning is the combustion chamber geometry, ignition timings, ignition energy and turbulence. To improve the power density of the natural gas engines, turbocharging technology is highly recommended.

3.2 Biodiesel Locomotives

3.2.1 Demonstration Projects

The National Railroad Passenger Corporation (AMTRAK) has tested 20% biodiesel blend B20 on a passenger locomotive GE P32-8 locomotive for 12 months in 2010. The Texas-based Direct Fuels was the supplier of the biodiesel fuel that is sourced from beef tallow [54, 55]. Based on the company report in 2011 [56], the emissions result of HC, CO and PM were well below the EPA emission limits for tire 0 locomotive engines. Canadian Pacific has used four GE Transportation AC4400 locomotives to test B5 in 2009. The test was carried in cold conditions that reach -40°C and show the viability of using B5 biodiesel in the cold weather for freight services [57, 58]. The South Florida RTA tested B100 for three months and B20 for eight year in 2002. They concluded that B100 is not suitable for cold weather and stop using B20 in 2010

because of the price problems [59]. Eastern Washington Gateway Rail road conducted six month test for B25 biodiesel locomotive in 2008 [60]. In 2010, Norfolk Southern Railway (NSR) partnered with Electro-Motive Diesel (EMD) and tested 11% biodiesel blend. In 2012, NSR started an experimental test for B100 biodiesel locomotive fuelled at Meridian, Miss. Terminal, but at late 2012, the terminal resume fuelling diesel only because the Louisiana plant that produces the biodiesel stopped by the plant owner[61-63]. The New Mexico Rail Runner (NMRR) was testing B20 biodiesel locomotive in 2009 using refurbished EMD 3600 HP (Tier 1) engines[64]. Iowa Interstate Railroad tested B20 biodiesel in 2010 and found out the NOx emissions had slight increased but other emissions had decreased with 35% [65].

In Brazil, Vale do Rio Doce (CVRD) has run a locomotive using B20 biodiesel mixed with palm oil. The locomotive was running since 2007, and CVRD planning to increase the number of locomotives that use biodiesel [66, 67]. During 2006 to 2007 the Russian Railways tested locomotives using 5%, 10% and 20% blends of biodiesel. The result of the demonstrated project found that the biodiesel characteristics are almost equal to the conventional fuel [68, 69]. Indian Railways had tested and compare the conventional diesel, B10, B20, B50, and B100. The comparison was based on the brake specific fuel consumption, engine power, and locomotives emissions. The main finding was that B10 and B20 are very similar to the conventional diesel in terms of the engine power and fuel consumption [70, 71]. French railway operator SNCF tested B20 locomotives and showed that there was a reduction on the smoke but increase in all other emissions [72].

3.2.2 Biodiesel Research Work

The area of biodiesel was covered by many researchers, where some of these studies are included in this section. Lahane et al. [73] made an experimental comparative study for biodiesel–diesel blends (B5, B10, B15, B20, B25, B50 and B100) to study the effect of the injection, spray, combustion, performance, and emissions of a direct injection diesel engine at speed of 1500 rpm. The test results indicate no wall impingement for the spray penetration with biodiesel–diesel blend up to B15, but B20 is to be a critical limit of wall impingement and for higher blends the probability of wall impingement is more. For B100 the engine torque reduced by 2.7% while for biodiesel with blended by 20% or less there is a significant reduction in the engine torque.   CO,

HC and smoke emissions decreased drastically for all biodiesel fuels compared with diesel, while NOx emission increased due to the oxygen content in biodiesel. B15 is the optimal biodiesel fuel for unmodified diesel engine, no wall impingement and increase in NOx emission.

An experimental investigation was done by Tesfa et al. [74] for CI to show the emission characteristics of various biodiesel types and fraction. The diesel was the base case and compared with the tested biodiesel fuels which are waste oil, rapeseed oil and corn oil. The analyses were carried for B10, B20, B50, B100 blended fuels. In the experimental setup, a four-cylinder, four-stroke, direct injection and turbocharged diesel engine was used with varying the engine speed from 1000 rpm to 1800 rpm with an increment f 200rpm. The result of the study indicated there is no significant effect of the biodiesel type on the emissions. The study concluded that compared to the diesel case, biodiesel have higher NOx emissions. However, the CO, CO_2 and THC emissions were reduced by 15%, 40% and 30%, respectively.

Yilmaz et al. [75] examined a diesel engine performance and emissions for biodiesel-butanol fuel blended. The performed test was for four-stroke, naturally aspirated, water-cooled, indirect injection diesel engine and compared the butanol blended with biodiesel, diesel and biodiesel B100. The biodiesel butanol blends were B95Bu5, B90Bu10 and B80Bu20. The results show that the butanol blends produce lower emissions NOx, CO and HC emissions, compared to biodiesel B100. Also, compared with diesel, butanol blended B95Bu5 and B90Bu10 showed lower CO and NOx emissions but no significant change in HC emissions. However, B80Bu20 produced higher CO and HC and lowered NOx emission than diesel.

Osborne et al. [76] studied the effects of biodiesel fuel blends on the emissions of a General Electric Tier 2 line-haul and switcher locomotives and compared with diesel. The test was performed at B2, B10, B20, B100 soybean biodiesel. The test results indicated the reduction of particular matter (PM) for biodiesel blend and noticed a small increase by increasing the biodiesel percentage in the fuel. In addition, the PM for line-haul duty was lower than switcher duty cycle. The B2, B10 and B20 NOx emissions were not greater than the expected test measurement variation, but for the line-haul NOx increased by 15% in case of B100. For both Line-Haul and Switch cycles, the HC emissions were reduced by 21% and 24%, respectively. Also for Switch cycle, the CO emissions were reduced by 11% and 35% for B20 and B100,

respectively. However for the Line-Haul cycle B20 and B100 CO emissions were reduced by 17% and 34%, respectively. Another conclusion is that an additional volume consumption of fuel is needed, in case of B100, an increase of the volume consumption nearly 7%.

3.3 Hydrogen Fuelled Projects

3.3.1 Demonstration Projects

The first experimental hydrogen fuel cell switch locomotive was developed by Burlington Northern Santa Fe (BNSF) railway and Colorado-based Vehicle Projects in 2009. The project was funded by the US department of defence. The locomotive used a set of batteries to drive electric traction motors, and a fuel cell power plant to supply additional power to traction motors, and recharge the batteries [77-79]. China North Vehicle Yongji Electric Motor Corporation, in partnership with Southwest Jiaotong University, has developed the first Chinese hydrogen fuel cell locomotive in 2010 [80].

Five fuel cell mine locomotives have been built by the partnership of Colorado-based Vehicle Projects and Anglo American Platinum (Amplats) in South Africa in 2012. PEM fuel cell has been used in this project, and 51% thermodynamic efficiency has been achieved during the actual operation [81, 82]. In 2003, JR East Group built the NE Train (New Energy Train) test hybrid locomotive that uses diesel and fuel cell to power the locomotive. The battery has been used to manage the power flow from the fuel cell [83-85].

3.3.2 Hydrogen Research Work

Several studies have been carried out to integrate the hydrogen in the locomotive system either by using it as fuel directly in the engine or using fuel cells to produce the required electricity. Miller et al. [86] examined the practicality of the fuel cells for commuter rail and long distance passenger train. The authors showed the results of pure fuel cells for 1200 kW locomotive and hybrid system that uses batteries in addition to the fuel cells that generate 200 to 700 kW. The results showed that in case of hybrid locomotive, the total cost can be reduced by 30% when the fuel cells produce 400 kW and batteries 752 kW.

Meegahawatte et al. [87] analysed a hybrid commuter railway vehicle that uses fuel cells and batteries. The authors studied the behaviour of the fuel cell stack and battery pack by varying the battery sizes, stack sizes, and control strategies. The study compared diesel and hybrid diesel vehicles with the hydrogen vehicle to show the energy performance and CO_2 emissions benefits. The results showed that the best configuration is a 670 kW fuel cell stack and 60 to 90kWh of energy storage and utilizing a load levelling control strategy. In this case, the hydrogen consumption is 27 kg that produce approximately 148.5 kg of CO_2 emissions. By comparing the fuel cell only locomotive, the hybrid one show better performance where it consumes 30% less fuel and emissions. For the diesel case, the hybrid system showed 45% reduction in the CO_2 emissions.

Peng et al. [88] developed and investigated the experimental prototype of a PEMFC shutting locomotive. The authors perform the test in two stages; PEMFC power plant test and locomotive running test. The purpose of the PEMFC power plant test was to verify the performance match between the PEMFC power plant and the power inverter, because of the delayed response of the PEMFC in the power load. In addition, this test means to ensure the temperature response of the cooling system for the PEMFC.

Schroeder et al. [89] analysed the technical and economic feasibility of the SOFC based locomotives using onboard gasified biodiesel. A long-haul locomotive was considered in this study with a peak load of 37000 kW. The locomotive uses biodiesel combustion to provide the required energy for the fuel cell operation. For the cost analyses, only the power generation equipment was considered, and the price of the biodiesel is not changing over 40 years. The fuel cells stack life time waste assumed to be 40000 h to produce 32000 MWh. The study concluded that when the stack has a lifetime of 8000 MWh, the SOFC became not cost effective. The efficiency of the diesel locomotive is 34.6% while for the SOFC is 47.6%, and it is more cost effective.

Martinez et al. [90, 91] studied the feasibility of the SOFC with gas turbine hybrid long-haul freight locomotive. The study used the diesel reformat and compared with the natural gas reformat and the hydrogen as fuel. The author concluded that efficiencies of the systems were in

the range of 65% to 70%, where the reformation of the hydrocarbon fuels was not counted. In case of diesel reformate, longer transit was noticed during the dynamic power change. Another finding is that by neglecting the electrical balance of the plant, the SOFC-GT space requirement is similar to the current diesel engine.

The performance of the hydrogen-powered prototype locomotive was evaluated by Hoffrichter et al. [92]. The study was 'Hydrogen Pioneer', the first hydrogen locomotive in UK and was built in 2012. Proton exchange membrane fuel cell power plant was sued to supply the required electricity to the traction motors or charge the onboard lead-acid batteries. The study tested the resistance to motion of the vehicle first, and then tests were conducted for the speeds 2 km/h, 6 km/h, 7 km/h, and 10 km/h on a 30 m. The results indicated that the efficiency of the power plant was 40%, and batteries were used on the peak power demand such as during the acceleration.

A comparison study was done between hydrogen and electrification locomotives with a case study in Ontario by Marin et al. [93, 94]. Their study focused on the implementation and operation of hydrogen passenger locomotive over a distance of 115 km. The study indicated that the electrical only locomotives depend on the source of the electricity to determine whether this option is clean or not. On the other hand, fuel cell power locomotives will generate electricity without the added cost, inconvenience and lake of flexibility of catenaries. Another note is that between refills, the fuel cell locomotive requires about 2900 kg of hydrogen to match a diesel power train requirement of 2694 gal. Due to the shorter range travelled by the hydrogen locomotives, more fuelling stations and refuelling stops are needed. Another drawback of the hydrogen locomotives is the fact that over 30% of the hydrogen energy is consumed during the liquefaction process and 10% to 15% in the compression process. Also, the fuel cell locomotive is heavier than the conventional electrical locomotive by 30%. Valuable information in the economic analyses is that PEMFCs expected to have a one-third life compared to diesel. The study concluded that the PEMFCs need about half of the hydrogen amount that is required by ICEs to run a locomotive. That shows the potential of PEMFCs as a locomotive prime mover for the better operational cost.

Chapter 4 : Systems Description

In this study, seven systems are investigated that include the baseline diesel-only locomotive power plant for the comparison. The purpose of these designed systems is to improve the performance of the overall locomotive system by examining different combinations of fuels with LNG. Depending on the fuels and system design, the suitable prime mover is selected. For systems 1, 2, and 3 the compression ignition engine is the prime mover of the system, where for systems 4 and 5 the spark ignition engine is used as prime mover. However, the solid oxide fuel cell (SOFC) is used in system 6 to generate power for the locomotive. Finally, system 7 uses gas turbine as prime mover. The internal combustion engines specifications used in the systems are given in Table 4.1.

Table 4.1: Internal combustion engines specifications.

Engine specification	Systems 1,2&3	Systems 4&5	Fumigate
Engine Model	(EMD) 16-710G3C-ES	(Cat) CG260-12	ISX12 G
Traction Horsepower, $\dot{W}_{THP}$ (hp)	4,300	4470	400
Traction Power, $\dot{W}_{TP}$ (kW)	3,207	3,333	298
Engine Speed, N_{CI}(rpm)	950	1000	2100
Brake mean effective pressure, bmep (kPa)	1399.4	2000	967.8
Displacement Volume, V_d(m3)	0.19407	0.204	0.0119
Compression ratio, r	16:1	12:1	---
Bore, (m)	0.23306	0.260	0.13
Stroke, s (m)	0.28433	0.320	0.150
Number of cylinders, n_c	16	12	6

Sources: [95-97]

4.1 System 1: Baseline Locomotive System (diesel-only)

The baseline locomotive system operates with ultra-low sulphur diesel (ULSD) only which is shown in Figure 4.1. A compression ignition two stroke engine is used for this system with a turbocharger. For steady operation, the air enters the compressor and exit with high pressure and temperature. Then, the air is cooled in the after cooler to increase its density and mass before entering the intake manifold. The cooled air then introduced to the internal combustion engine to produce the required power for the locomotive operation. The exhaust gases of the engine are passed through the turbocharger turbine for the expansion that runs the turbocharger compressor.

The cooling system uses a mixture of water and ethylene glycol as antifreeze. The cooling fluid is drawn from the coolant reservoir and used to cool the internal combustion engine and the air that exit the compressor and enter the intake manifold of the engine. The lubrication system uses a petroleum base lubricant that is preferable for each engine to lubricate and cool the engine. Two reservoirs are used for the lubrication system where one of them is used to collect the oil that come from the system and the other one is used for the cooled and clean oil that is supplied to the engine.

4.2 System 2: LNG-ULSD Locomotive System

In this system, a dual operation uses LNG and ULSD as fuels is proposed in Figure 4.2. This system can operate with diesel only if the LNG is not available where, in this case, the fuels that run the main engine consist of 60% diesel and 40% LNG. Since LNG is used, a cryogenic system should be placed in the locomotive such as a cryogenic tank and pump. During the operation, the LNG is pumped by the cryogenic pump from the cryogenic tank to the evaporator to increase its temperature and convert it into natural gas. Then the natural gas is introduced to a carburetor to be mixed with air and enter the intake manifold of the main engine. The combustion of the natural gas occurs because of the piloted diesel at the end of the compression stork.

A fumigate small capacity spark ignition engine is used to overcome the boil-off gases problem from the cryogenic tank. The fumigate engine is used to run the locomotive auxiliaries where it can produce a maximum of 10% of the total power and the remaining 90% produced by the main engine. Since the fumigate engine is used to run the auxiliaries, a pump is introduced to take more fuel if needed to run the auxiliaries. The exhaust gases from the fumigate engine are used to heat the boil-off gases before entering the carburetor.

The cooling system has similar functions to system one but in addition of cooling the main engine and the intake air there are two more functions. The first is that the cooling system cool the fumigate engine which means more energy is required to remove that heat from that cooling water. The second function is that the cooling fluid is used to after cooling the engine to evaporate the LNG, which helps to reduce the energy of that required to cool the cooling fluid.
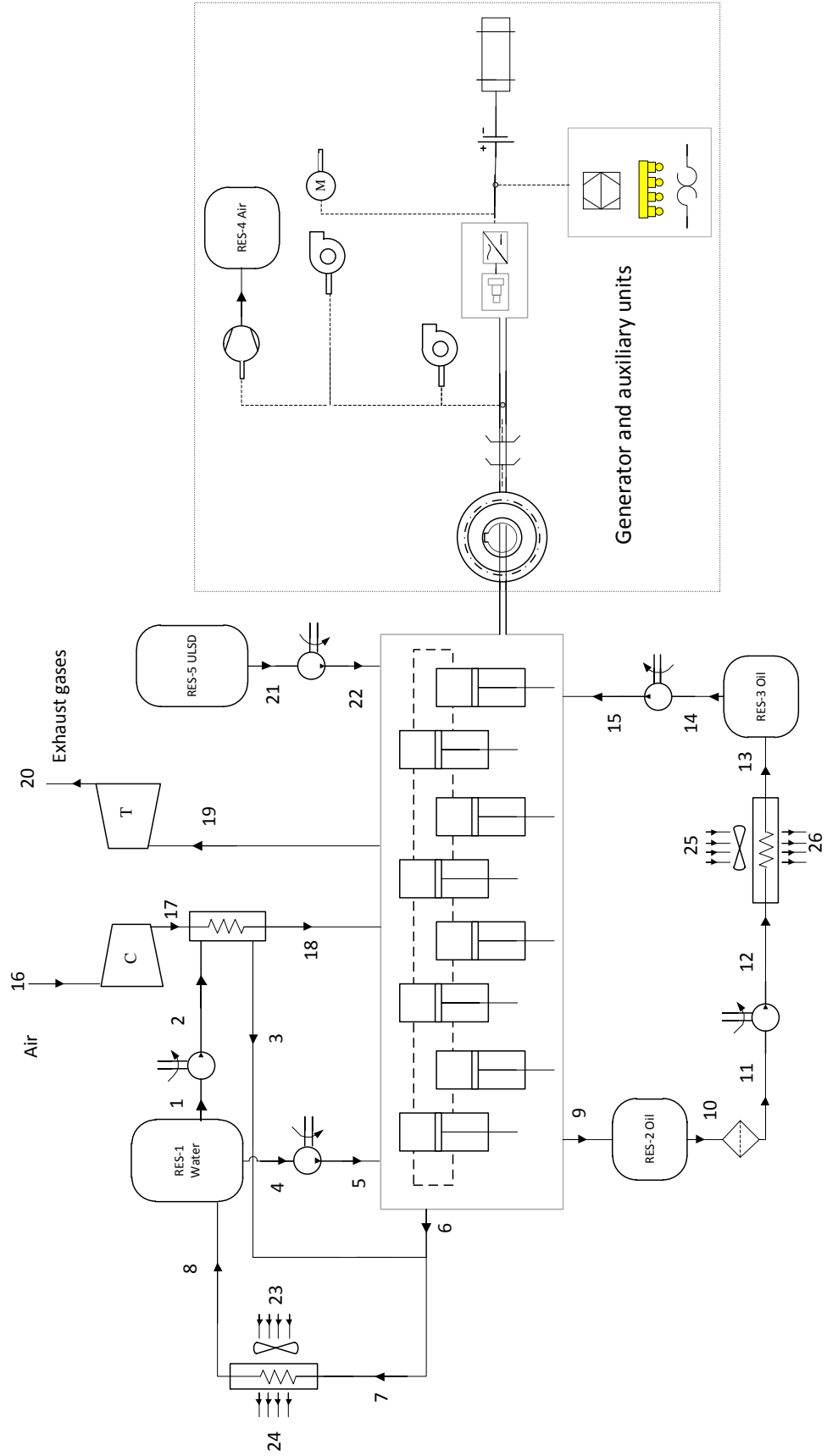
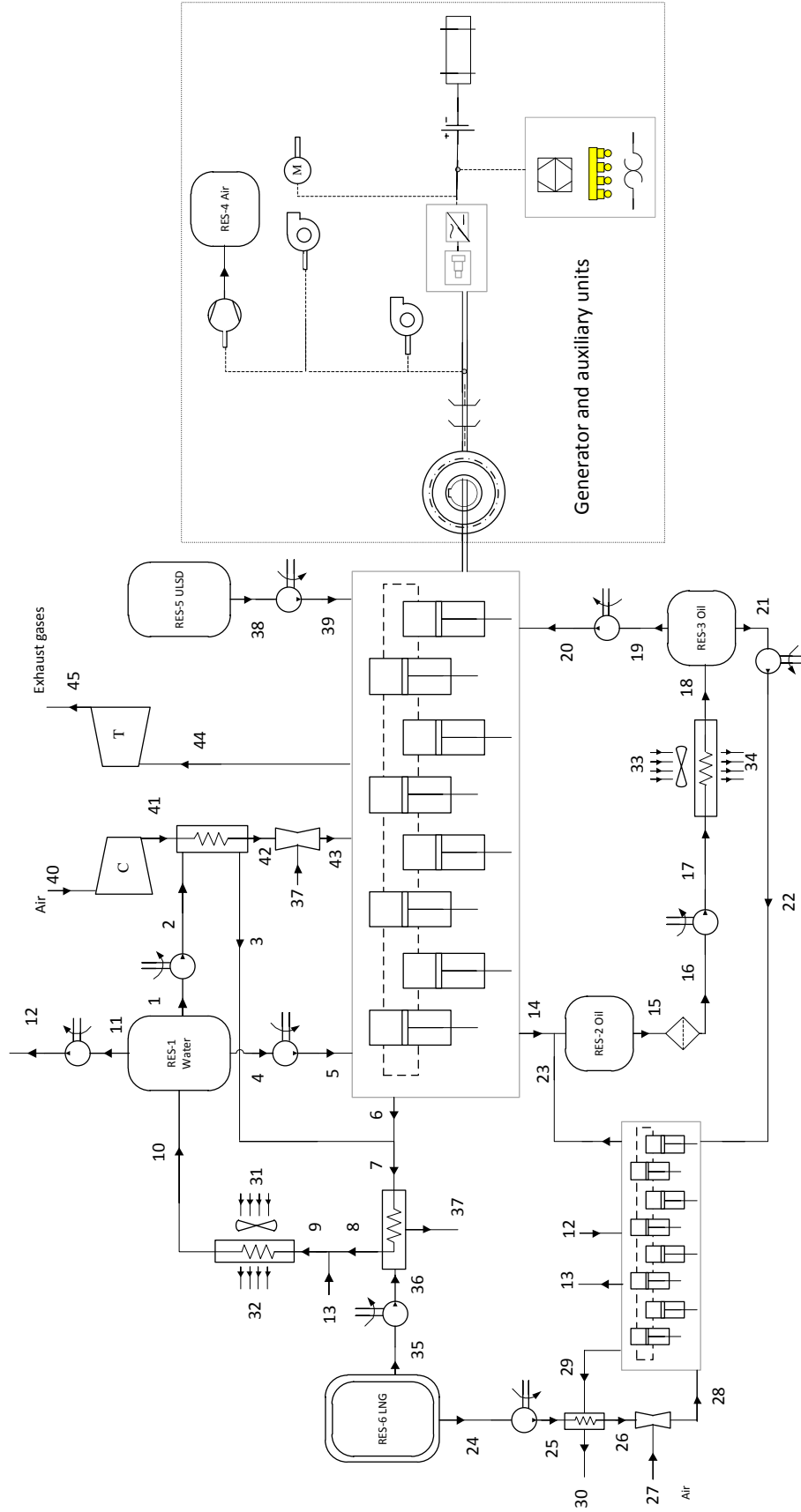Figure 4.1: System 1, baseline system (diesel only).

Figure 4.2: System 2 (diesel and LNG).

4.3 System 3: LNG-ULSD Locomotive System

LNG and ULSD are the fuels used in system 3 where the locomotive cannot operate in the diesel only mode; system 3 is shown in Figure 4.3. In this case, the LNG accounts for 90% of the total fuel introduced to the main engine and the diesel is used only for piloting using dual injection system. This system has similar components to system 2, where the fumigated engine and lubrication system are working same as system 2. System 3 uses a high pressure direct injection method to inject the natural gas along with diesel into the main engine.

An exhaust gas recirculation is used to reduce the NOx emissions, where the exhaust gases from the turbine are controlled by a controlling valve to monitor the amount the recycled gases. The regulation of the exhaust gas recirculation is important because the more gas recycled the engine become less efficient, because less oxygen is introduced to the engine because of the place taken by the recycled exhaust gases that reduce the amount of fuel needed for the combustion. The cooling fluid cools the recycled exhaust gases before entering the compressor because the compressor is not designed to withstand a very high temperature.

4.4 System 4: LNG-LPG Locomotive System

A combination of liquefied natural gas (LNG) with liquefied petroleum gas (LPG) is used to fuel system 4 which is shown in Figure 4.4. This system can operate in LPG only mode where it accounts for 65% of the total fuel used to run the locomotive. Spark ignition engine is used as the prime mover and main engine for this system where no diesel introduced to the engine. The LPG is stored in a cryogenic tank where the fluid pumped using a cryogenic pump to the evaporator and then injected to the main engine. The LNG leaves the evaporator after the conversion to natural gas and split into two streams, one stream enter the carburetor, and the other stream enters a catalytic membrane reforming unit. The catalytic membrane reforming recovers the heat from the exhaust gases to operate the steam methane reforming to produce hydrogen. The hydrogen is only 2% by mass and introduced to the carbureted which is mixed with methane and air, and then enters the intake manifold of the engine.
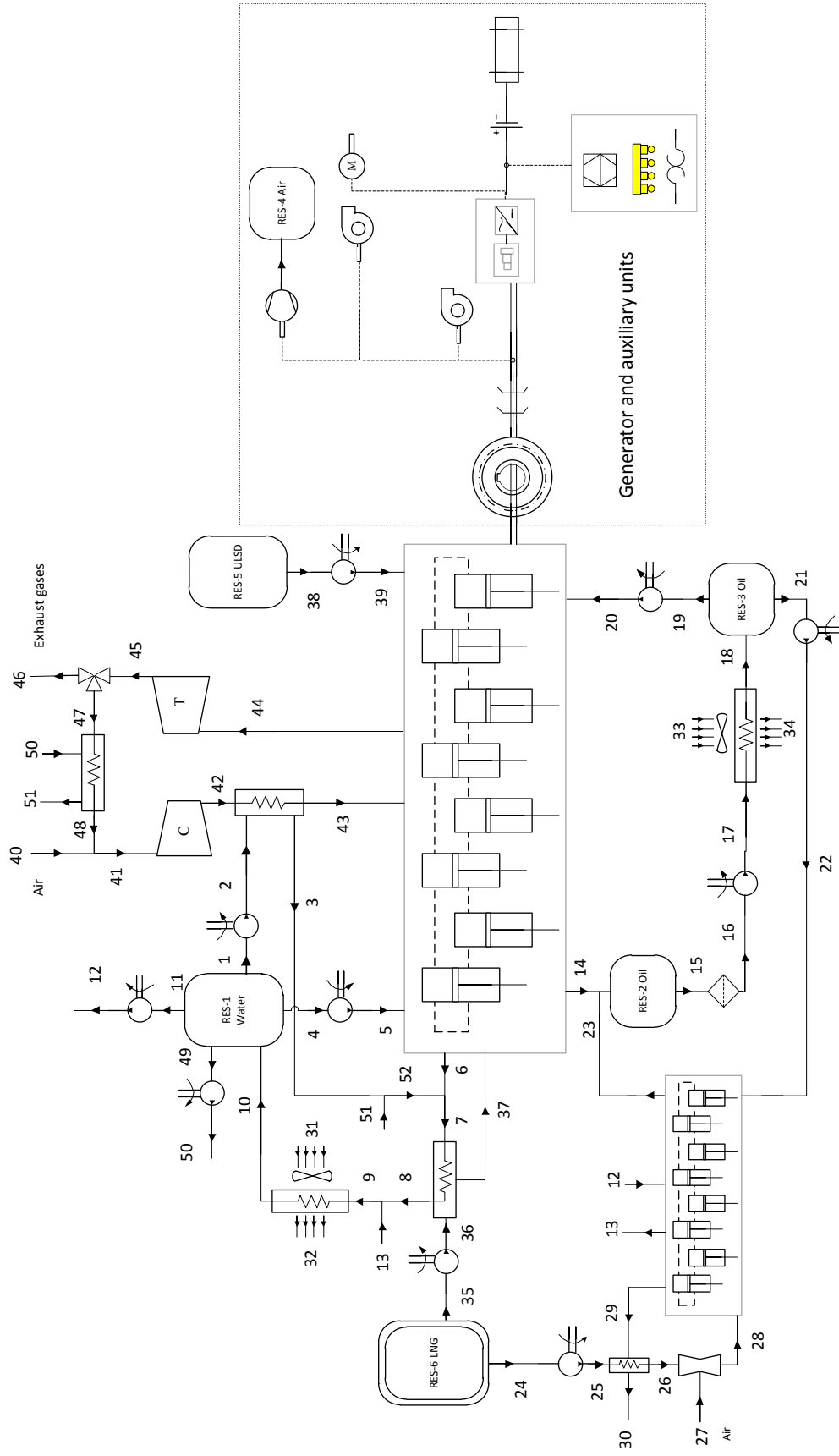
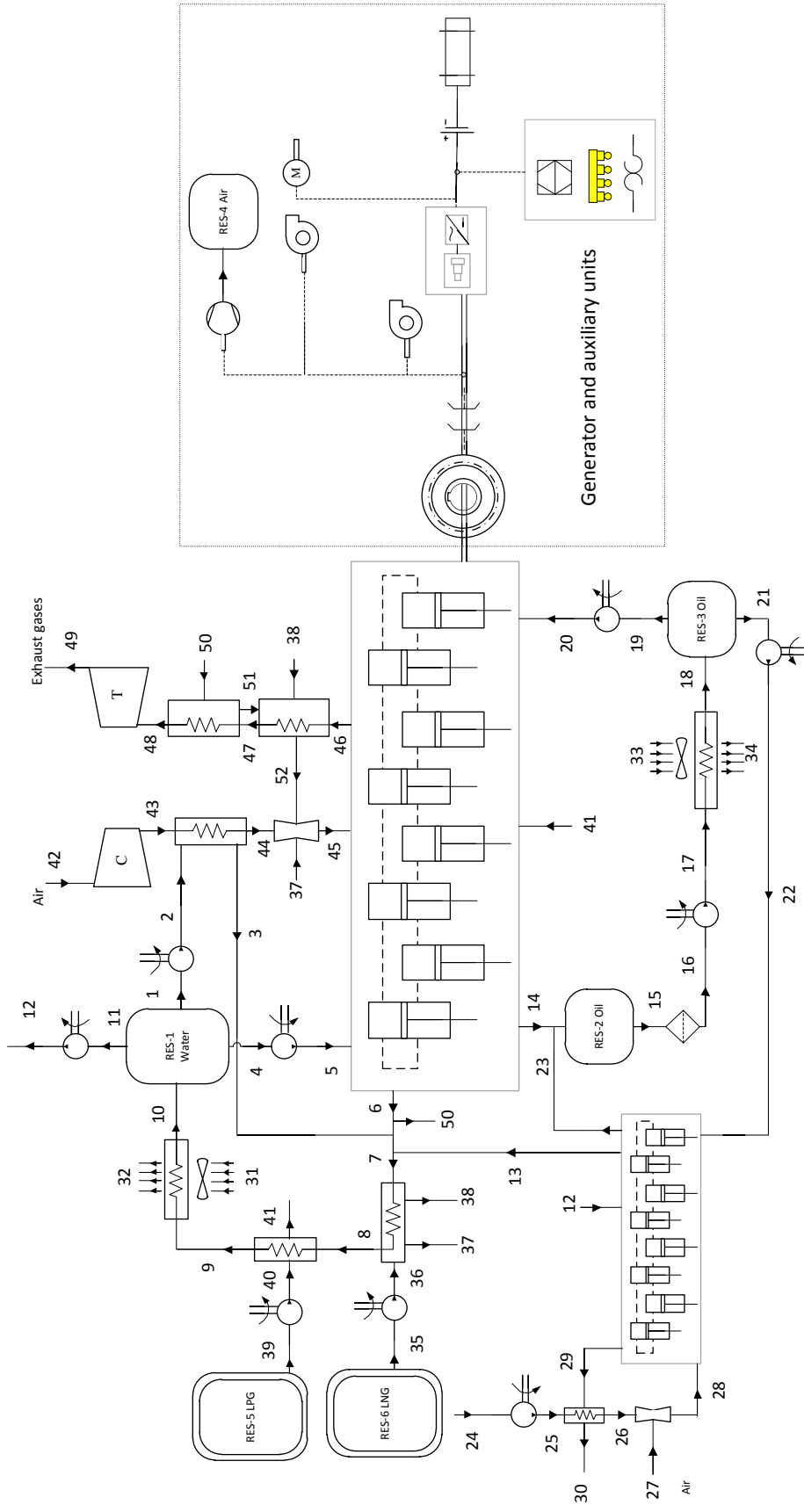Figure 4.3: System 3 (diesel and LNG).

Figure 4.4: System 4 (LNG and LPG).

The lubrication and fumigate engine are similar to system 3. However the cooling system is used to supply the hot water that exit the main engine and further heat is added to convert it into steam. This was achieved by utilizing some of the exhaust gases energy and introduced it to the steam methane reforming process. Also, the LPG evaporator is used to cool the cooling fluid to save more energy.

4.5 System 5: LNG-H_2 Locomotive System

The fifth system, shown in Figure 4.5, uses the LNG with compressed hydrogen to operate the locomotive. This system is similar to system 4 where fumigated engine, lubrication system and LNG system are almost the same. The compressed hydrogen is introduced into the carburetor with air, methane and the additional hydrogen obtained from the catalytic membrane reforming. This system operates with 70% LNG with 30% compressed hydrogen.

4.6 System 6: LNG only Locomotive System (SOFC)

System 6 is presented in Figure 4.6 where only LNG is used to run the locomotive. The system consists of gas turbine with Solid Oxide Fuel Cell with internal methane reforming. The primary power generation of the locomotive comes from the SOFC, where the gas turbine is used for the auxiliaries and fast startup. The system starts by compressing air and heat it up using the turbine exhaust gases; then the air enters the SOFC cathode part. The water needed for the SOFC is drawn from the recirculated gases that exit the anode and introduced with methane to enter the SOFC anode where the chemical reaction occur and electricity is generated due to the movement of electrons. At the exit of the SOFC the cathode part, the exit is the remaining of the excess air, where the anode part include CO_2, CO, H_2O and the remaining H_2 and CH4. These gases enter the combustion chamber where more methane is added to the combustion. For the LNG system, the cryogenic pump pumps the fluid from the tank and split it into two flows both are heated by the turbine exhaust gases. The first stream enters the SOFC for internal methane reforming and the second stream is introduced into the combustion chamber that helps during the startup.

4.7 System 7: LNG only Locomotive System (GT)

In system 7, LNG is the only fuel that is used to operate the system. In this system, the gas turbine is the prime mover and ORC has been integrated and run by using a heat recovery.
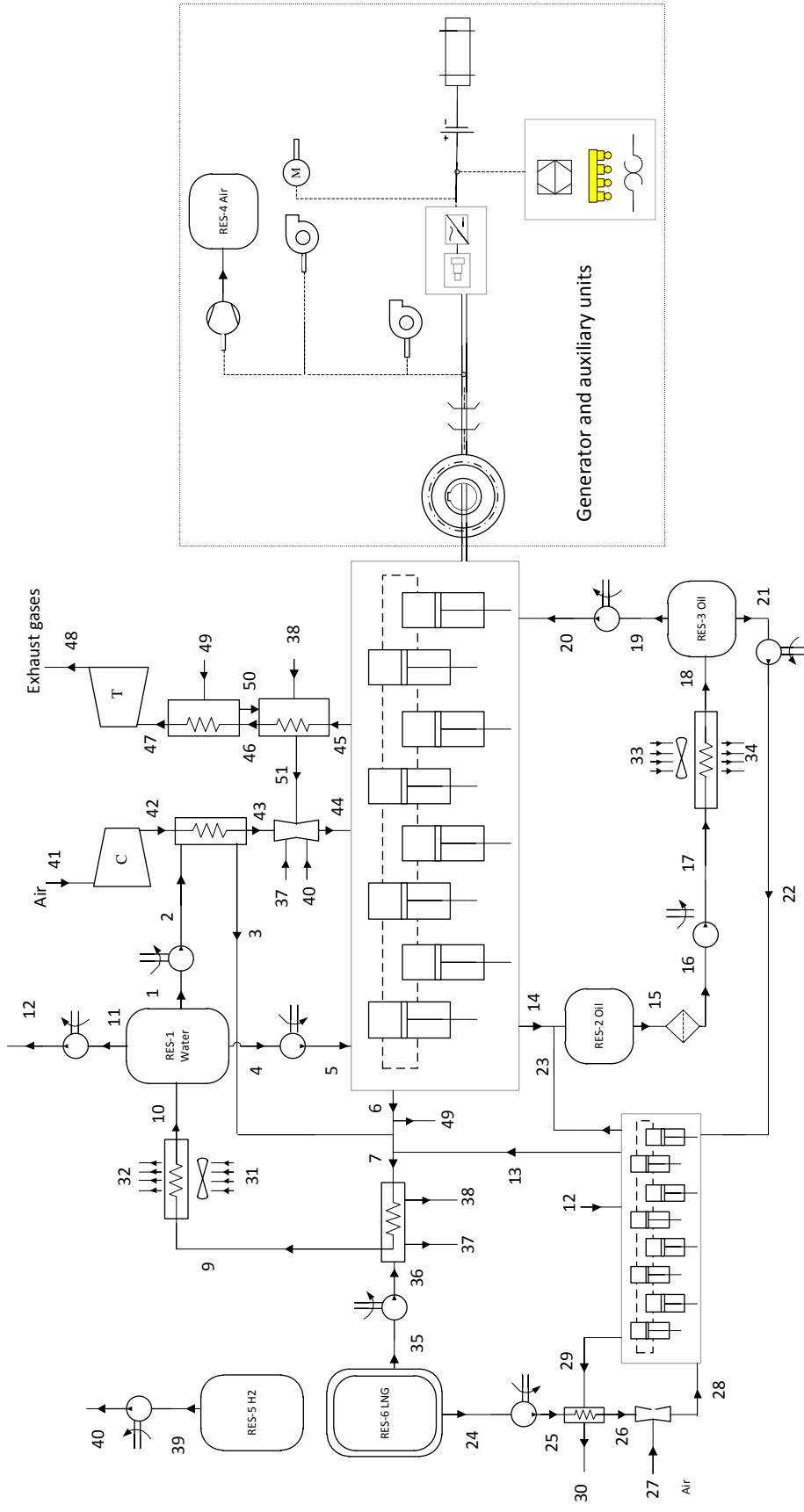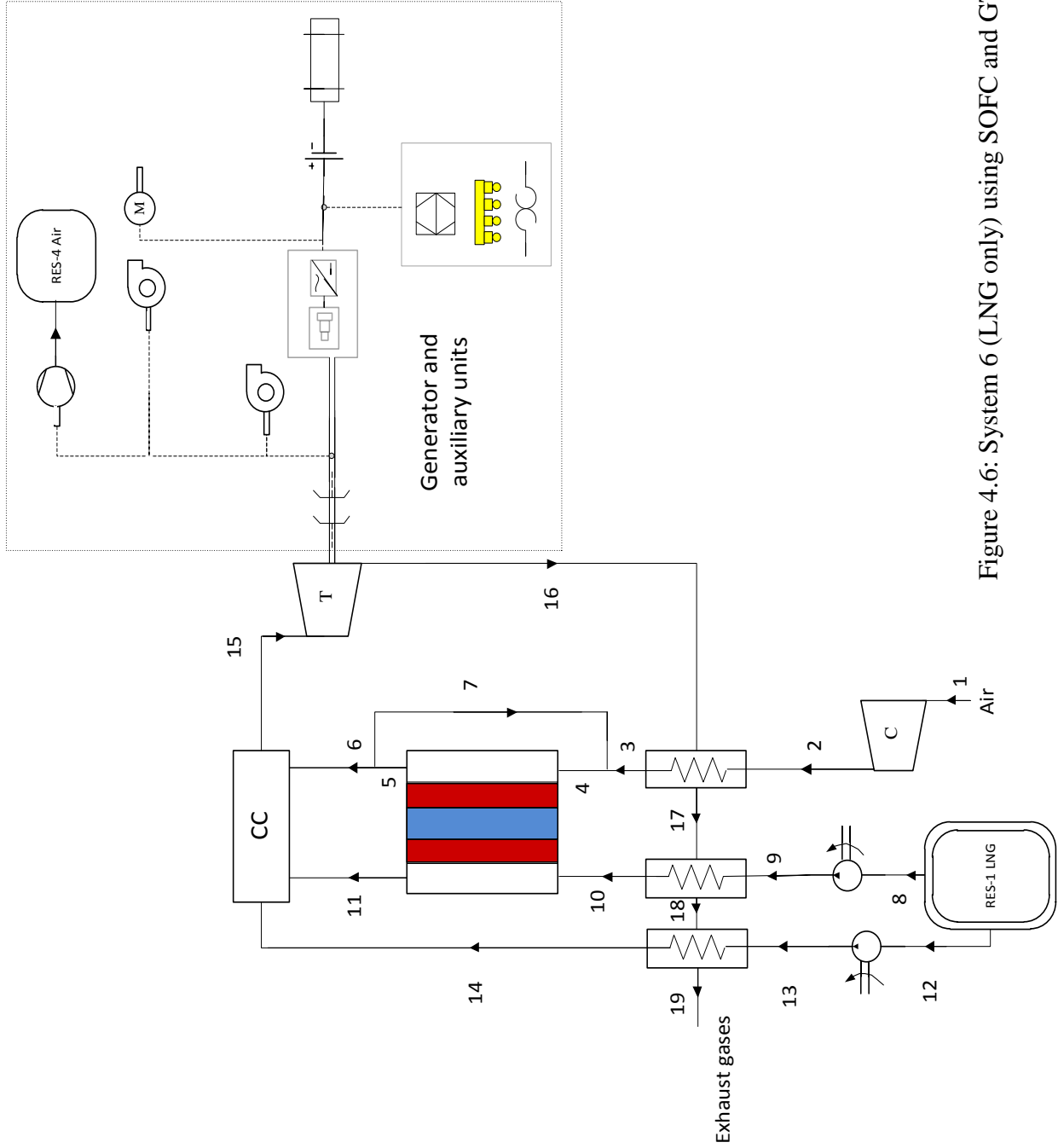
Figure 4.5: System 5 (LNG and H_2).

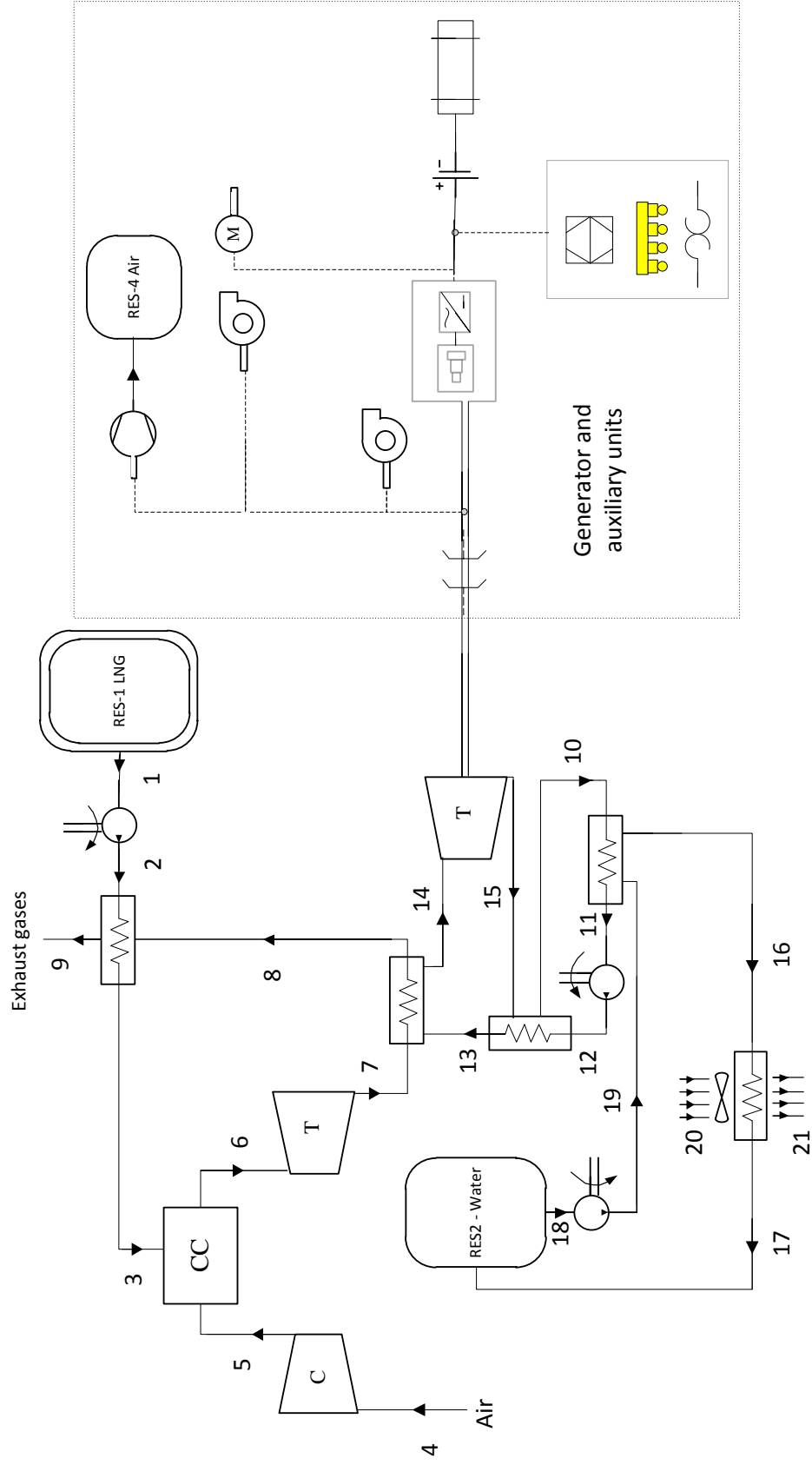Figure 4.6: System 6 (LNG only) using SOFC and GT.

Figure 4.7: System 7 (LNG only) using GT and ORC.

The LNG is evaporated by the exhaust gases from the gas turbine and then introduced to the combustion chamber. At state 4 the air is compressed and enter the combustion chamber, after the combustion process the gases pass through the turbine for the expansion process to generate power for the locomotive. Then, the gases exit the turbine and enter the ORC evaporator to supply the required heat to run the ORC. The n-octane is used as the ORC fluid that is heated by the exhaust gases and enters the turbine for the expansion process to produce power to run the auxiliaries. After that, the stream enters a heat exchanger to be cooled and heat the stream that exits the pump. By doing so, decreasing heat transfer in the condenser results in an increase in the ORC efficiency.

Chapter 5 : Analyses

In this chapter, the analyses and assumptions of the developed systems are introduced and described. It also provides the thermodynamic analyses that include mass, energy, entropy, and exergy balance equations and then the internal combustion engines cycle, engine parameters and chemical reaction analyses. In next section, the solid oxide fuel cell analyses are presented, and the final section discusses the environmental and economic aspects.

5.1 Thermodynamic Analyses

In this section, the thermodynamic analyses are performed for proposed systems. The general balance equations are written, where some special cases of these equations are indicated in the respective sections.

Mass Balance Equation (MBE)

The mass balance equation for control volume in steady state condition is defined as that total mass flow rate entering the control volume equal to the total mass flow rate exiting the control volume and expressed as

$$\sum \dot{m}_i = \sum \dot{m}_e \tag{5.1}$$
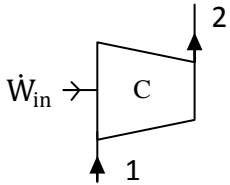
where i and e are the inlet and the exit, respectively.
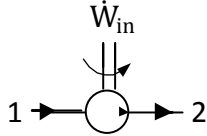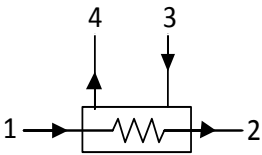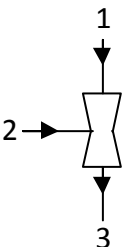
Energy Balance Equation (EBE)

The energy balance equation for steady state control volume process can be written as

$$\dot{Q}_i + \dot{W}_i + \sum_i \dot{m}(h + \frac{v^2}{2} + gz) = \dot{Q}_e + \dot{W}_e + \sum_e \dot{m}(h + \frac{v^2}{2} + gz) \tag{5.2}$$

where v is the velocity in m/s, g is the gravitational acceleration, $\dot{Q}$ is the heat transfer rate, and $\dot{W}$ is the work rate. Also, h and z are the specific enthalpy and the elevation.

Table 5.1: Mass, energy, entropy, and exergy balance equations of the system components.

Component	Component name	Balance equation
	Compressor	MBE : $\dot{m}_1 = \dot{m}_2$ EBE : $\dot{m}_1 h_1 + \dot{W}_{in} = \dot{m}_2 h_2$ EnBE : $\dot{m}_1 s_1 + \dot{S}_{gen} = \dot{m}_2 s_2$ ExBE : $\dot{m}_1 ex_1 + \dot{W}_{in} = \dot{m}_2 ex_2 + \dot{Ex}_{Dest}$
	Turbine	MBE : $\dot{m}_1 = \dot{m}_2$ EBE : $\dot{m}_1 h_1 = \dot{m}_2 h_2 + \dot{W}_{out}$ EnBE : $\dot{m}_1 s_1 + \dot{S}_{gen} = \dot{m}_2 s_2$ ExBE : $\dot{m}_1 ex_1 = \dot{m}_2 ex_2 + \dot{W}_{out} + \dot{Ex}_{Dest}$
	Pump	MBE : $\dot{m}_1 = \dot{m}_2$ EBE : $\dot{m}_1 h_1 + \dot{W}_{in} = \dot{m}_2 h_2$ EnBE : $\dot{m}_1 s_1 + \dot{S}_{gen} = \dot{m}_2 s_2$ ExBE : $\dot{m}_1 ex_1 + \dot{W}_{in} = \dot{m}_2 ex_2 + \dot{Ex}_{Dest}$
	Heat exchanger	MBE : $\dot{m}_1 + \dot{m}_3 = \dot{m}_2 + \dot{m}_4$ EBE : $\dot{m}_1 h_1 + \dot{m}_3 h_3 = \dot{m}_2 h_2 + \dot{m}_4 h_4$ EnBE : $\dot{m}_1 s_1 + \dot{m}_3 s_3 + \dot{S}_{gen} = \dot{m}_2 s_2 + \dot{m}_4 s_4$ ExBE : $\dot{m}_1 ex_1 + \dot{m}_3 ex_3 = \dot{m}_2 ex_2 + \dot{m}_4 ex_4 +$ $\dot{Ex}_{Dest}$
	Carburetor	MBE : $\dot{m}_1 + \dot{m}_2 = \dot{m}_3$ EBE : $\dot{m}_1 h_1 + \dot{m}_2 h_2 = \dot{m}_3 h_3$ EnBE : $\dot{m}_1 s_1 + \dot{m}_2 s_2 + \dot{S}_{gen} = \dot{m}_3 s_3$ ExBE : $\dot{m}_1 ex_1 + \dot{m}_2 ex_2 = \dot{m}_3 ex_3 + \dot{Ex}_{Dest}$

Entropy Balance Equation (EnBE)

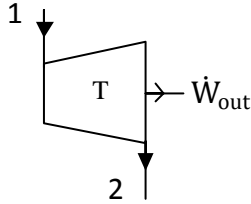The entropy generated in a process called entropy generation, $\dot{S}_{gen}$, which is included in the entropy balance equation. The entropy balance equation for steady state control volume process is defined as

$$\sum_i \dot{m}s + \dot{S}_{gen} + \sum \left(\frac{\dot{Q}_k}{T_k}\right) = \sum_e \dot{m}s \tag{5.3}$$

where s is the specific entropy, and $\dot{Q}_k$ is the heat transfer from the system boundary at temperature T_k and location k.

Exergy Balance (ExBE)

The exergy balance equation includes exergy destruction term that measure the amount of exergy destroyed in a process [98]. By neglecting the kinetic and potential energies, the exergy balance equation can be written as

$$\sum_i \dot{m} \; ex + \sum \left(1 - \frac{T_0}{T}\right) \dot{Q} = \sum_e \dot{m} \; ex + \dot{W} + \dot{E}_{Dest} \tag{5.4}$$

where ψ is the exergy at the inlet or exit of a process.

For the common components in studies systems, the mass, energy, entropy, exergy balance equations are listed in Table 5.1. The streams numbers are not the actual numbers used as state numbers in the analyses, the streams numbers in Table 5.1 are only used for the illustration purposes.

General Assumptions for the Systems

All studied systems are assumed to have the same power output to run the locomotive where the comparison occur in the amount of energy input to measure the efficiencies of the systems. All processes steady state and steady flow processes and the changes in the kinetic and potential energies are neglected. There is no drop in the pressure across all heat exchangers and pipes. The isentropic efficiency of the turbines, pumps and compressors are assumed to be 80%, and the dead state properties are $T_0 = 25\ °C$ and $P_0 = 101.3\ kPa$.

5.2 ICE Locomotives

5.2.1 Internal Combustion Engine Cycle

The majority of the locomotives use internal combustion engine as prime mover. In current study, two-stroke compression ignition engine is used for three systems, where the four stroke spark ignition engine is used for two systems. The ICE cycle assumed to be Dual cycle instead of

Otto or Diesel cycles due to the simplification of these cycles and the fact that the Dual cycle is closer to the actual engine cycle. Both Diesel and Otto cycles are special cases of the Dual cycle [99]. The Dual cycle uses two heat addition processes, the first one at constant volume and the second one at constant pressure. The amount of heat added in each process is adjusted to approximate the actual operation. The ideal Dual cycle consist of five processes: isentropic compression state 1 to 2, constant volume heat addition state 2-3, constant pressure heat addition state 3-4, isentropic expansion state 4-5, and constant pressure heat rejection state 5-1. By assuming constant heat coefficient of k=1.35, the processes in the cycle have the following relations:

For isentropic compression (1 to 2)

$$P_2 = P_1 r^k$$

$$T_2 = T_1 r^{(k-1)}$$

For constant volume heat addition (2-3), where $V_2 = V_3$

$$\dot{Q}_{2-3} = \dot{m}c_v (T_3 - T_2)$$

For constant pressure heat addition (3-4), where $P_3 = P_4$

$$\dot{Q}_{3-4} = \dot{m}c_p (T_4 - T_3)$$

where the total heat addition is defined as

$$\dot{Q}_{in} = \dot{Q}_{2-4} = \dot{Q}_{2-3} + \dot{Q}_{3-4}$$

For isentropic expansion process (4-5)

$$P_5 = P_4 \left(\frac{1}{r}\right)^k$$

$$T_5 = T_4 \left(\frac{1}{r}\right)^{k-1}$$

For heat rejection (5-1), where $V_5 = V_1$

$$\dot{Q}_{5-1} = \dot{m}c_v (T_5 - T_1)$$

5.2.2 Engine Parameters

There are several engine parameters that are useful for internal combustion engine analyses. The total displacement volume of the engine can be given by the engine manufacturer or calculated as follows [98]:

$$V_d = N_c \cdot st \cdot \pi \cdot \left(\frac{b}{2}\right)^2 \tag{5.5}$$

where N_c, st and b are the number of the cylinders in the engine, the engine stroke and cylinder bore, respectively. Another useful parameter is the brake mean effective pressure that is defined as

$$BMEP = \frac{\dot{W}}{V_d\left(\frac{N}{60}\right)} \qquad \text{(2 stroke engine)} \tag{5.6a}$$

$$BMEP = \frac{2\dot{W}}{V_d\left(\frac{N}{60}\right)} \qquad \text{(4 stroke engine)} \tag{5.6b}$$

where $\dot{W}$ is the traction power in kW, V_d is the engine displacement in m^3, and N is the engine speed in rpm. In addition the specific fuel consumption is used to measure the amounts of power that can be produced by unit of fuel and defined as follows:

$$SFC = \frac{\dot{m}_f}{\dot{W}} \tag{5.7}$$

where $\dot{m}_f$ is the mass flow rate of the fuel. To find the amount of air that enter the intake manifold, the volumetric efficiency is used and assumed to be 0.85. For direct injection system where only air enter the cylinder, the volumetric efficiency is calculated as

$$\eta_v = \frac{\dot{m}_{air}}{\rho_a V_d\left(\frac{N}{60}\right)} \qquad \text{(2 stroke engine)} \tag{5.8a}$$

$$\eta_v = \frac{2\dot{m}_{air}}{\rho_a V_d\left(\frac{N}{60}\right)} \qquad \text{(4 stroke engine)} \tag{5.8b}$$

where $\dot{m}_a$ is the mass flow rate of the air and ρ_a is the density of the air. In case of early injection systems where the fuel is introduced with the air into the cylinder, the volumetric efficiency is defined as follows:

$$\eta_v = \frac{\dot{m}_{air} + \dot{m}_{fuel}}{\rho_a V_d \left(\frac{N}{60}\right)} \qquad \text{(2 stroke engine)} \qquad (5.9a)$$

$$\eta_v = \frac{2(\dot{m}_a + \dot{m}_{fuel})}{\rho_a V_d \left(\frac{N}{60}\right)} \qquad \text{(4 stroke engine)} \qquad (5.9b)$$

5.2.3 Chemical Reactions

By performing the mass balance equation for the ICE, the mass flow rate of the exhaust gases mixture is the summation of the air and fuel entering the engine is $\dot{m}_{mix} = \dot{m}_a + \dot{m}_f$. The stoichiometric combustion within the ICE for one mole of fuel that has a chemical formula, $C_\alpha H_\beta$, can be written as

$$C_\alpha H_\beta + X_1 (O_2 + 3.76 N_2) \rightarrow X_2 CO_2 + X_3 H_2O + X_4 N_2 \qquad (5.10)$$
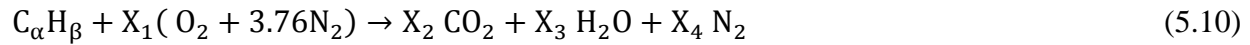
where X_1, X_2, X_3, and X_4 are the number of moles of air, carbon dioxide, water vapor and nitrogen, respectively. Some of the combustion properties for, methane, ULSD, hydrogen and propane are listed in Table 5.2.

Table 5.2: Combustion properties of the fuels.

Propriety	ULSD	Methane	Propane	Hydrogen
Chemical formula	$C_{12}H_{26}$	CH_4	C_3H_8	H_2
Molecular weight	170.3	16.04	44.1	2.02
Flammability limit (% volume in air)	0.6 - 5.5	5 - 15	2.1 - 9.5	4 – 75
Auto ignition temperature (℃)	~ 225	627	502	571
Lower heating value (kJ/kg)	43,200	50,050	46,340	120,000
Higher heating value (kJ/kg)	46,100	55,530	50,330	141,800

Source: [6, 100,101]

To analyze the ICE, the system boundary should be specified. The ICE engine inlets are the coolant fluid, air, fuel, and lubrication oil. While the outputs are the exhaust gases, warm coolant fluid, lubrication oil, and work. The heat transfer rate from the engine to the coolant and lubrication oil is represented as $\dot{Q}_{loss}$. The energy balance equation for the ICE can be written as

$$\sum \dot{m}_i h_i = \sum \dot{m}_e h_e + \dot{W}_{net} + \dot{Q}_{loss} \qquad (5.11)$$

where $\dot{W}_{net}$ is the net work produced by the ICE. Since there is a chemical reaction in the ICE, it is more explicit to write the energy balance equation in molar base as follows:

$$\sum \dot{n}_r \left(\overline{h}_f{}^\circ + \overline{h} + \overline{h}^\circ \right)_r = \sum \dot{n}_p \left(\overline{h}_f{}^\circ + \overline{h} + \overline{h}^\circ \right)_p + \dot{W}_{net} + \dot{Q}_{loss} \qquad (5.12)$$

where $\dot{n}_r$ and $\dot{n}_p$ are the molal flow rates of the reactants r and products p, respectively. While $\overline{h}_f{}^\circ, \overline{h}$, and $\overline{h}^\circ$ are the enthalpy of formation at the reference state, sensible enthalpy at specific state, and sensible enthalpy at reference state, respectively. In the combustion process, the highest temperature can reached by the combustion under the adiabatic flame temperature case. The adiabatic flame temperature is calculated when there is no heat transfer or work crossing the system boundary where in this case equation (5.12) becomes

$$\sum \dot{n}_r \left(\overline{h}_f{}^\circ + \overline{h} + \overline{h}^\circ \right)_r = \sum \dot{n}_p \left(\overline{h}_f{}^\circ + \overline{h} + \overline{h}^\circ \right)_p \qquad (5.13)$$

Since the sensible enthalpy of the products depends on the temperature of the products which is not known, the calculation of the adiabatic flame temperature is not straightforward. The temperature is found by trial and error to find the temperature that met the condition in equation (5.13).

The energy efficiency of the ICE is defined as the ratio of the useful power output to the fuel input to the engine and written as

$$\eta_{ICE} = \frac{\dot{W}_{TP} + \dot{W}_{TC}}{\eta_{comb} \, \dot{Q}_{in}} \qquad (5.14)$$

where η_c is the combustion efficiency assumed to be 1 for complete combustion. While $\dot{Q}_{in}$ is the amount of energy that is supplied by the fuel and defined as

$$\dot{Q}_{in} = \sum \dot{m}_i \, LHV_i \qquad (5.15)$$

where LHV is the lower heating value of fuel i. The ratio of the mass flow rate of specific fuel to the total fuel used in the system called fuel ratio and defined as

$$FR_i = \frac{\dot{m}_i}{\dot{m}_{fuel,total}} \qquad (5.16)$$

where i is the fuel type such as LNG, LPG, or H_2.

In the current investigation, the gases are assumed to have the ideal gas behavior. In this case, the entropy of component j of an ideal gas mixer in kJ/kmol · K is written as

$$\bar{s}_j(T, P_j) = \bar{s}_j°(T, P_0) - R_u \ln \frac{P_j}{P_0} \tag{5.17}$$

where $\bar{s}_j°$ is the absolute entropy in kJ/kmol · K at temperature T and reference pressure P_0. Also, R_u is the gas constant that is 8.31447 kJ/kmol · K and P_j is the partial pressure of the component j which can be found by multiplying the molar fraction y_j of component j by the pressure of the gas mixer.

The exergy of a substance consist of two parts, physical and chemical exergy and can be written as follows:

$$ex = ex_{phys} + ex_{chem} \tag{5.18}$$

The physical exergy is defined as

$$ex_{phys} = (h - h_0) - T_0(s - s_0) \tag{5.19}$$

where h_0 and s_0 are the enthalpy and entropy at the reference conditions T_0 and P_0. However for the exhaust gases, equation (5.18) can be written in more explicit way as follows:

$$ex_{exhaust,phys} = \sum_{j=1}^{L} y_j[(h_j - h_{j0}) - T_0(s_j - s_{j0})] \tag{5.20}$$

where h_j and s_j are the enthalpy and entropy of substance j at specific state. Also, h_{j0} and s_{j0} are the enthalpy and entropy of substance j at the reference conditions.

Since there is a chemical reaction occurs in the ICE, the chemical exergy should be considered in the exergy calculations. According to [97], the chemical exergy of gas mixer is written as

$$ex_{chem} = \sum_{j=1}^{L} y_j \overline{ex}_{ch}^j + R\,T_0 \sum_{j=1}^{L} y_j \ln(y_j) \tag{5.21}$$

where $\overline{ex}_{ch}^j$ is the standard chemical exergy of element j. However, the standard chemical exergy values of the studied fuels which are ULSD, methane, propane, and hydrogen are taken from [102].

The exergy efficiency of the ICE is defined in a similar way to the energy efficiency that is the ratio of the useful work output to the fuel exergy input to the engine and written as follows:

$$\psi_{ICE} = \frac{\dot{W}_{TP} + \dot{W}_{TC}}{\dot{E}x_{in}} \qquad (5.22)$$
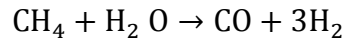
where

$$\dot{E}x_{in} = \sum \dot{m}_{fuel,i} \cdot ex_{fuel,i} \qquad (5.23)$$

Here, $\dot{E}x_{in}$, $\dot{m}_{fuel,i}$ and $ex_{fuel,i}$ are the exergy input of the fuel, mass flow rate of fuel and standard chemical exergy of the fuel i, respectively.

5.3 Solid Oxide Fuel Cell Analyses

The SOFC with internal reforming modeling is presented in this section. There are three streams enter the SOFC stake to generate electricity; steam and methane enter the anode while the air enters the cathode. A portion of the anode exhaust gases is circulated and mixed with methane to enter the anode again, by doing do the internal steam methane reforming can occur. The chemical and electrochemical reactions occur in the SOFC are written as

$$CH_4 + H_2O \rightarrow CO + 3H_2$$

$$CO + H_2O \leftrightarrow CO_2 + H_2$$

$$H_2 + \frac{1}{2}O_2 \rightarrow H_2O$$
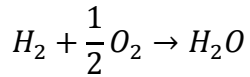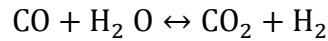
It is assumed that at the outlet of the SOFC stack, the thermodynamic and chemical equilibrium are achieved. The cell analyses and performance is conducted from the literature [104].

The cell voltage is defined as

$$E = E_r - \gamma_{ohm} - \gamma_{act} - \gamma_{conc} \qquad (5.24)$$

where $E, E_r, \gamma_{ohm}, \gamma_{act}$, and γ_{conc} are the cell voltage, revisable voltage, ohmic, activation polarization, and concentration polarization. Using the well-known Nernst equation, the reversible voltage is defined as

$$E_{rev}(T, P_i) = E_{rev}(T, P) + \frac{RT}{2F} \ln\left(\frac{P_{H_2} P_{O_2}^{1/2}}{P_{H_2O}}\right) \qquad (5.25)$$

where $E_r(T, P)$ is the reversible voltage at the standard conditions, R is the universal gas constant, T is the cell operating temperature, n is the number of transferred electrons, F is Faraday's constant (96,487 C/mol), and P_i is the species partial pressure.

The ohmic losses are defined by Bossel [104] as follows:

$$\gamma_{ohm} = \delta_a L_a + \delta_c L_c + \delta_{el} L_{el} + \delta_{int} L_{int} \tag{5.26}$$

where ρ and L are the material electrical resistivity and the thickness for the anode, cathode, electrolyte, and interconnect.

The electrical resistivity is a function of temperature [104] and defined as

$$\delta_{el} = \left(B1_{el} \exp\left(\frac{B2_{el}}{T_{FC,exit}}\right) \right)^{-1} \tag{5.27a}$$

$$\delta_a = \left(\frac{B1_a}{T_{FC,exit}} \exp\left(\frac{B2_a}{T_{FC,exit}}\right) \right)^{-1} \tag{5.27b}$$

$$\delta_c = \left(\frac{B1_c}{T_{FC,exit}} \exp\left(\frac{B2_c}{T_{FC,exit}}\right) \right)^{-1} \tag{5.27d}$$

$$\delta_{int} = \left(\frac{B1_{int}}{T_{FC,exit}} \exp\left(\frac{B2_{int}}{T_{FC,exit}}\right) \right)^{-1} \tag{5.27e}$$

where $B1_{el}$ to $B2_{int}$ are constants as shown in Table 5.3.

Table 5.3: Resistivity constants.

	B1 (S/m)	B2 (K)
Electrolyte	33,400	$-10,300$
Anode	95×10^6	-1150
Cathode	42×10^6	-1200
Interconnect	9.3×10^6	-1100

Source: [104]

The activation polarization is defined as

$$\gamma_{act} = \gamma_{act,a} + \gamma_{act,c} \tag{5.28}$$

where

46

$$\gamma_{act,a} = \frac{RT_{FC,exit}}{F} \left(\sinh^{-1} \left(\frac{j}{2j_{Oa}} \right) \right) \tag{5.29}$$

$$\gamma_{act,c} = \frac{RT_{FC,exit}}{F} \left(\sinh^{-1} \left(\frac{j}{2j_{OC}} \right) \right) \tag{5.30}$$

Here, j_{Oa} and j_{OC} are the exchange current density of the anode and cathode, respectively.

The concentration polarization is defined as

$$\gamma_{cons} = \gamma_{cons,a} + \gamma_{cons,c} \tag{5.31}$$

where

$$\gamma_{cons,a} = \frac{RT_{FC,exit}}{2F} \left(-\ln \left(1 - \left(\frac{j}{j_{as}} \right) \right) + \ln \left(1 + \frac{P_{H_2} \, j}{P_{H_2O} \, j_{as}} \right) \right) \tag{5.32}$$

$$\gamma_{cons,c} = \frac{RT_{FC,exit}}{2F} \left(-\ln \left(1 - \left(\frac{j}{j_{cs}} \right) \right) \right) \tag{5.33}$$

with

$$j_{as} = \frac{2FP_{H_2} D_a^{eff}}{R \, T_{FC,exit} \, L_a} \tag{5.34a}$$

$$j_{ac} = \frac{4FP_{O_2} D_c^{eff}}{R \, T_{FC,exit} \, L_c \left(\frac{P_0 - P_{O_2}}{P_0} \right)} \tag{5.34b}$$

where D_a^{eff} and D_c^{eff} are the effective gaseous diffusivity through the anode and cathode, respectively.

The current of the cell is defined as

$$I = j \, A_{ac} \tag{5.35}$$

where A_{ac} is the active surface area.

The power of the fuel cell is defined as

$$\dot{W}_{FC} = E \, I \tag{5.36}$$

where E is the cell voltage including all losses.

Table 5.4: SOFC parameters

Parameter	Value
Cell operating temperature (°C)	800
Current density (A/cm^2)	0.8
Fuel utilization factor	0.8
Active surface area (cm^2)	100
Exchange current density of anode (cm^2)	0.65
Exchange current density of cathode (cm^2)	0.25
Effective gaseous diffusivity through the anode (cm^2/s)	0.2
Effective gaseous diffusivity through the cathode (cm^2/s)	0.05
Anode thickness of the (cm^2)	0.07
Cathode thickness of the (cm^2)	0.01
Electrolyte thickness of the (cm^2)	0.004
Interconnect thickness of the (cm^2)	0.004

5.3 Energy and Exergy Efficiencies

To compare the designed systems with the baseline diesel system, energy and exergy efficiencies are performed. The energy and exergy efficiencies for the baseline system are defined as

$$\eta_{sys\ 1} = \frac{\dot{W}_{CI} + \dot{W}_{TC} - \dot{W}_{aux}}{\dot{Q}_{in}} \tag{5.37}$$

$$\psi_{sys\ 1} = \frac{\dot{W}_{CI} + \dot{W}_{TC} - \dot{W}_{aux}}{\dot{Ex}_{in}} \tag{5.38}$$

where $\dot{W}_{CI}, \dot{W}_{TC},$ and $\dot{W}_{aux}$ are the work done by the compression ignition engine, the work produced from the turbocharger turbine, and the work consumed in the system by the auxiliaries and other components, respectively. Also, $\dot{Q}_{in}$ and $\dot{Ex}_{in}$ are the energy and exergy input of the diesel fuel which can be calculated using equation (5.15).

Systems 2 and 3 have similar energy and exergy efficiency definitions, which are written as follows:

$$\eta_{sys2,3} = \frac{\dot{W}_{CI} + \dot{W}_{SI} + \dot{W}_{TC} - \dot{W}_{aux}}{\sum \dot{Q}_{in}} \tag{539}$$

$$\psi_{sys2,3} = \frac{\dot{W}_{CI} + \dot{W}_{SI} + \dot{W}_{TC} - \dot{W}_{aux}}{\sum \dot{Ex}_{in}} \tag{5.40}$$

where $\dot{W}_{SI}$ is the work done by the spark ignition engine. However, systems 4 and 5 use two spark ignition engines where the efficiencies are defined as

$$\eta_{sys\,4,5} = \frac{\dot{W}_{SI,m} + \dot{W}_{SI} + \dot{W}_{TC} - \dot{W}_{aux}}{\sum \dot{Q}_{in}} \tag{5.41}$$

$$\psi_{sys\,4,5} = \frac{\dot{W}_{SI,m} + \dot{W}_{SI} + \dot{W}_{TC} - \dot{W}_{aux}}{\sum \dot{Ex}_{in}} \tag{5.42}$$

where $\dot{W}_{SI,m}$ is the power produced by the main spark ignition engine. System 6, uses gas turbine and fuel cells to run the locomotive, where the efficiencies are written as

$$\eta_{sys\,6} = \frac{\dot{W}_{GT} + \dot{W}_{FC} - \dot{W}_{aux}}{\dot{Q}_{in}} \tag{5.43}$$

$$\psi_{sys\,6} = \frac{\dot{W}_{GT} + \dot{W}_{FC} - \dot{W}_{aux}}{\dot{Ex}_{in}} \tag{5.44}$$

where $\dot{W}_{GT}$ and $\dot{W}_{FC}$ are power produced by the gas turbine and fuel cell, respectively. The energy and exergy efficacies for system 7 are defined as

$$\eta_{sys\,7} = \frac{\dot{W}_{GT} + \dot{W}_{ORC} - \dot{W}_{aux}}{\dot{Q}_{in}} \tag{5.45}$$

$$\psi_{sys\,7} = \frac{\dot{W}_{GT} + \dot{W}_{ORC} - \dot{W}_{aux}}{\dot{Ex}_{in}} \tag{5.46}$$

where $\dot{W}_{ORC}$ is the power produced by the Organic Rankine Cycle turbine.

5.4 Environmental Impact and Economic Assessments

The GHG are considered for the fuels environmental impact assessment. Table 5.3 list the emission factors for the ULSD, LNG and LPG in terms of kilogram of gas emitted to the

environment per liter of fuel. The hydrogen is not included in the table because there is no carbon atoms in the hydrogen to produce CO_2. The US Environmental Protection Agency (EPA) emissions standards for freight locomotives are listed in Table 5.6. Tire 3 emissions standard is applicable for locomotives that run in 2012 to 2015, where Tire 4 is for locomotives after 2015.

Table 5.5: Emission factors for ULSD, LNG, and LPG.

Gas Species	ULSD	LNG	LPG	GWP_i
Carbon Dioxide CO_2 (g/L)	2.663	1.178	1.500	1
Methane CH_4 (g/L)	0.00015	0.000037	0.00013	21
Nitrous oxide N_2O (g/L)	0.00110	0.000035	0.000058	310

GWP_i is the global warming potential.
Source:[2,105,106]

In the current study, the costs for the fuels are presented in dollar per liter of fuel. It is assumed that the cost of one liter of diesel is 0.9959 $, where the natural gas has 0.3652 $/L. However, the price of hydrogen is 1.62 $/L, it is expensive as compared to other fuels used here. In addition, propane has a relatively high price with 0.81365$/L. These costs have been used to analyse the systems fuel costs [107].

Table 5.6 EPA locomotives exhaust emissions standards (g/kWh)

Standards	Year	NO_x	CO	PM	HC
Tire 3	2012 – 2015	7.38	2.01	0.134	0.402
Tire 4	2015 +	1.74	2.01	0.0402	0.188

Source: [2]

5.5 Optimization

In the current study, the Genetic Algorithm optimization (GA) method is used as the optimization method. This method is inspired from the biological evolution by natural selection. The independent variables of the problem are bounded to create the initial sample points, also known as initial population, and these points are coded into a binary system. The fitness value of each individual is determined by substituting that solution into the objective function. A selection criterion is applied to choose two solutions, based on their fitness value where higher fitness value leads to higher probability of selection. A crossover operation is then applied to form a

new offspring based on the selected solutions or parents, where the offspring chromosome takes a portion of each parent chromosome in the encoding form. A random variation and change are introduced by the mutation rate where one of the genes can evolve to create different solution that helps the algorithm to explore for more solutions. This process is repeated until the number of the new solutions is equal to the size of the initial population. The new population replaces the initial population and the process is repeated until the stopping criterion is satisfied [108].

In this study, the objective function is defined as

$$Ob = w_{eff}\ \psi + w_{emissions}\ Em + \ w_{cost}\ Cf_{Duty} \tag{5.47}$$

where w_{eff}, $w_{emissions}$, and w_{cost} are the weighting factors for the exergy efficiency, emissions and fuel cost in one duty cycle. In addition Em is the CO_2, NOx, CO, HC, PM emissions in one duty cycle. Cf is the fuel cost in one duty cycle. The parameters and constrains in this optimization study are defined according to [109,110] as

$$0.75 \leq \eta_{isentropic} \leq 0.85 \tag{5.48a}$$

where $\eta_{isentropic}$ is the isentropic efficiency of the pumps and turbines.

$$1.3 \leq k \leq 1.4 \tag{5.48b}$$

$$150\ kPa \leq P_{in,engin} \leq 300\ kPa \tag{5.48c}$$

where k and $P_{in,engin}$ are the heat coefficient and inlet pressure to the main engine.

$$20°C < T_{ref} < 30°C \tag{5.48d}$$

$$0.75 \leq \eta_v \leq 0.85 \tag{5.48e}$$

where T_{ref} and η_v are the reference environment temperature and the volumetric efficiency of the internal combustion engine.

$$0.6\ \frac{A}{cm^2} \leq j \leq 0.8\ \frac{A}{cm^2} \tag{5.48f}$$

$$750°C < T_{SOFC} < 850°C \tag{5.48g}$$

where j and T_{SOFC} are the current density and the SOFC operating temperature.

$$10 \leq r \leq 20 \qquad (5.48h)$$

where r is the compression ratio for the gas turbine cycle.

Chapter 6 : Results and Discussion

The results of the studies conducted on these newly developed systems are discussed in this chapter. The main findings and parametric studies are discussed in addition to specifying the maximum exergy destruction location for the systems. The environmental impact results include CO_2, NOx, CO, HC, and PM for all systems are then explained. The systems are compared and optimized in terms of their performances, fuel cost and environmental impact in one duty cycle.

6.1 System 1 (Diesel Only) Results

The main results of system 1 are presented in this section where the parametric study was not performed for this system because it is an already exist system, and the results are used for the reference. The exergy flow of the system is shown in Figure 1, where the right circle is the exergy destruction part. The baseline locomotive generates 3207 kW traction power and consumes 0.2065 kg/s of diesel is 8919 kW of power. For this system, the GHG are presented in CO_2 equivalent where it generates 0.7391 kg/s of $CO_{2,eq}$. The energy and exergy efficiencies of system 1 are 35.9% and 32%, respectively. However, the exergy destruction of the system is 3573 kW.
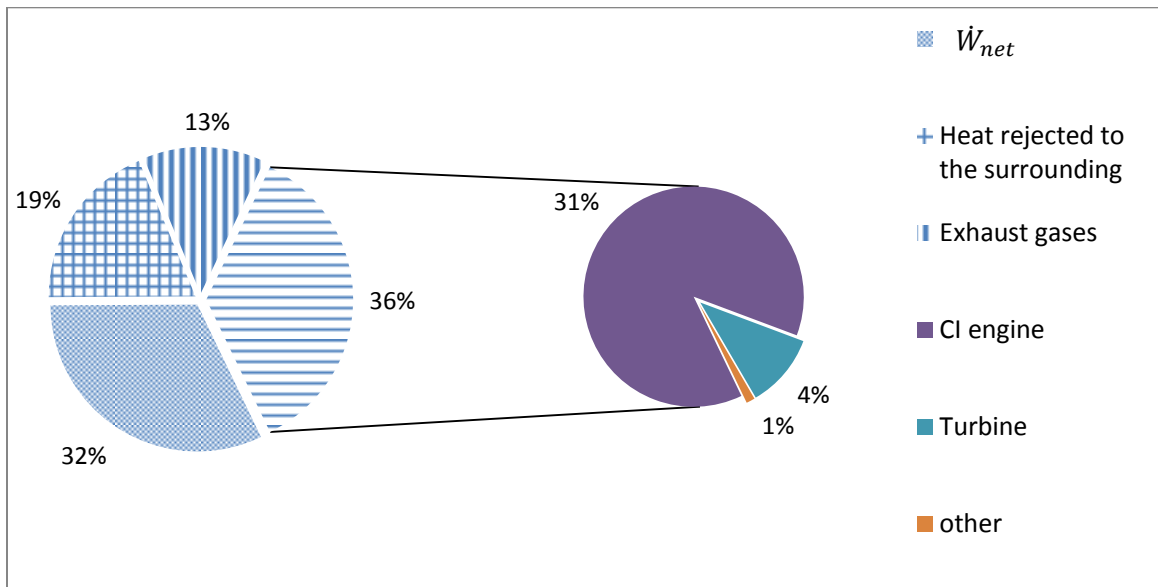

Figure 6.1: Exergy content for System 1.

6.2 System 2 (LNG and Diesel) Results

System 2 is a dual fuel system that uses diesel and LNG. Figure 6.2 shows the system performance corresponding to mass fraction of LNG in fuel blend. By varying the LNG mass fraction from 5% to 75% both the energy and exergy efficiencies increase from 37.8 to 40% and 33.9% to 37%, respectively. That is to the fact the LNG increase leads to more boil-off gas in the tender because of the large contact area with the tender wall. Since the boil-off gas is supplied to the fumigated engine, the increase of the boil-off gas results in increasing the work produced by the fumigated engine. It is applicable to a certain limit where the small engine does not operate at its maximum output, where, in that case, the gas is vented from the tank.
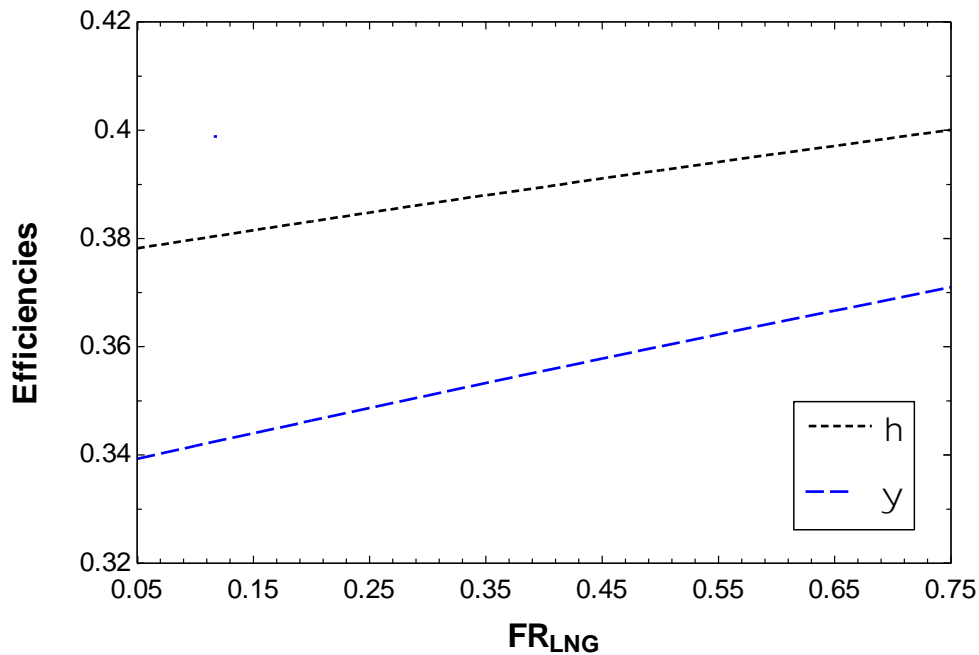
Figure 6.2: Effects of the LNG percentage on the energy and exergy efficiencies of System 2.

Figure 6.3 shows the change of the adiabatic flame temperature and mass base air-fuel ratio for the CI engine, as it is the prime mover, with respect to the LNG percentage. As the LNG percentage change from 5% to 75%, the adiabatic flame temperature decreases from 2146 to 2085. This drop is because the adiabatic flame temperature of the natural gas is lower than diesel. A low adiabatic flame temperature is desired since the temperature of the combustion related directly to the formation of the emissions and the material selection for the engine. In addition, the variation of the LNG% increases the mass base air fuel ratio in the combustion from 15 to

16.6. This increase results from the fact that the chemical reaction of one mole of methane needs lesser air to combust than one mole of diesel.
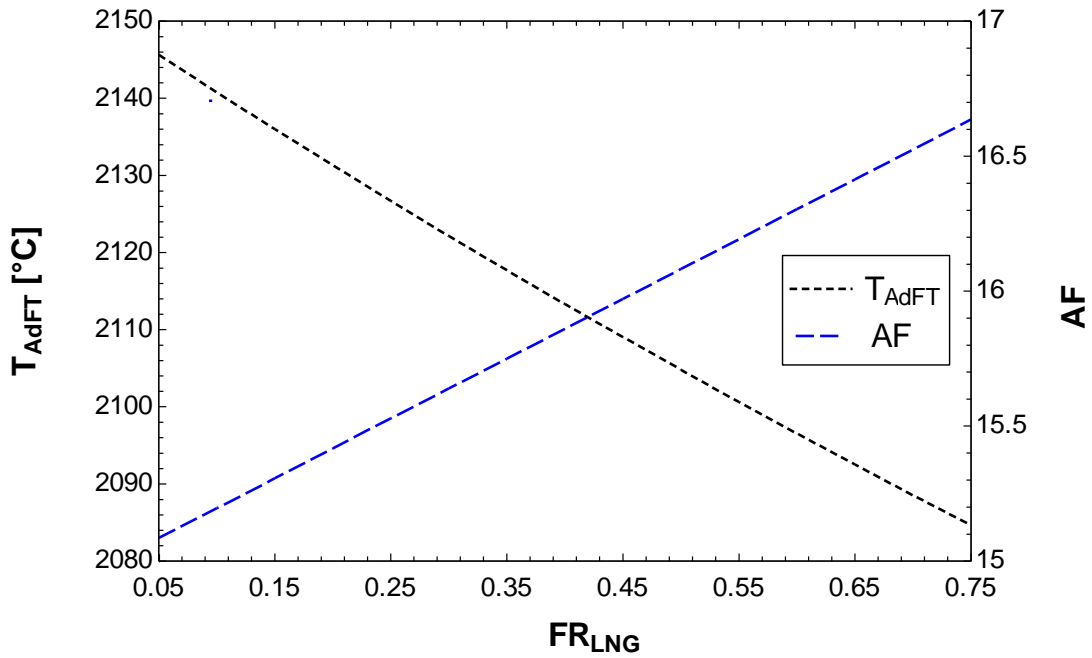

Figure 6.3: Effects of the LNG percentage on the adiabatic flame temperature and the air-fuel ratio for System 2 prime mover.
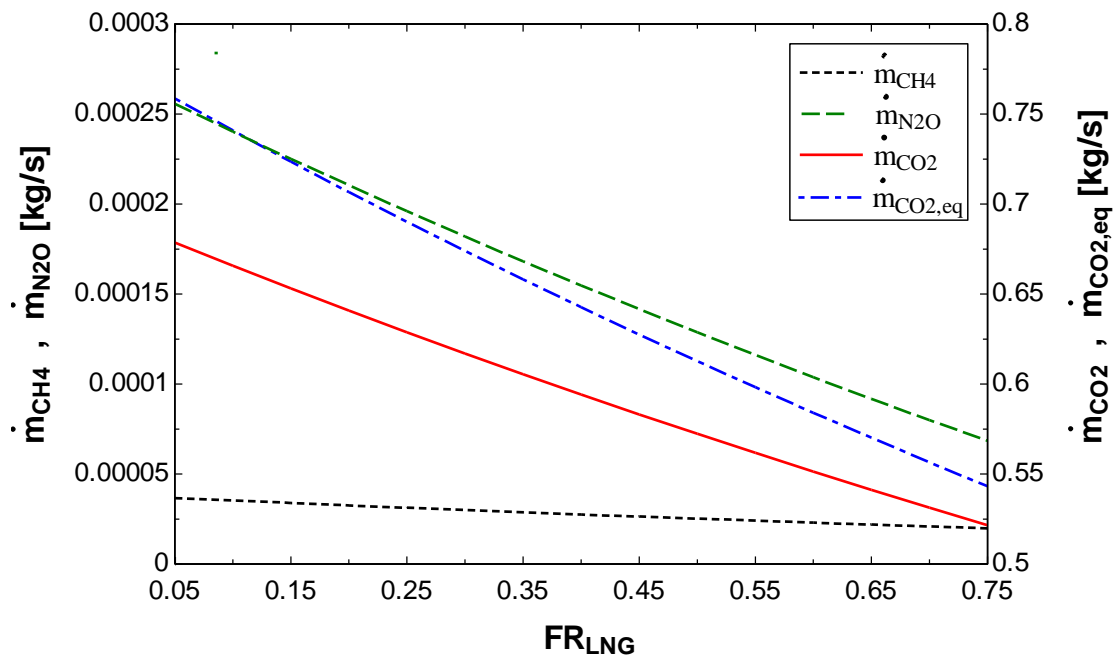

Figure 6.4: Effects of the LNG percentage on System 2 GHG emissions.

In terms of the greenhouse gas emissions; Figure 6.4 illustrates the change of the mass flow rates of CH_4, N_2O, CO_2 and the CO_2 equivalent of the system. All GHG emissions reduce with increase in the LNG percentage due to the low carbon content of methane compared to diesel where the mass flow rate of the CO_2 equivalent drop from 0.7587 to 0.5432 kg/s or 2731.3 to 1955.52 kg/h.

Figure 6.5 presents the effect of varying the after cooler temperature with respect to the adiabatic flame temperature and heat lost by the CI engine. By varying the after cooler temperature from 30 to 75°C, the adiabatic flame temperature and heat lost by the engine increase from 2103 to 2134 °C and 3801 to 3899 kW. It is due to the higher energy content of air at a higher temperature, but the lower density, which means less oxygen is introduced to the engine. Table 6.1 shows the performance and the main results for system 2.
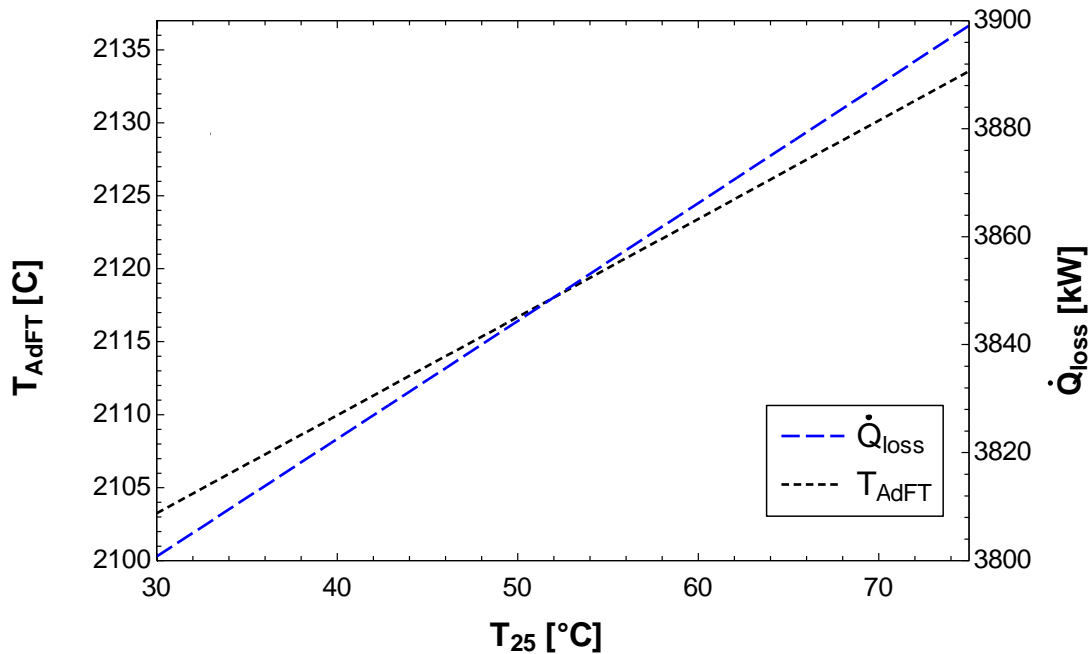

Figure 6.5: Effects of the after cooler temperature on adiabatic flame temperature and heat loss from System 2 prime mover.

Figure 6.6 shows the exergy flow of system 2, where 35 % of the fuel exergy is converted into useful power, where the right pie shows the exergy destruction part. However, the exergy of the heat rejected to the environment from the CI, and SI engines amount to 17%. In addition, the exhaust gases carry 11% of the fuel exergy that also rejected to the environment. Exergy destruction is the largest part of the exergy flow where 37% of the fuel exergy is destructed in the system process and devices. The CI engine is the main contributor in the exergy destruction,

which accounts for 31% of the total fuel exergy that is due to the fact that the IC is the prime mover, which produces most of the work needed to run the locomotive, in addition to the combustion process, which occurs within the engine.
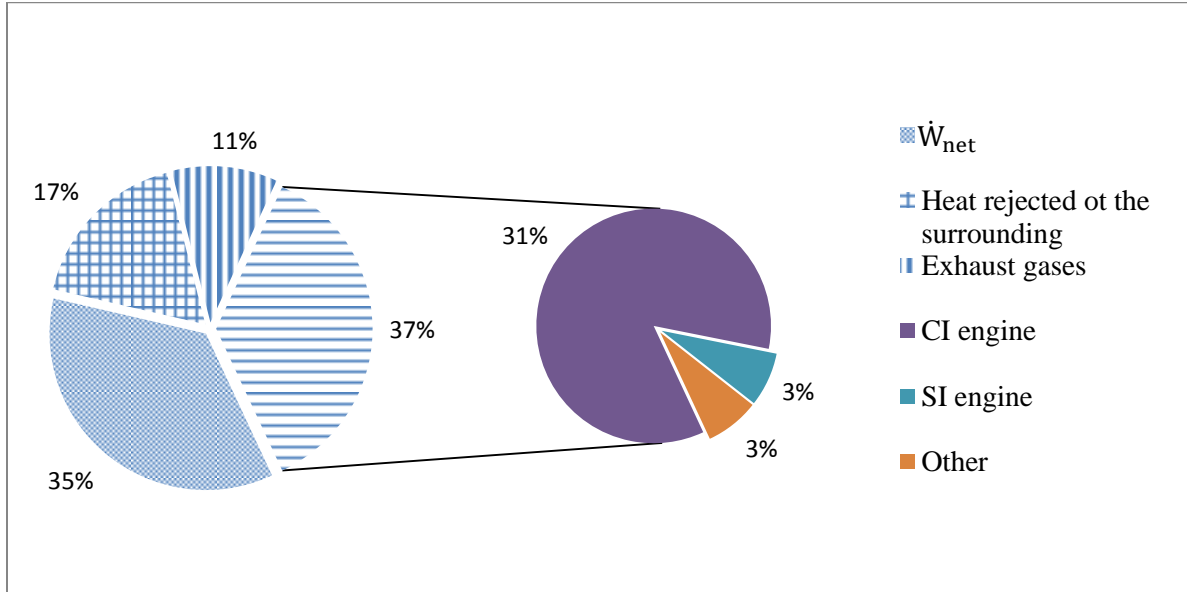

Figure 6.6: Exergy content for System 2.

Table 6.1: System 2 (Diesel – LNG) main inputs and outputs.

Parameter	Value
Diesel mass flow rate (kg/s)	0.1128
Natural gas mass flow rate (kg/s)	0.08836
Mass base AF ratio for CI engine	15.86
Adiabatic flame temperature of the CI engine (°C)	2113
Work input for the CI engine air compressor (kW)	243.1
Equivalent carbon monoxide emissions, $CO_{2,eq}$ (kg/s)	0.6427
Energy efficiency (%)	37.13
Exergy efficiency (%)	33.83

6.3 System 3 (LNG and Diesel) Results

This system uses HPDI as an injection method to increase the system efficiency in addition to EGR to reduce the emissions from the locomotive prime mover. This system does not run in diesel mode only where the LNG is the primary energy supply to the system. That reveals the importance of studying the effects of the LNG percentage in fuel on several important

parameters. Figure 6.7 shows the effect of increasing the LNG percentage on the system performance where both the energy and exergy efficiencies of the system indicate slight improvement. These improvements in the results because LNG is pressurized by the high pressure pump that consumed a considerable amount of work but in return the efficiency of the engine increases.
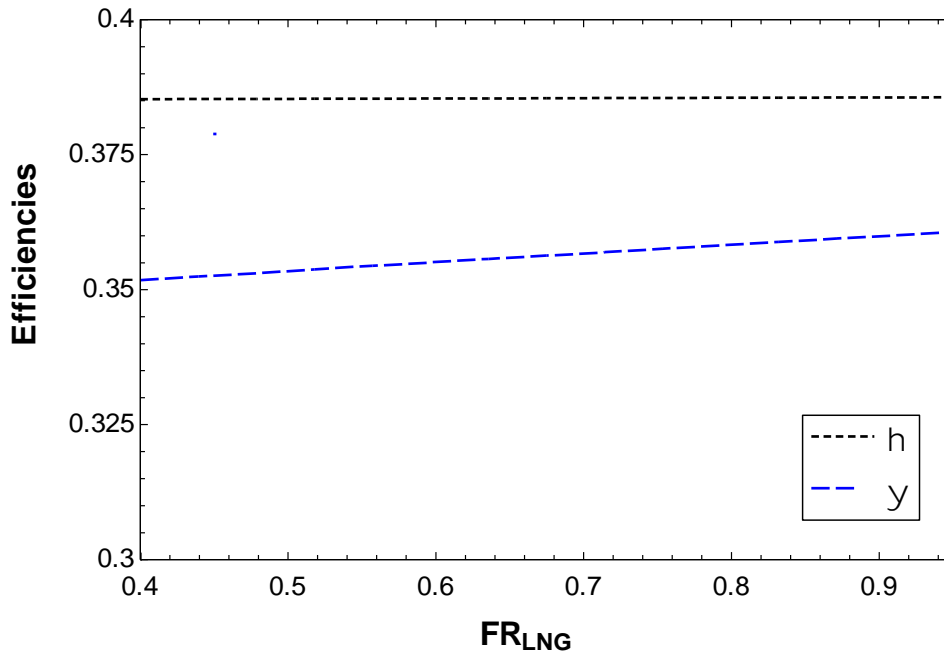

Figure 6.7: Effects of the LNG percentage on the energy and exergy efficiencies of System 3.

Figure 6.8 shows the variation of the LNG percentage with respect to the adiabatic flame temperature and air-fuel ratio in the mass base for system3 prime mover. By increasing the LNG percentage from 40% to 95%, the adiabatic flame temperature decreases from 1857℃ to 1823℃ because the natural gas has a low adiabatic flame temperature as compared to diesel. However, the air-fuel ratio increases from 15.86 to 17.08 with increasing the LNG percentage.

Figure 6.9 illustrate the effect of the LNG percentage from the total fuel uses to run the locomotive on the greenhouse gas emissions for system 3.As the LNG percentage increases, all greenhouse gas emissions mass flow rate, $\dot{m}_{CH_4}, \dot{m}_{N_2O}$, and $\dot{m}_{CO_2}$ decrease due to the fact LNG has lower emission factor than diesel as shown in Table 5.2. The mass flow rate of the equivalent CO_2 emissions for this system vary from 0.5657 kg/s to 0.4521 kg/s as the LNG percentage increases from 45% to 95%.
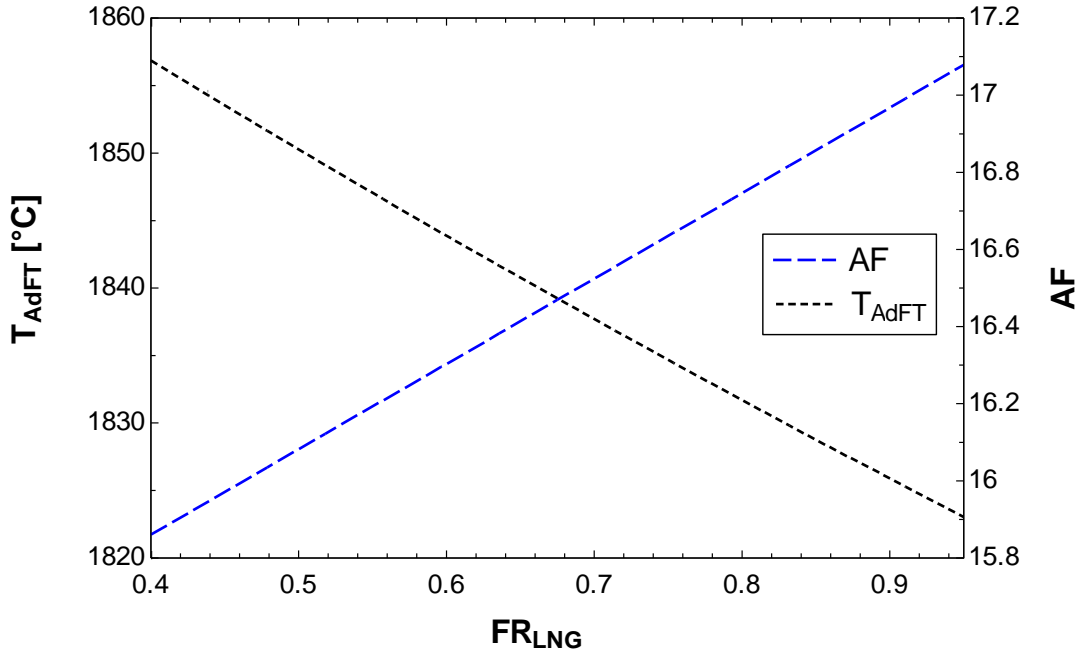
Figure 6.8: Effects of the LNG percentage on the adiabatic flame temperature and the air-fuel ratio for System 3 prime mover.
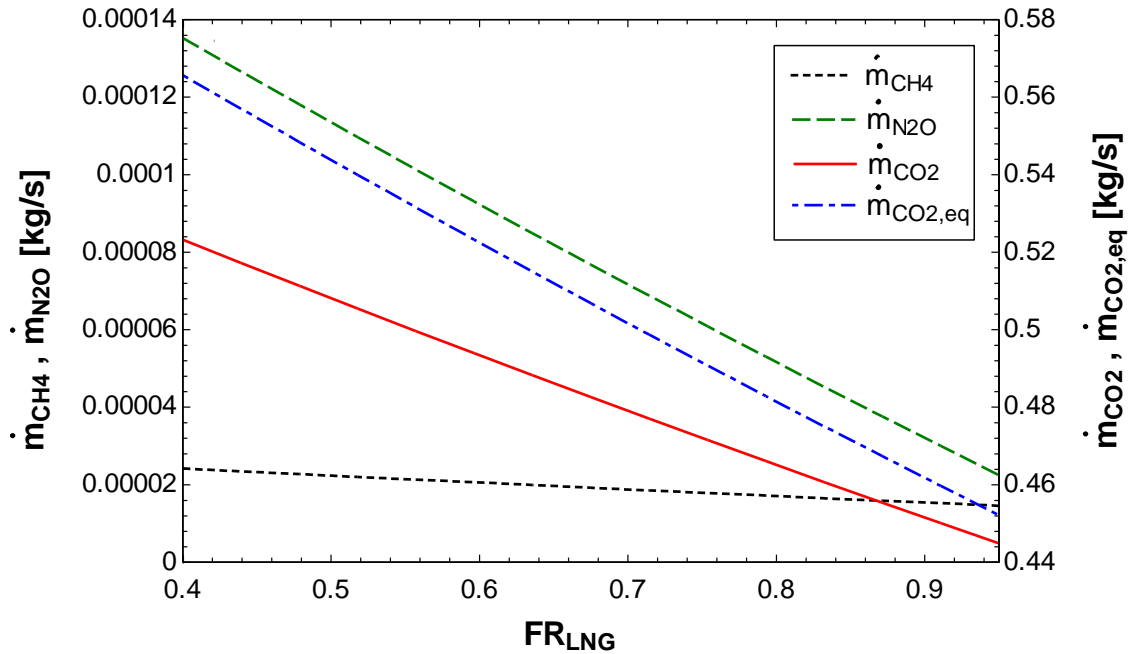

Figure 6.9: Effects of the LNG percentage on system 3 GHG emissions.

The effect of the amount exhaust gas recirculation in the adiabatic flame temperature and the equivalent carbon monoxide emission from system 3 is shown in Figure 6.10. As the ratio of the exhaust gas recirculation increases from 0 to 0.3, the adiabatic flame temperature decreases from

2073°C to 1564°C. That serve the purpose of this device that is lowering the combustion temperature to limit the formation of the emissions mainly NO_x emission. In addition, the mass flow rates of equivalent CO_2 emissions from system 3 decrease 0.5276 kg/s to 0.3733 kg/s. However, high EGR is not recommended for higher load operation conditions, because the recirculated gases affect the engine performance. It is because EGR reduces the amount of oxygen that can be introduced to the engine to perform the combustion. Table 6.2 shows the main parameters and results of system 3 analysis.
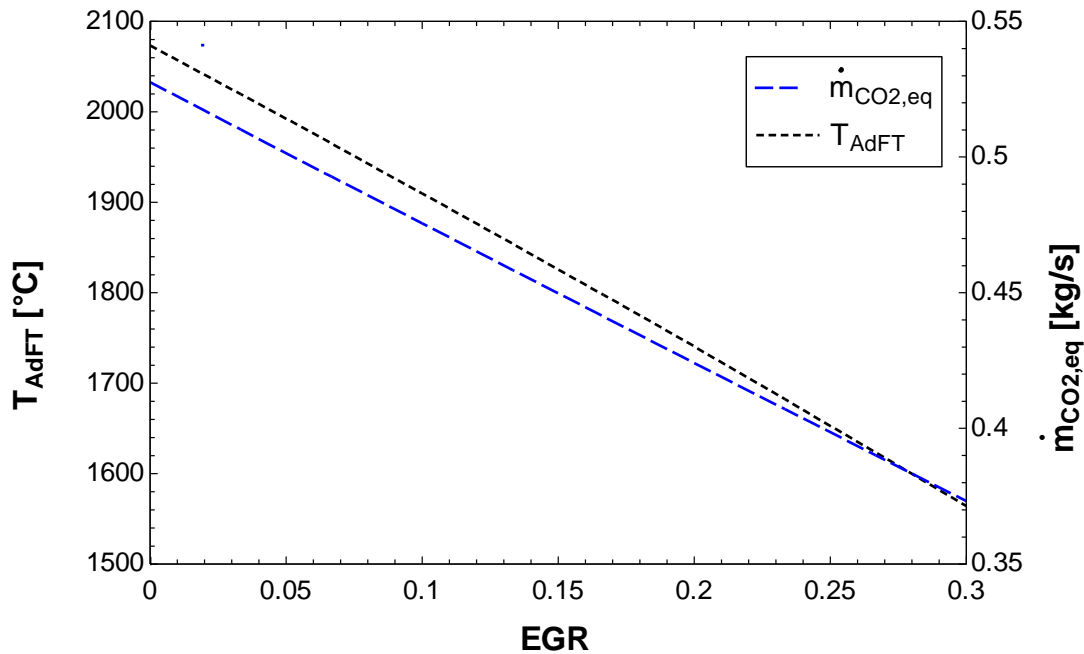

Figure 6.10: Effects of the EGR ratio in the adiabatic flame temperature of the CI engine and mass flow rate $CO_{2,eq}$ of System 3.

The exergy content for system 3 is shown in Figure 6.11, where the right circle is the exergy destruction part. It indicates that, 35% of the fuel exergy has been utilized and converted in to work. A total of 34% of the fuel exergy is lost due to exhaust gases and heat rejected to the environment from the internal combustion engines. In addition, 26% of the total fuel exergy is destroyed in the CI engine and 3% in the SI engine. The other system components have a total of exergy destruction about 2%, respectively.
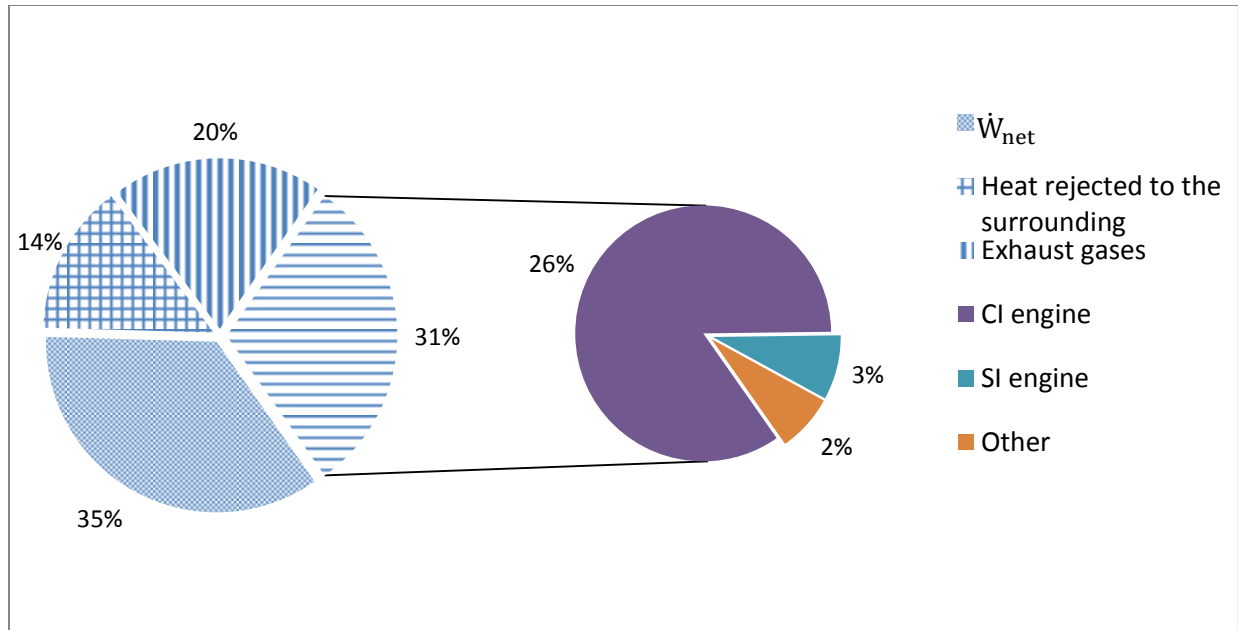
Figure 6.11: Exergy content for System 3.

Table 6.2: System 3 (Diesel – LNG) main inputs and outputs.

Parameter	Value
Diesel mass flow rate (kg/s)	0.01535
Natural gas mass flow rate (kg/s)	0.16585
Mass base AF ratio for CI engine	16.97
EGR ratio	0.15
Adiabatic flame temperature of the CI engine (℃)	1828
Work input for the CI engine air compressor (kW)	252.1
LNG high pressure pump work input (kW)	242.9
Equivalent carbon monoxide emissions, $CO_{2,eq}$ (kg/s)	0.4618
Energy efficiency (%)	38.56
Exergy efficiency (%)	35.9

6.4 System 4 (LNG and LPG) Results

System 4 uses the combination of LNG and LPG to run a spark ignition engine locomotive with a reformer that convert a small portion of the natural gas into hydrogen and introduce it into the combustion engine. The effect of varying the amount of LPG used as fuel in the system on the system performance is shown in Figure 6.12. The energy and exergy efficiencies are decreased from 33.8% to 32.1% and 33.2% to 31.8%, respectively. This system uses LPG and LNG to

remove some of the water coolant heat, which means more heat, is removed by the LNG due to the very temperature of LNG compared to LPG. By increasing the percentage of LPG as fuel, results in decreasing the LNG percentage and reduce the cooling effect in the coolant water that leads to more power input to remove such a heat. In addition, the energy content of LPG is lower than LNG, which means increasing LPG results in less efficient system.
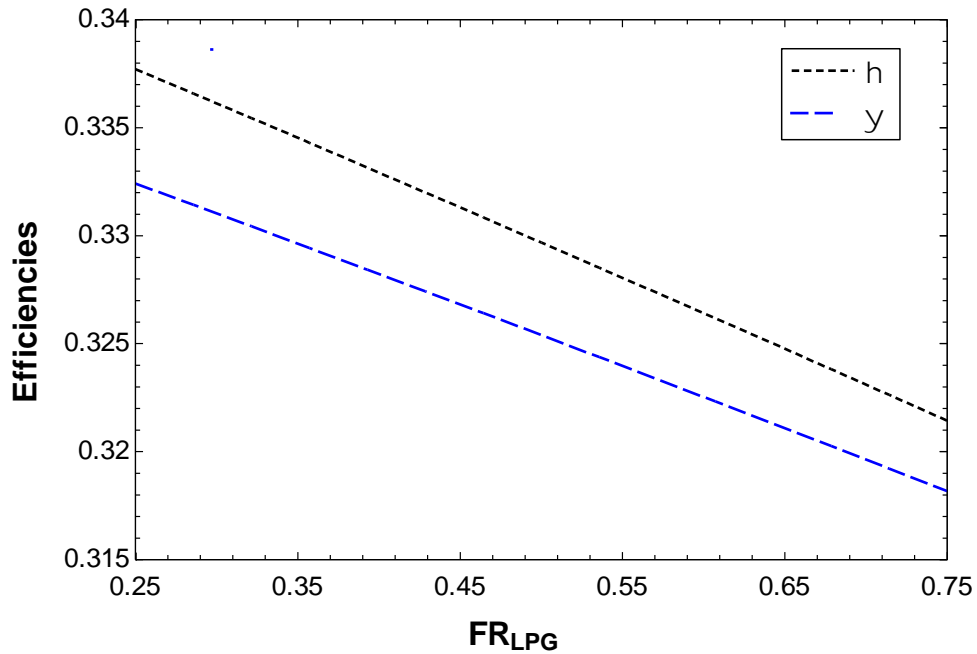

Figure 6.12: Effects of the LPG percentage on the energy and exergy efficiencies of System 4.

Figure 6.13 shows the effect of varying LPG percentage with respect to the adiabatic flame temperature and heat loss from system 4 prime movers. By varying the percentage of LPG from 25% to 75% of the total fuel used in the system, the adiabatic flame temperature of the prime mover increases from 2089°C to 2121°C. This increase results from the higher adiabatic flame temperature of LPG. However, the air-fuel ratio of decrease from 17.14 to 16.36 with increasing the LPG percentage since less air is needed to perform the combustion of propane as compared to methane.

Figure 6.14 illustrates the effect of varying the LPG percent in the GHG emissions mass flow rate. By increasing the propane percentage in the fuel from 25% to 75%, all GHG are increasing. This could occur because the propane has more carbon content than methane that results in more carbon monoxide emissions. As a result, the equivalent carbon monoxide flow rate of system 4

increases from 0.54 kg/s to 0.63 kg/s. The important parameters and results for system 4 are shown in Table 6.3.
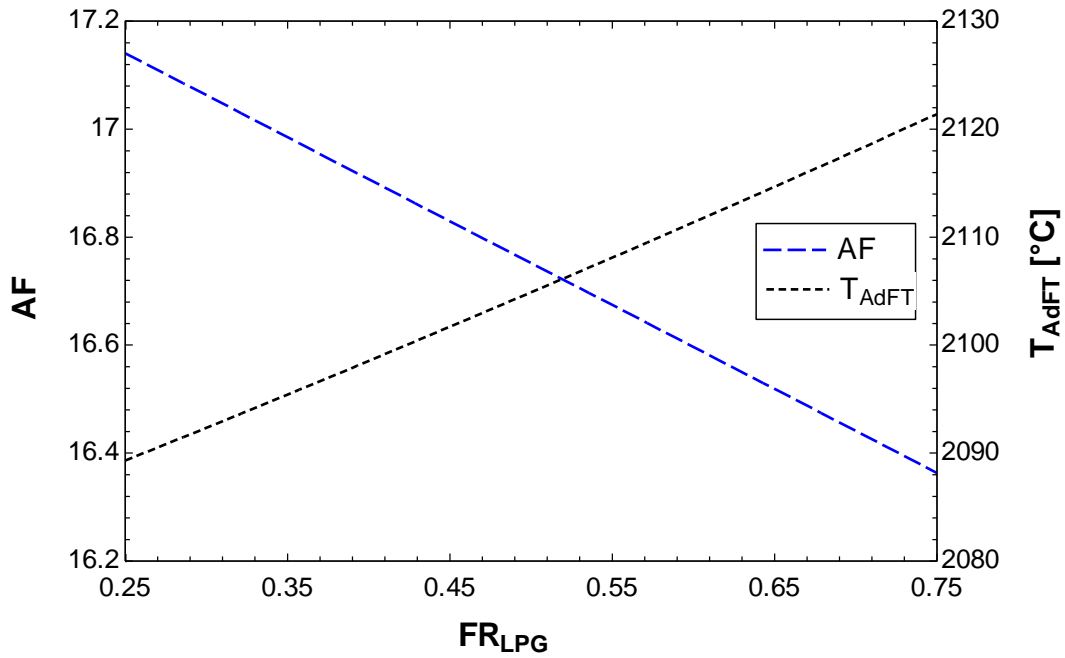

Figure 6.13: Effects of the LPG percentage on the adiabatic flame temperature and air-fuel ratio
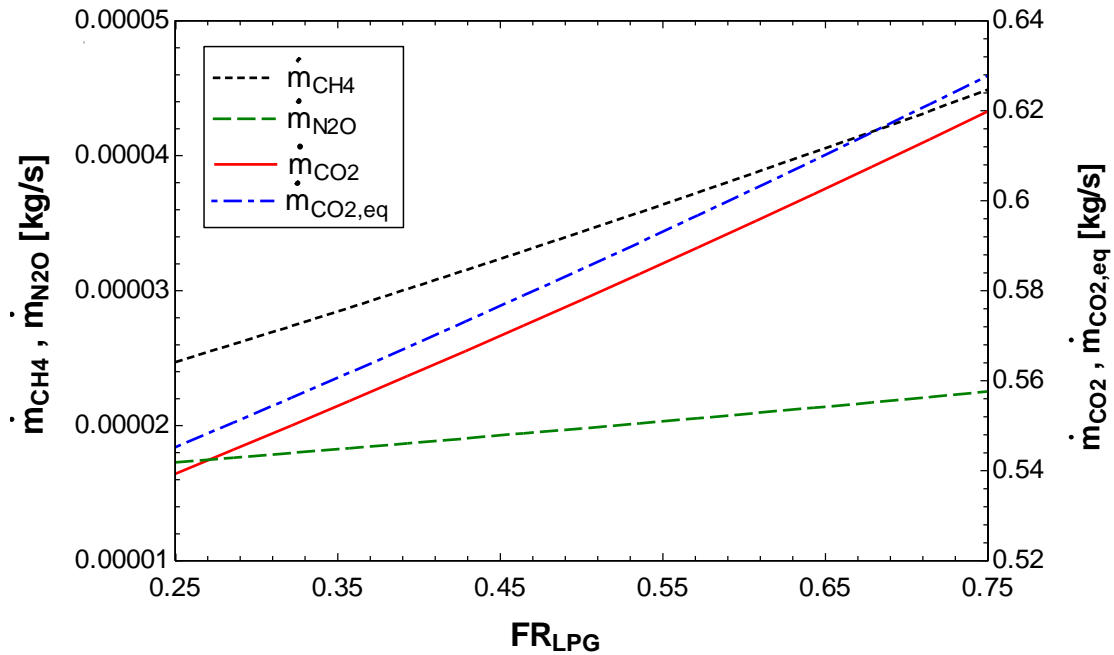

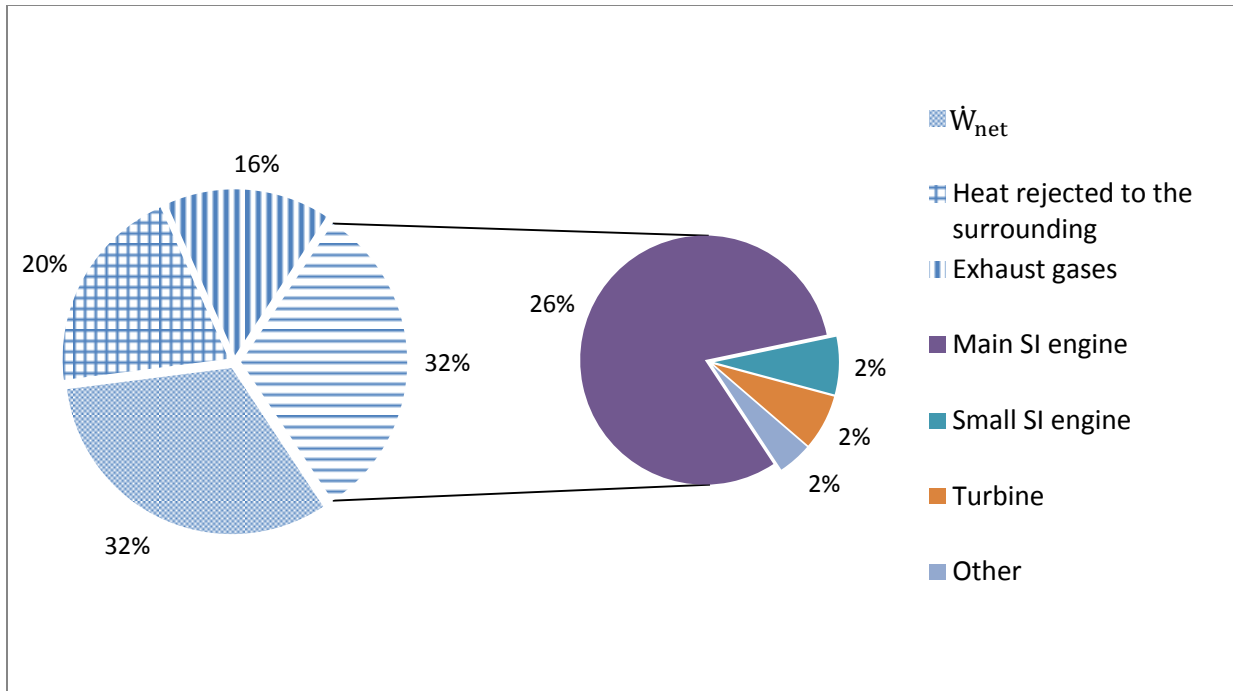Figure 6.14: Effects of the LPG percentage on System 4 GHG emissions.

Figure 6.15: Exergy content for System 4.

Table 6.3: System 4 (LNG – LPG) main inputs and outputs.

Parameter	Value
Propane flow rate (kg/s)	0.1533
Natural gas mass flow rate (kg/s)	0.09217
Mass base AF ratio for system 4 prime mover	16.6
Adiabatic flame temperature of the prime mover engine (℃)	2111
Work input for the prime mover air compressor (kW)	269.3
Equivalent carbon monoxide emissions, $CO_{2,eq}$ (kg/s)	0.6016
Energy efficiency (%)	32.64
Exergy efficiency (%)	32.25

Figure 16.15 shows the exergy content of system 4, where the right pie gives the exergy destruction part. The useful exergy of the system accounts for 32% whereas the heat rejected by both the main and small SI engine is 20% of the exergy input to the system. The exergy destruction in the system is 32% where 26% of this 32% is the exergy destruction in the main spark ignition engine. However, the small SI engine contributes to 2% exergy destruction from the total exergy input to the system. In addition, the turbine of the turbocharger and the system other components have a total of 4% of the exergy destroyed.

6.5 System 5 (LNG and H_2) Results

System 5 uses LNG and compressed hydrogen to run the locomotive. The amount of hydrogen used in this system important parameter to analyze this system. The variation of the hydrogen used to fuel the locomotive affect the system performance, as shown Figure 6.16. With the increase in the hydrogen percentage in fuel, both energy and exergy efficiencies decrease from 32.25% to 30.8% and 31.3% to 30.5%. That could be due the increase in the energy input but no increase in the power output that result in a decrease in the efficiencies.
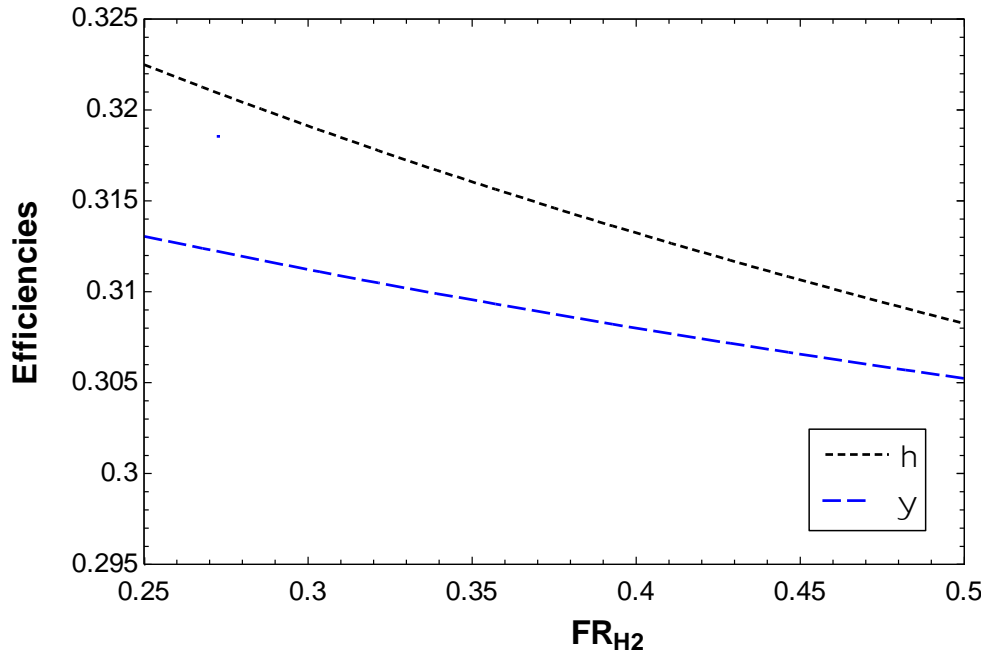

Figure 6.16: Effects of the H_2 percentage on the energy and exergy efficiencies of System 5.

The effect of varying the compressed hydrogen from 25% to 50% on the air fuel ratio and adiabatic flame temperature of system 5 prime mover is shown in Figure 6.17. The air fuel ratio increases from 21.78 to 26.03 by increasing the hydrogen percentage that enters the engine. This is because hydrogen has higher air fuel ratio compare to methane that leads to an overall increase in the air-fuel ratio of the combustion. In addition, the adiabatic flame temperature increases because hydrogen adiabatic flame temperature is high.

Figure 6.18 shows the effects of varying the hydrogen percentage on the mass flow rate of CO_2 and $CO_{2,eq}$ emissions. As the hydrogen percentage increases from 25% to 50%, both CO_2 and $CO_{2,eq}$ deceases due to the fact that the hydrogen does not contain any carbon atoms

which mean all of the CO_2 emissions are due to methane combustion. The product of the hydrogen combustion is water vapor which has no effect on the environment. However other emissions, like NOx, are possible due to high combustion temperature of the hydrogen. The main results of system 5 are presented in Table 6.4.
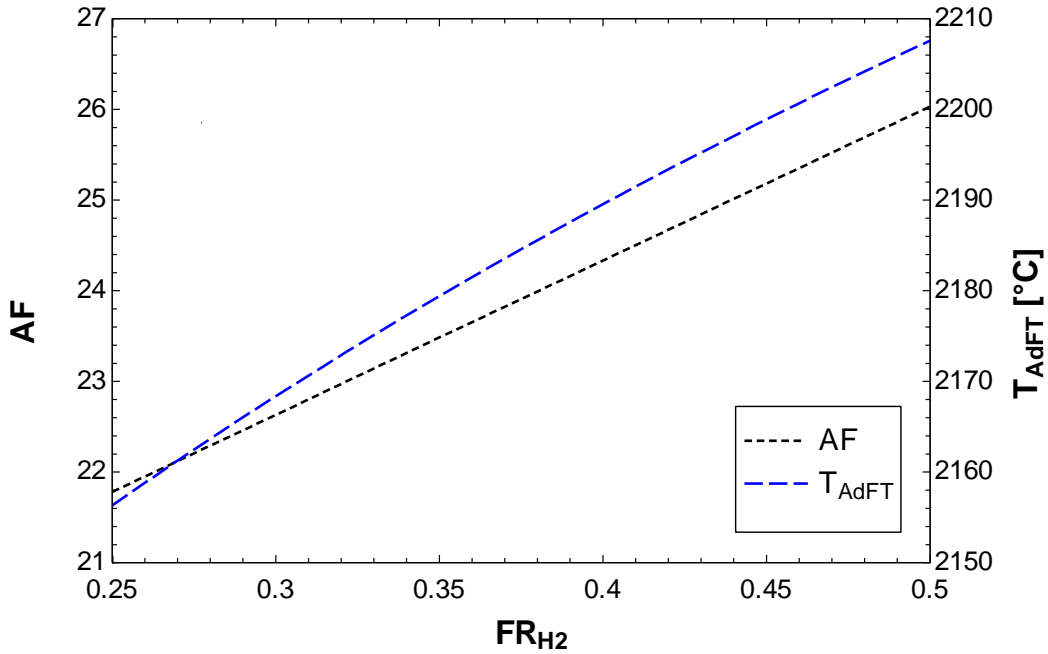

Figure 6.17: Effects of the H_2 percentage on the adiabatic flame temperature and air-fuel ratio.
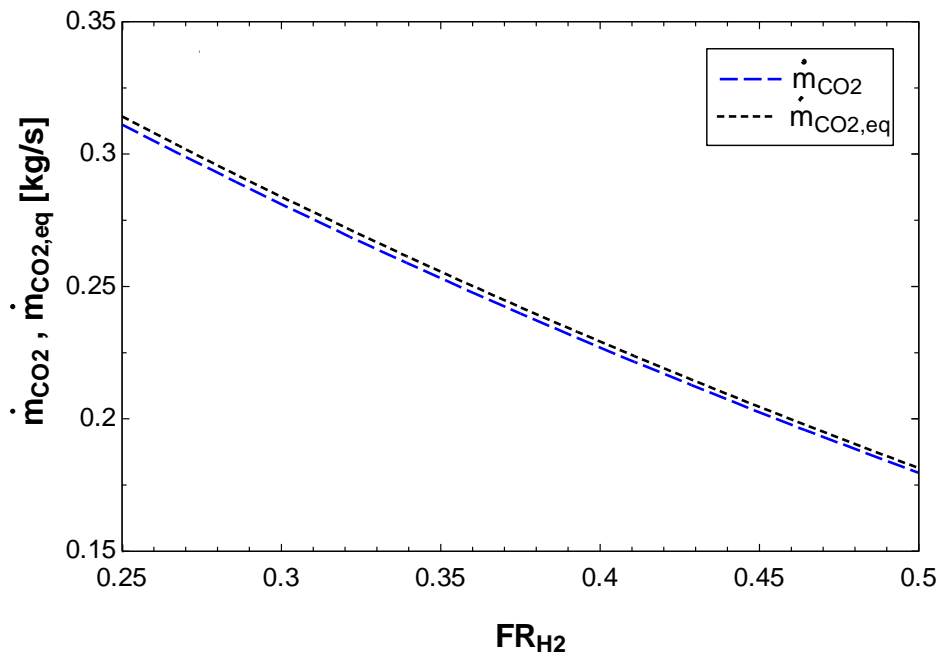

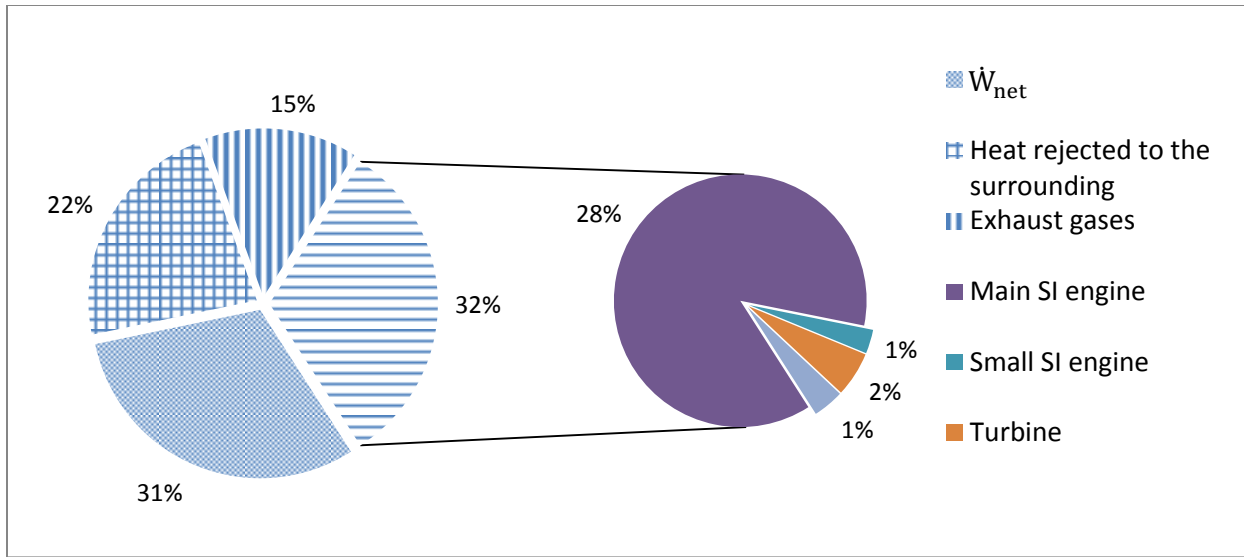Figure 6.18: Effects of the H_2 percentage on System 5 CO_2 emissions.

Figure 6.19: Exergy content for System 5.

Table 6.4: System 5 (LNG $-H_2$) main inputs and outputs.

Parameter	Value
Hydrogen flow rate (kg/s)	0.05254
Natural gas mass flow rate (kg/s)	0.08739
Mass base AF ratio for system 5 prime mover	24.3
Adiabatic flame temperature of the prime mover engine (℃)	2190
Work input for the prime mover air compressor (kW)	260.6
Equivalent carbon monoxide emissions, $CO_{2,eq}$ (kg/s)	0.2292
Energy efficiency (%)	31.32
Exergy efficiency (%)	30.8

Figure 6.19 shows the exergy input flow through system 4, where the right pie exhibits the exergy destruction part. A considerable amount of exergy is rejected into the environment as heat exergy that is about 22% of the used fuel exergy. On the other hand, 31% of the exergy input is used to produce the required amount work needed to run the locomotive. The exhaust gases from both SI engines accounts for 15% of the total exergy input to the system. The exergy destruction has the highest exergy flow which is 32% of the exergy input where the 28% of the system exergy input is destroyed in the main SI engine, while only 1% is destroyed in the small SI engine. The turbine has about 2% exergy destroyed in terms of the total exergy supplied to the system.

6.6 System 6 (LNG only) Results

This system uses pure LNG to run the locomotive, where the solid oxide fuel cell is used as prime mover. Since the SOFC is the main component in the system, the effect of varying the main parameters is studied. Figure 6.20 shows the effect of varying the current density in the cell potential at different operating pressures. By increasing the current density, all cell potentials at different pressures decrease due to the fact that the ohmic, activation polarization and concentration polarization losses increase. The increase in the pressure results in higher cell potential and power. However, high operational pressure in not always recommended, due to mechanical work required to pressurize the gases.
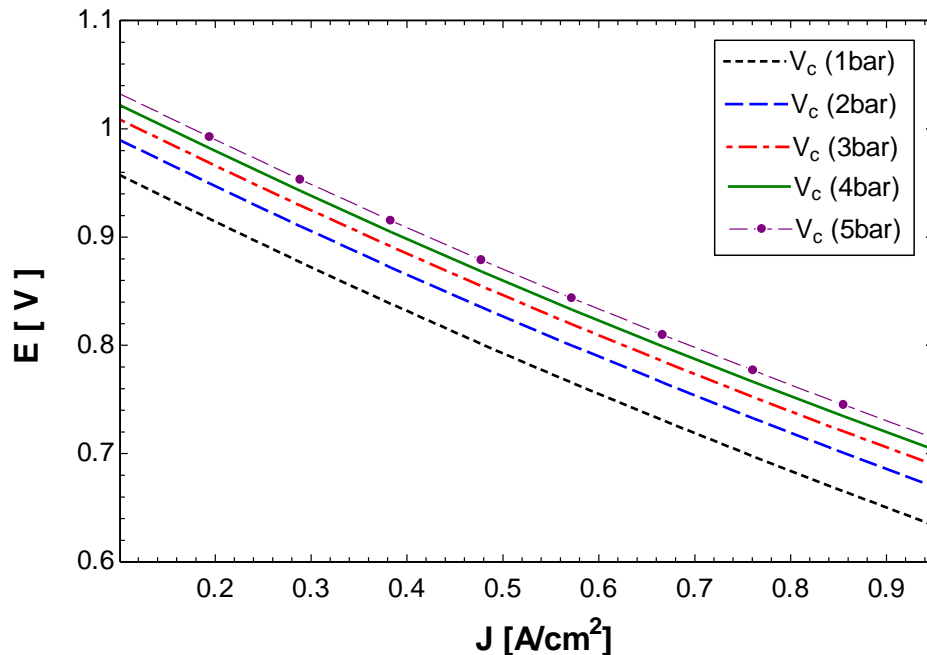

Figure 6.20: Effects of the current density in the cell potential at different operational pressure.

The effect of varying the SOFC operational pressure in the fuel cell and system performance is shown in Figure 16.21. By varying the operational pressure from 100 kPa to 500 kPa, the energy and exergy efficiencies of the fuel cell increase from 41.6% to 46.4% and 38.9 to 43.5, respectively. On the other hand, the energy and exergy efficiencies of the system decreased from 49.8% to 44.8%, respectively. The drop results from the high power input to the compressor and pumps to raise the operational pressure, where this work input is greater than the increase in the fuel cell electrical output. The main results of system 6 are shown in Table 6.4.
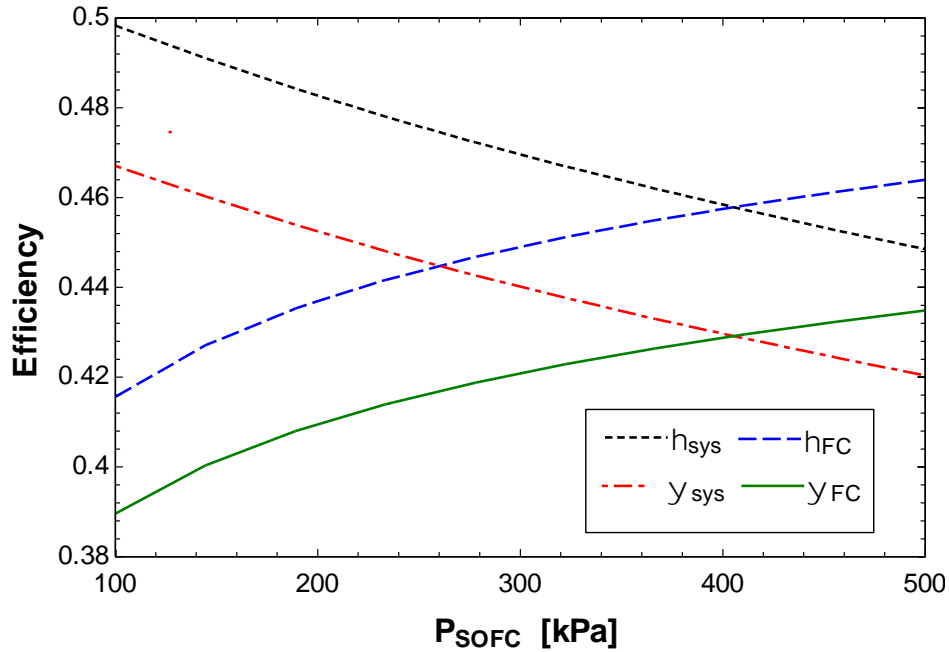
Figure 6.21: Effects operational pressure in the energy and exergy efficiencies of the fuel cell and System 6.
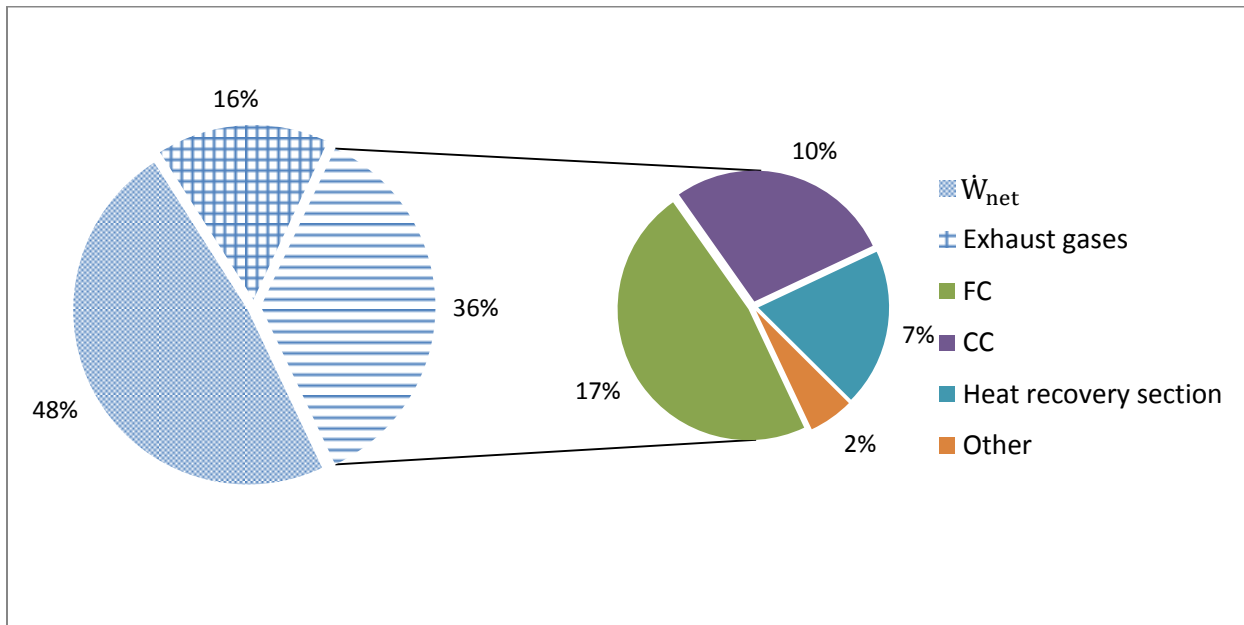

Figure 6.22: Exergy content for System 6.

The exergy flow and exergy destruction for system 6 are shown in Figure 6.22, where the right pie presents the exergy destruction part. The system has an exergy efficiency of 0.41 which indicate that 41% of the exergy input has been converted into useful work. However, there is no exergy lost due to the heat rejection because both the SOFC and CC were assumed adiabatic.

Additionally, 16% exergy input is rejected into the environment with the exhaust gases. The CC and SOFC are the two main components that account for majority of the exergy destruction nearly 16% and 18%, respectively. The heat recovery section accounts for 7% from the total exergy input that include the heat exchangers used to evaporate the LNG and heat the air before entering the SOFC.

Table 6.5: System 6 (LNG only) main inputs and outputs.

Parameter	Value
Natural gas mass flow rate (kg/s)	0.166
Cell voltage (V)	0.71
Work input for air compressor (kW)	296.8
Equivalent carbon monoxide emissions, $CO_{2,eq}$ (kg/s)	0.4453
System energy efficiency (%)	48.23
System exergy efficiency (%)	45.21

6.7 System 7 (LNG only) Results

System 7 uses LNG only as fuel to run the gas turbine, which is the prime mover, in addition to a bottoming ORC to recover some of the heat from the exhaust gases. The effect of varying the compression ratio in the system performance is shown in Figure 16.23. By varying the compression ratio from 10 to 20, both the energy and exergy efficiencies of system 7 increase from 30.3% to 36.7 and 28.4.4% to 34.4%, respectively. This increase is due to relatively higher enthalpy that enters the combustion and results an increase in the combustion temperature. This is reflected in the improvement of turbine inlet temperature, finally delivers more power. In addition, the increase in the pressure of the air drives more power from the turbine in the expansion process.

Figure 6.24 shows the effect of varying the ORC turbine inlet temperature in the energy and exergy efficiencies of the system. By varying the ORC turbine inlet temperature from 150℃ to 300℃, both the energy and exergy efficiencies increase from 33.4% to 34.3% and 31.3% to 32.2%, respectively. This increase occurs due to the increase of the enthalpy of the fluid that enters the ORC turbine, which leads to more power can be extracted from the fluid. The increase of this temperature means better utilization and heat recovery from the gas turbine exhaust gases.
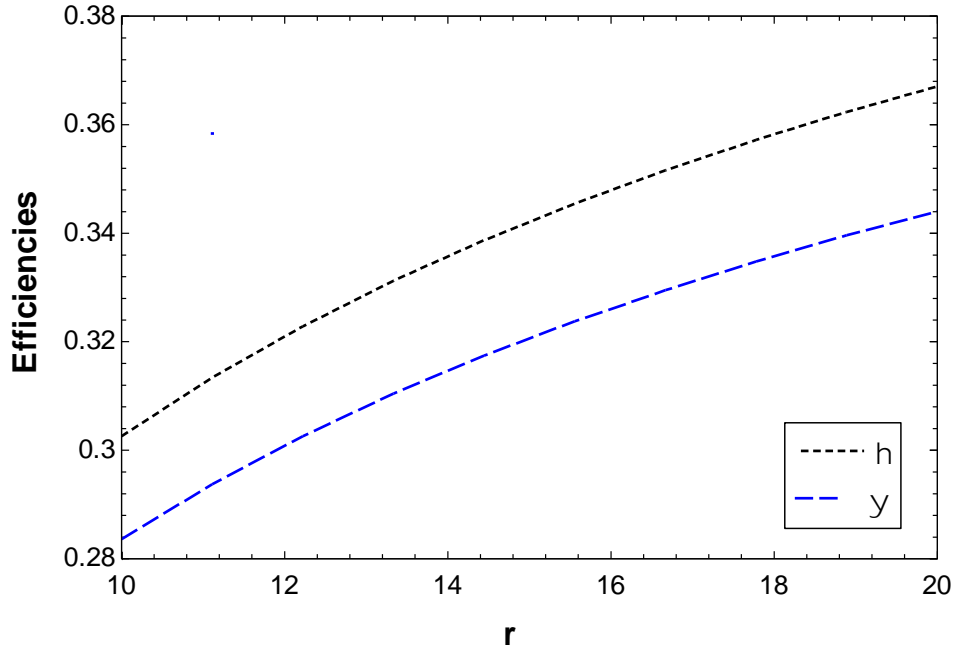
Figure 6.23: Effects of the compression ratio in the system energy and exergy efficiencies.
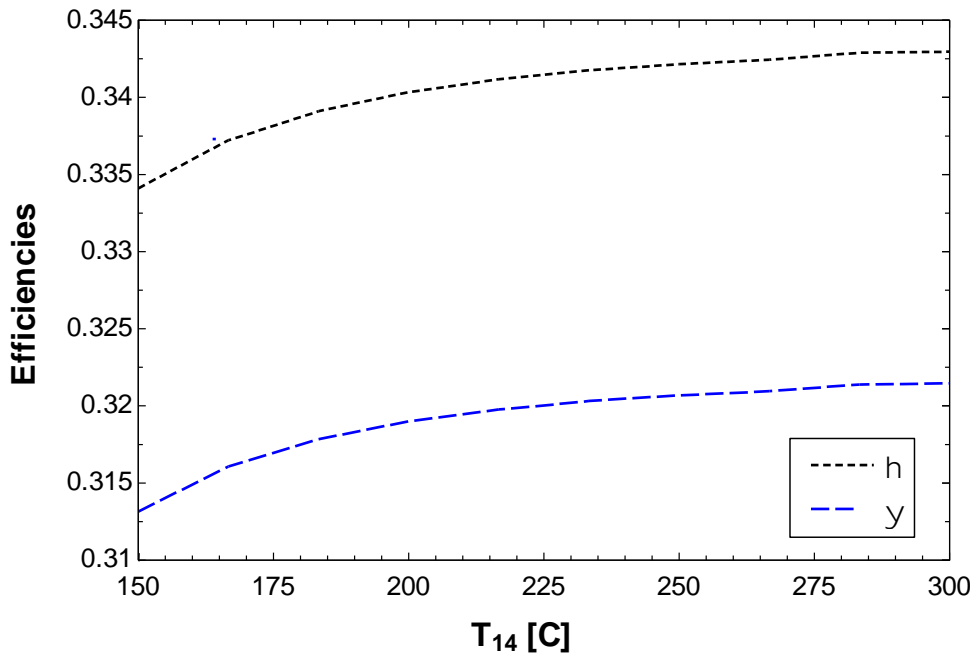

Figure 6.24: Effects of natural gas flow rate in the system energy and exergy efficiencies.
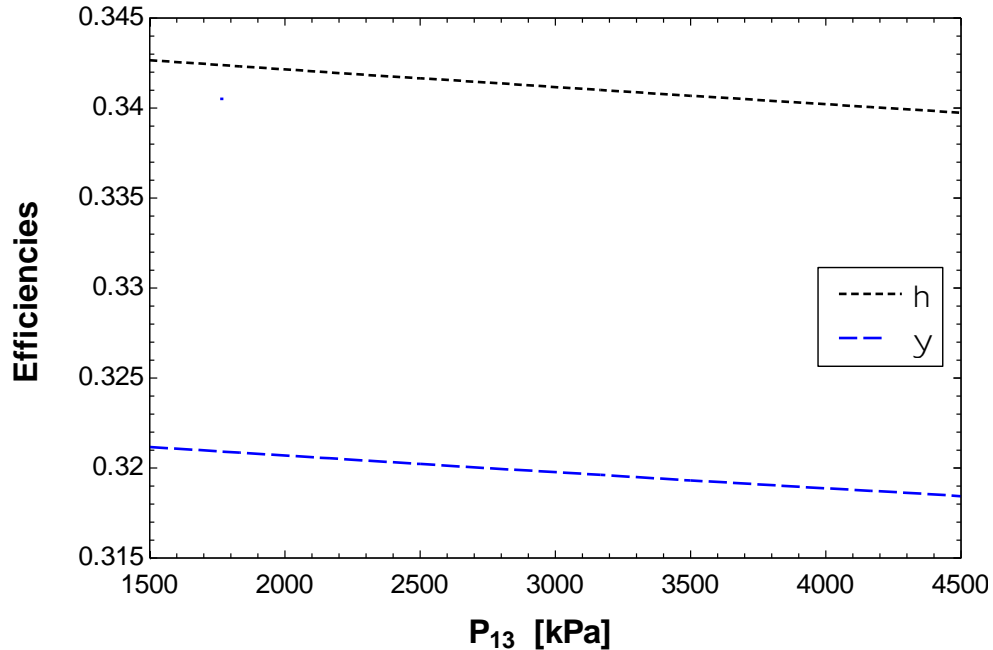
Figure 6.25: Effects of ORC turbine inlet pressure in the energy and exergy efficiencies.

Figure 6.25 shows the effect of varying the ORC turbine inlet pressure in the energy and exergy efficiencies of the system. By increasing ORC turbine inlet pressure from 1500kPa to 4500kPa, the energy and exergy efficiencies decreases from 34.3% to 34% and 32.1% to 31.8% This effect is relatively small because the ORC produces a small amount of power compare to the gas turbine which means the change in the ORC has an effect on the system performance but not a significant effect. The decrease in the efficiency can be caused by the increase in the energy input of the ORC pump that results in a total reduction of the system performance. The main inputs and output parameters of system 7 are included in Table 6.6.

The exergy content of system 7 including the exergy destruction is presented in Figure 6.26, where the right pie shows the exergy destruction part. 32% of the exergy input to the system has been converted into useful exergy work. The exergy of the exhaust gases carry 20% to the environment. However, the exergy destruction is counted for 48% of the total exergy input to the system, where the highest exergy destruction occurs in the combustion chamber with 37% from the total exergy input. The ORC evaporator has 8% exergy destruction from the total exergy input. In addition, the gas turbine, air compressor and other system components account for 1%, 1%, and 1%, respectively.
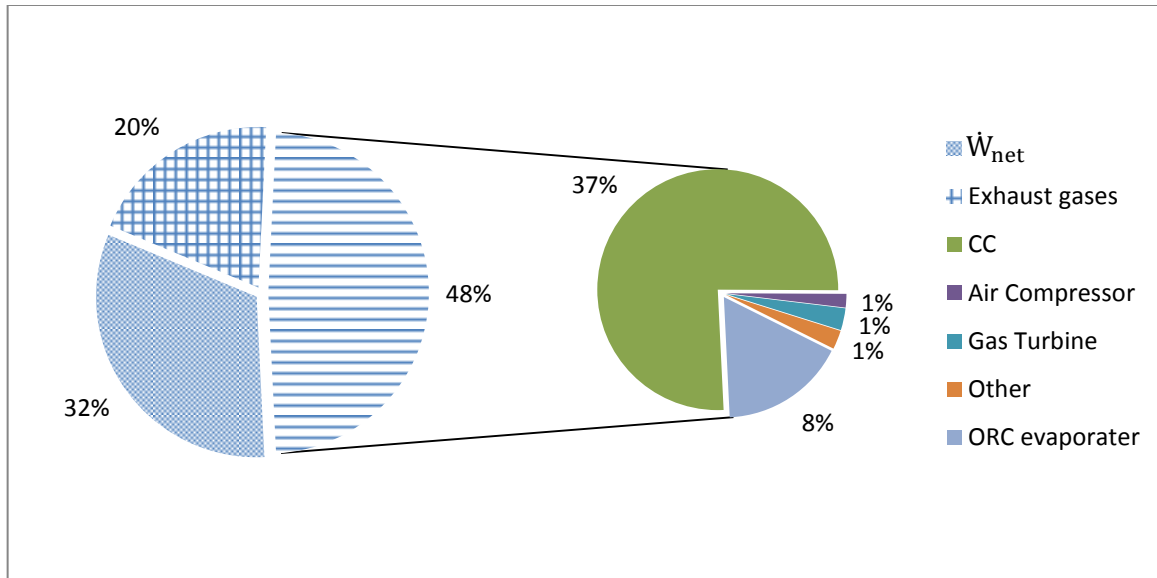
Figure 6.26: Exergy content for System 7.

Table 6.6: System 7 (LNG only) main inputs and outputs.

Parameter	Value
Natural gas mass flow rate (kg/s)	0.2135
Mass base AF ratio for system 7 prime mover	17.19
Work input to the air compressor (kW)	1505
Equivalent carbon monoxide emissions, $CO_{2,eq}$ (kg/s)	0.5773
Energy efficiency (%)	34.2
Exergy efficiency (%)	32.1

6.8 Systems Performance Results

The systems energy and exergy efficiencies are presented in Figure 16.27. The figure shows that system 6 has the highest energy and exergy efficiency which uses LNG only as fuel and SOFC as prime mover. The system has high efficiency due to the higher value of the SOFC efficiency because it is not limited by the Carnot engine. The energy and exergy efficiencies for systems 4&5 are low compared to the baseline diesel only locomotive. That is because the prime mover of these systems is a spark ignition engine that has a lower thermal efficiency than the compression ignition engine. For the compression ignition engine systems, system 3 has the best performance.
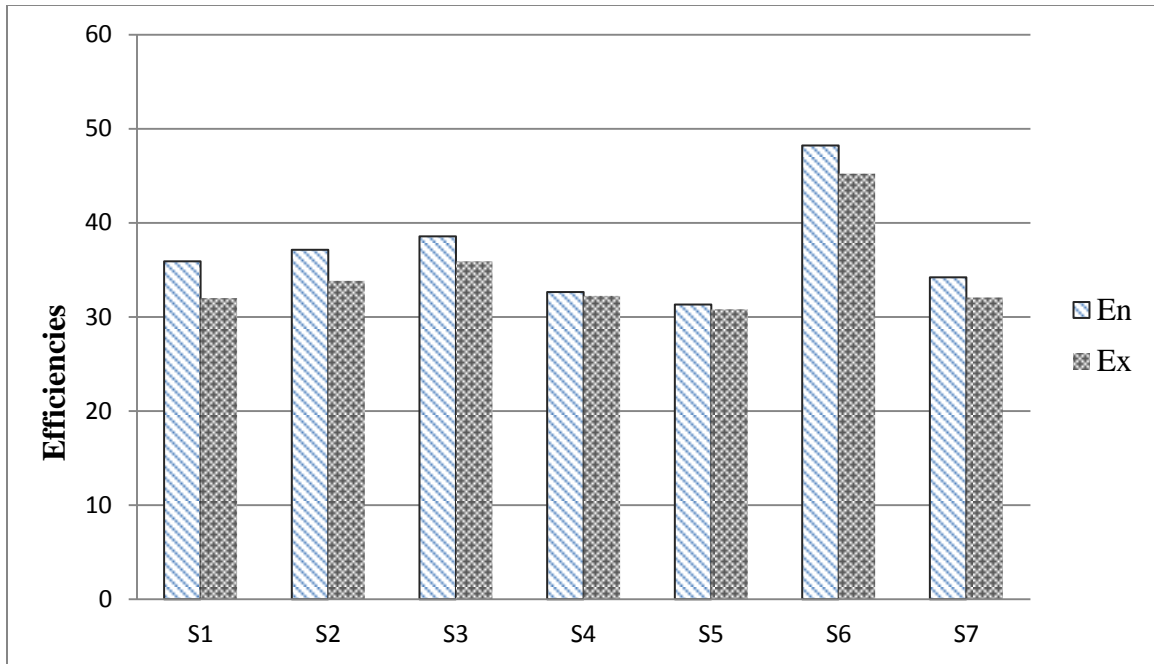
73

Figure 6.27: Energy and exergy efficiencies for all seven systems.

6.9 Environmental Impact Results

The environmental impacts of all systems are presented in this section. Figure 6.28 shows the mass flow rates of the equivalent carbon dioxide for all systems. The CO_2 emissions depend mainly in the carbon content in the fuels used, where the baseline system which uses diesel only has the highest $CO_{2,eq}$. However, system 5 has the lowest $CO_{2,eq}$ emissions because a considerable amount of the fuel that runs the locomotive is hydrogen, which has zero carbon content. Comparing systems 2 and 3 where both of them uses the diesel and LNG to operate the locomotive, system 3 has lower $CO_{2,eq}$ because the percentage of the LNG used as fuel in this system is about 90% and the natural gas process less $CO_{2,eq}$ compared to diesel. However for system 4, the emissions are higher than system 3 because of the existence of the propane which produces lower $CO_{2,eq}$ than diesel but more than natural gas. System 7 has a high $CO_{2,eq}$ emissions compare to the LNG only systems because of the low efficiency of the system which require more fuel to run the locomotive compared to SOFC.
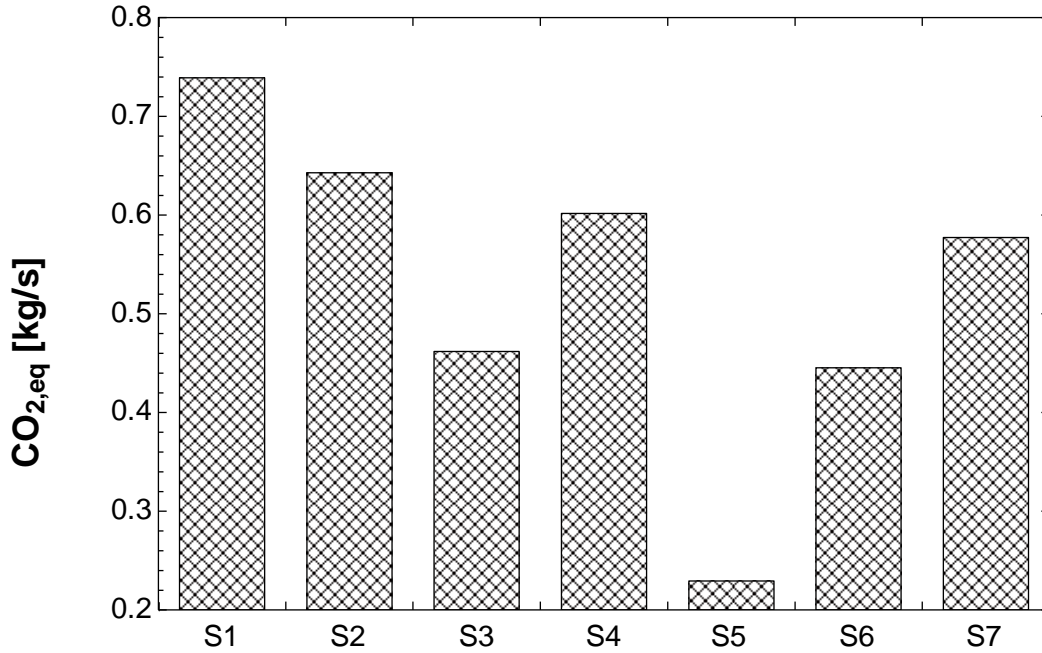
Figure 6.28: Mass flow rate of the $CO_{2,eq}$ for all systems .

Figure 6.29: NO_x emissions for all systems.

Figure 6.29 shows the NO_x emissions for all systems and Tire 3&4 standard emissions. The NO_x formation is affected mainly by the combustion temperature or adiabatic flame temperature of the combustion .The baseline system has the highest NO_x emissions due to the high adiabatic flame temperature of the diesel and that makes system one not meeting the emissions standards.

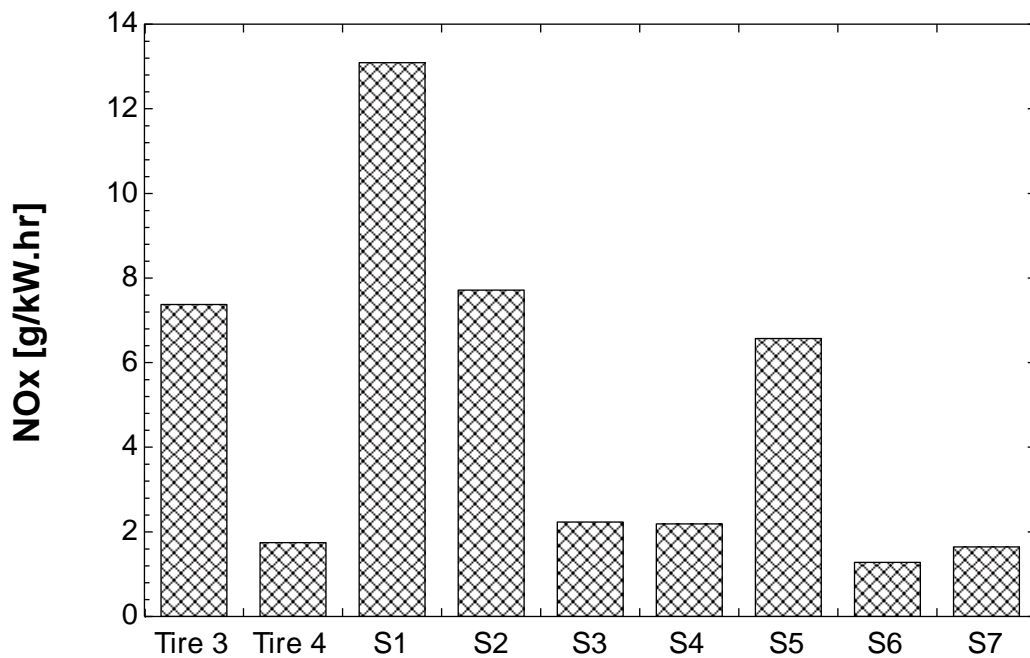System 2 has lower NO$_x$ emissions as compared to the baseline system because it uses LNG which has low adiabatic flame temperature as compared to diesel, which makes it slightly higher than Tire 3 emissions standard. However, the third system has low NO_x emissions and met Tire 3 standards. This low emission has two main reasons which are, the system uses EGR to lower the combustion temperature which affects and reduces the formation of NO_x.

In addition, system 3 uses LNG as the main fuel where only small amount of diesel is used for piloting, which means the combustion process has the form of natural gas combustion temperature, which is lower than diesel. System 4 meet Tire 3 emissions standard because the propane has lower adiabatic flame temperature than diesel which results in less emissions. On the other hand system 5 has high NO_x emissions because of the high combustion temperature that results from the hydrogen combustion which help the formation of NO_x. Systems 5&6 met Tire 4 emissions because both of then use LNG only as fuel.

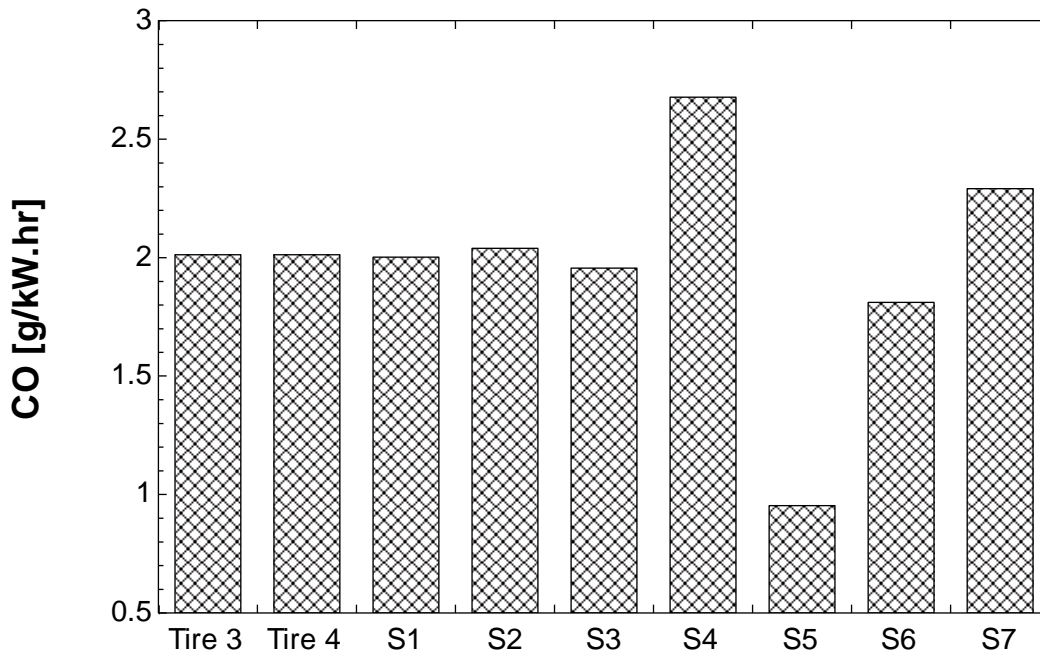Figure 6.30: CO emissions for all systems.

Figure 6.30 shows the carbon monoxide emissions and the standard emissions which are Tire 3 and Tire 4. Systems 1&2 have CO emissions that are closed to the standards due to the high combustion temperature of the diesel that reduces the formation of CO because CO increases in incomplete combustion. However, system 3 has similar CO emissions even though it runs on

mostly natural gas. That is because of the use of the EGR which lower the combustion temperature and that allow for more CO formation. System 4 has the highest CO emissions because of the use of propane with high mass flow rate. System 5 has low CO because they run on spark ignition engine that uses hydrogen which has no carbon atoms. Systems 6&7 they run on natural gas only which allow for more CO to be formed because of the low adiabatic flame temperature and low combustion pressure.
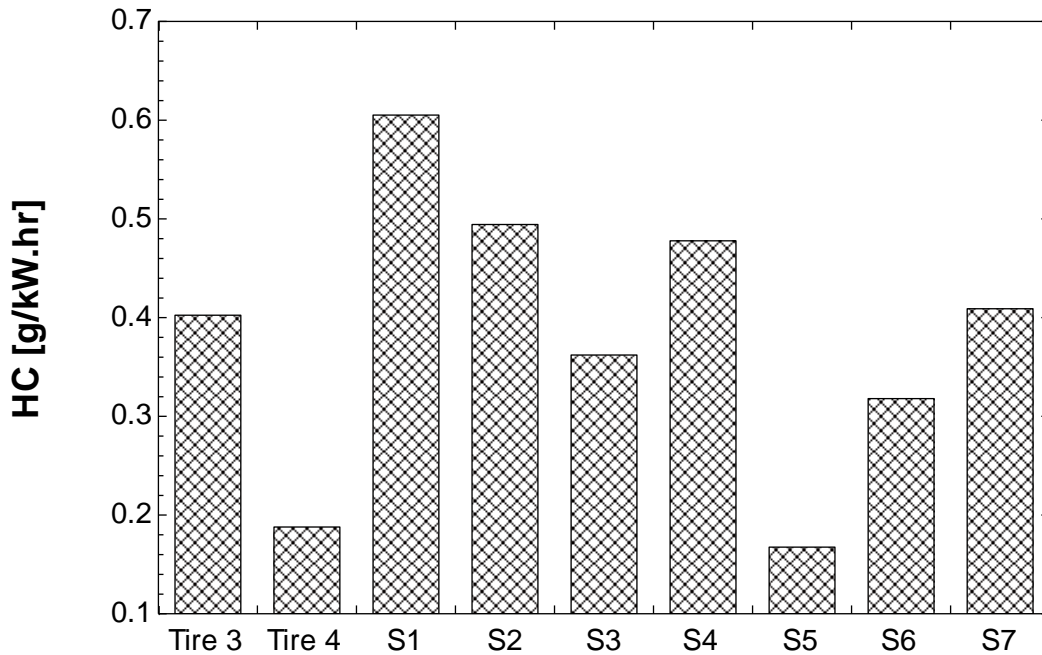

Figure 6.31: HC emissions for all systems.

The HC emission for all systems and the emissions standards are shown in Figure 6.31. In the figure, system 1 has the highest HC emissions because of the use of diesel. For system 2, the emissions are not meeting Tire 3 or 4 which is caused by the amount of diesel used to run the locomotive. However, System 3 has low HC emissions which met Tire 3 standard because the system uses EGR which recirculate part of the exhaust gases to be burned completely which reduces the amount of unburned hydrocarbons. In addition, system 3 uses mostly natural gas to operate the locomotive which has lower carbon content compared to diesel. System 4 has high HC emissions because the carbon atoms in propane are more than natural gas. The low HC emissions from system 5 are due to the use of hydrogen in addition to the LNG which does not contain carbon that allows it to meet Tire 4 standard. System 6 uses SOFC which convert most of the natural gas into hydrogen where fuels driven into the combustion are hydrogen and natural

gas in addition to the carbon dioxide from the reformer. That allows for less carbon to form HC because some of the carbon atoms have already form CO_2.System 7, has low HC because of the use of LNG.
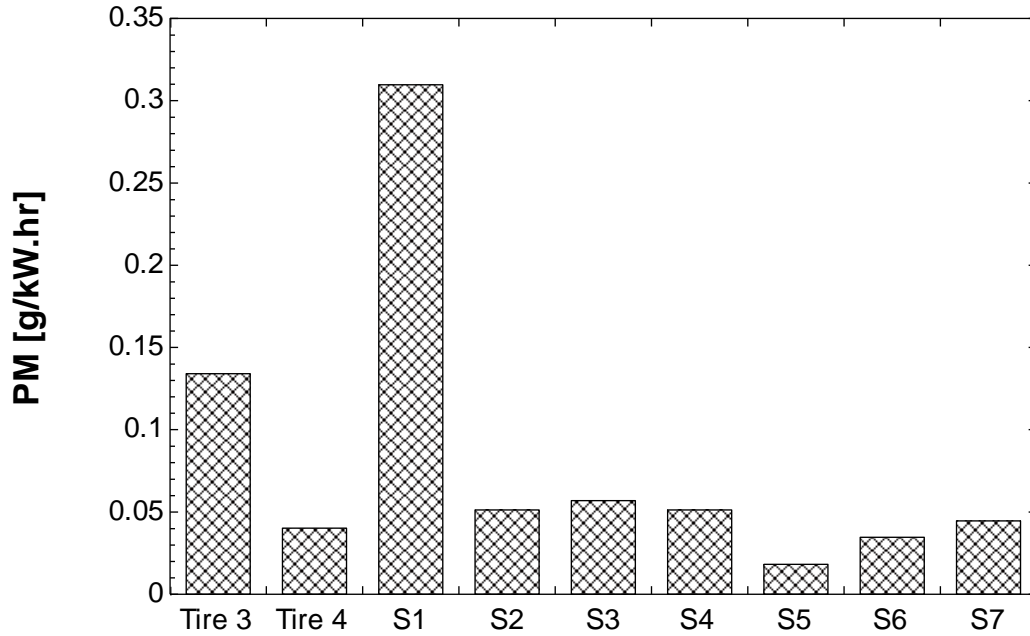

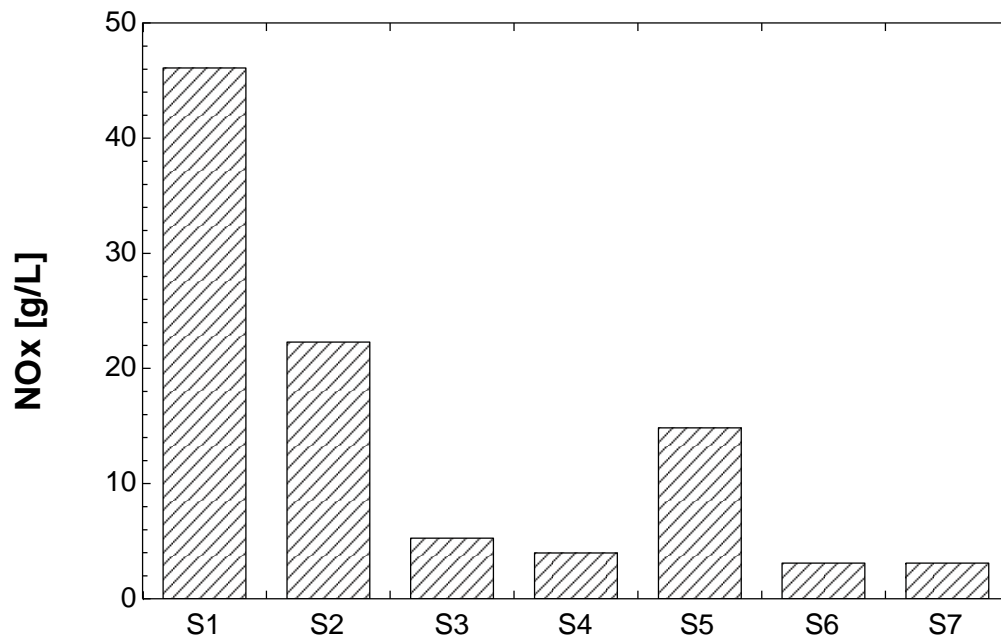Figure 6.32: PM emissions for all systems.

Figure 6.33 : NOx emissions in g/L for all systems.

Figure 6.32 shows the PM emissions for all systems and the standard emissions. Systems 1&2 have high PM emissions because these use diesel that is considered as the main reason of forming these emissions. However, system 3 met Tire 3 emissions where it uses mostly natural gas to operate the locomotive. Systems 4&7 met Tire 3 standards where the low emissions are obtained because of the use of the gases fuels. However, systems 5&6 met Tire 4 emissions because system 5 uses hydrogen and system 6 uses SOFC, which has high efficiency and low mass flow rate of the fuel that reduce the amount of emissions.

The amount of emissions in one liter of fuel is presented in Figures 6.33-6.37 for further illustration. Depending on the fuel type and combination of fuels the emissions of one liter of fuel is calculated. On these calculations, the density of the fuel and the percentage of one type of fuel in the total fuel consumed are important. Based on that, diesel has the highest fuel density that is proportional to the effect of diesel in the emissions. However, hydrogen has low emissions in addition to low density, and that makes it ideal fuel from the emissions perspective.
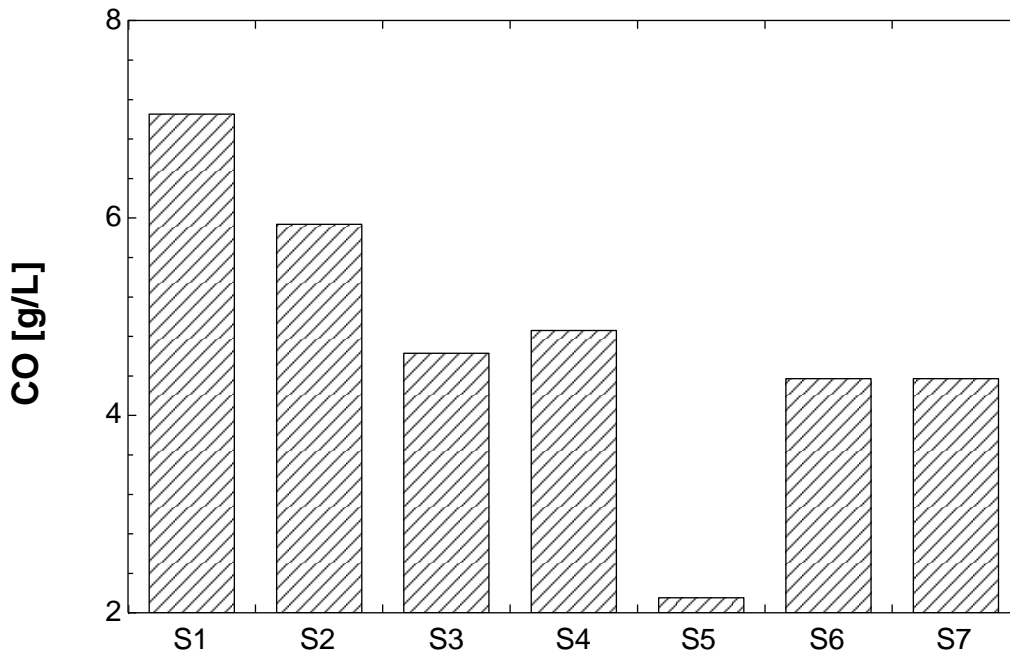
Figure 6.34: CO emissions in g/L for all systems.
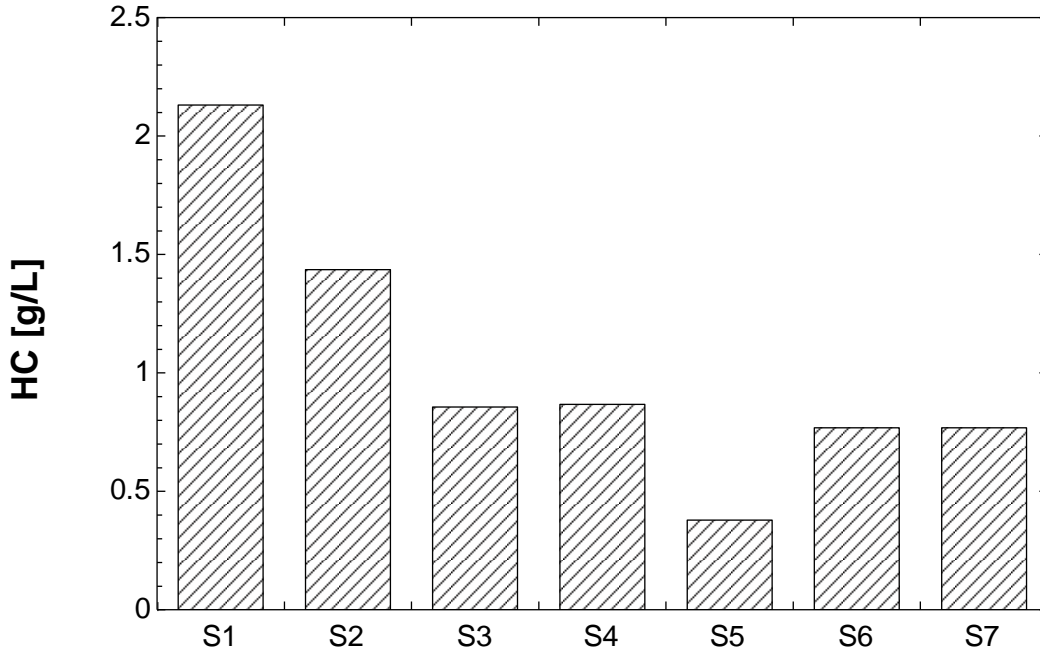
Figure 6.35: HC emissions in g/L for all systems.
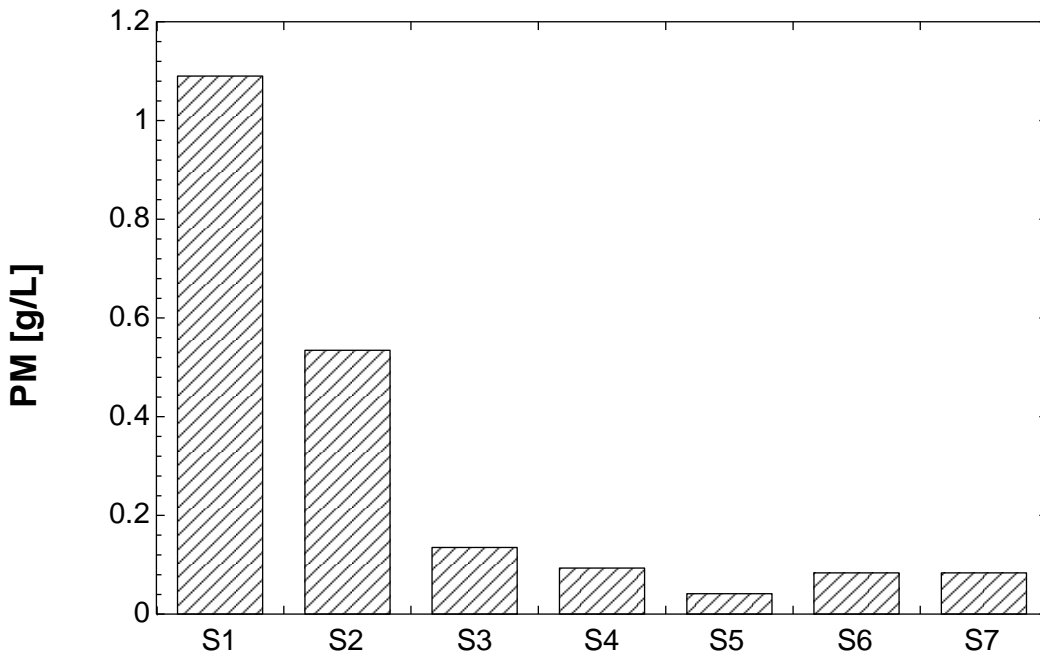
Figure 6.36: PM emissions in g/L for all systems.

Figure 6.38 shows the cost of fuel in Dollar per liter of fuel. Depending upon the percentage of the fuel used in the system the cost was calculated. The hydrogen comes out to be the most expensive fuel used in this study, but since it has been combined with natural gas, which has the lowest cost, system 5 still has a total fuel cost that is lower than the baseline that uses diesel only.

However systems 6 and 7, has the lowest fuel cost because natural gas is the only fuel that is used in these systems. System 2 has the combination of diesel and natural gas that made a moderate fuel cost. In addition, the fuel cost of system 4 is lower than the baseline but higher than the natural gas only systems because it contains propane that has a cost lower than diesel but higher than natural gas. System 3 has slightly higher cost than the natural gas operated systems due to the small amount of diesel that is used in the system.
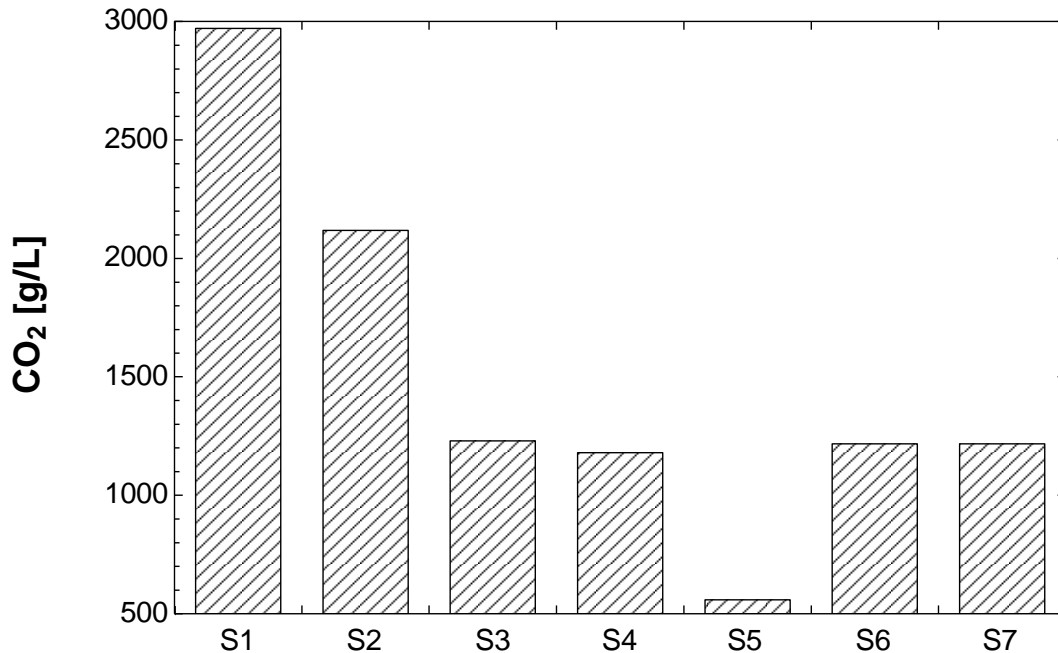
Figure 6.37: CO_2 emissions in g/L for all systems.

6.10 Case Study Results of Freight Locomotive

A Class 1 mainline freight locomotive duty cycle has been selected to evaluate and compare the proposed systems with the baseline system operation. Table 6.7 shows the spent time and power for each notch for the locomotive operation. The fuel cost in dollar per duty cycle for all systems is shown in Figure 6.39. In the figure, system 6 is the most economic system in terms of fuel cost because the system uses natural gas only to fuel the locomotive. However, system 5 has the most expensive fuel cost per duty cycle; it is due to the high cost of hydrogen which is used in this system with a considerable amount. System 2 has slightly lower fuel cost per duty cycle than the baseline system that uses diesel only. This reduction is because of the amount of natural gas used to run the locomotive where natural gas is cheaper than diesel. Further reduction is achieved by

system 3 which uses mostly natural gas and a small amount of diesel for piloting. However, system 4 shows high fuel cost per duty cycle because of the use of propane.
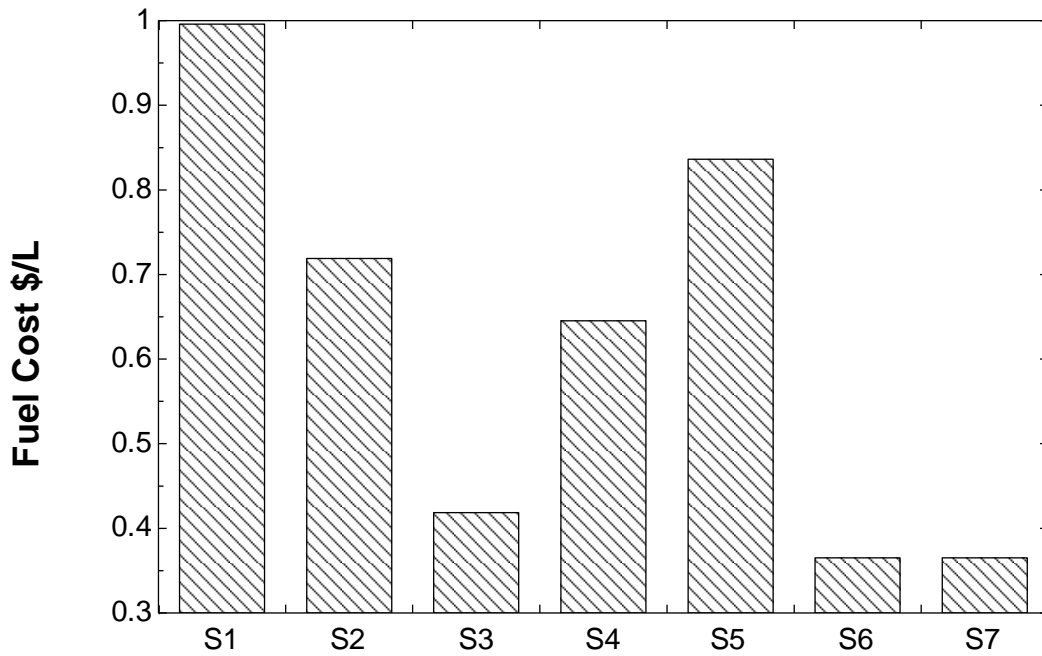
Figure 6.38: Fuel costs in the studied systems.
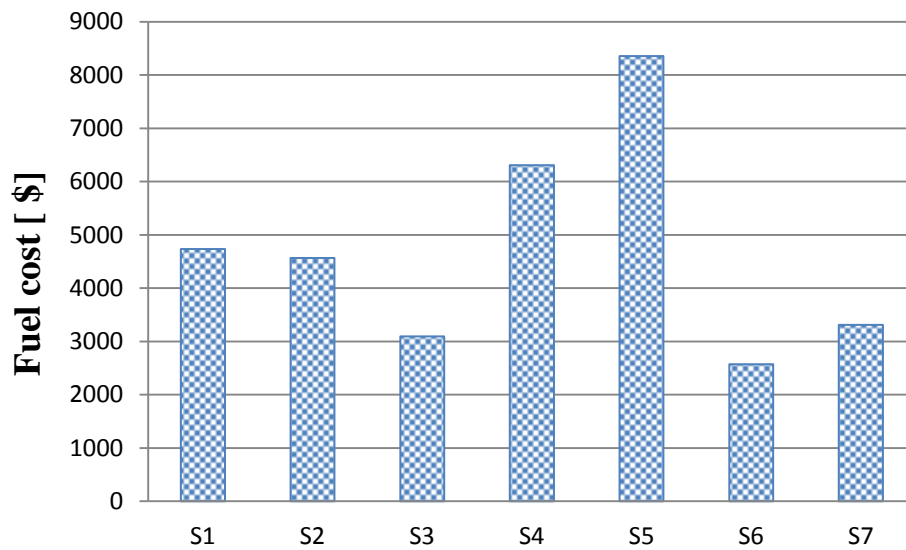
Figure 6.39: Fuel cost in $ per duty cycle.

Table 6.7: Freight locomotive duty cycle.

	Idle	N1	N2	N3	N4	N5	N6	N7	N8	DB
Operation in daily time (%)	51.3	4.7	5.7	4.7	3.8	3.2	3.0	1.6	14.0	8.0
Percent of rated power (%)	0.0	4.5	11.5	23.5	35	48	64	85	100	0

Source: [111]
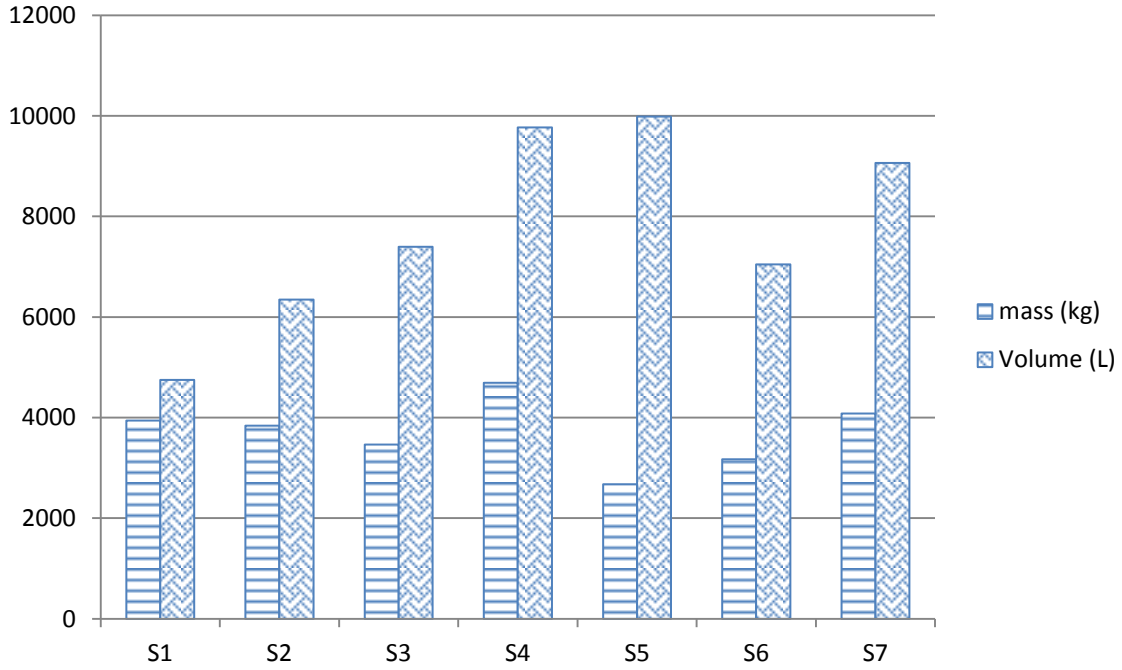
Figure 6.40: Mass and volume of fuel used in one duty cycle.

Figure 6.41: NOx emissions reduction compare to the baseline system in terms of one duty cycle.

Figure 6.40 shows the mass and volume of the fuel used per duty cycle for all systems. The mass of the fuels indicate that systems 2, 3, 5 and 6 have lower mass compare to the baseline system. However, the amount of fuel used in liter per duty cycle shows that systems 2, 3, 5 and 6 have significantly high volume of fuels. System 5 has the lowest mass of fuel per duty cycle but in terms of volume it is one of the highest that is due to the low density of the hydrogen used in this system.
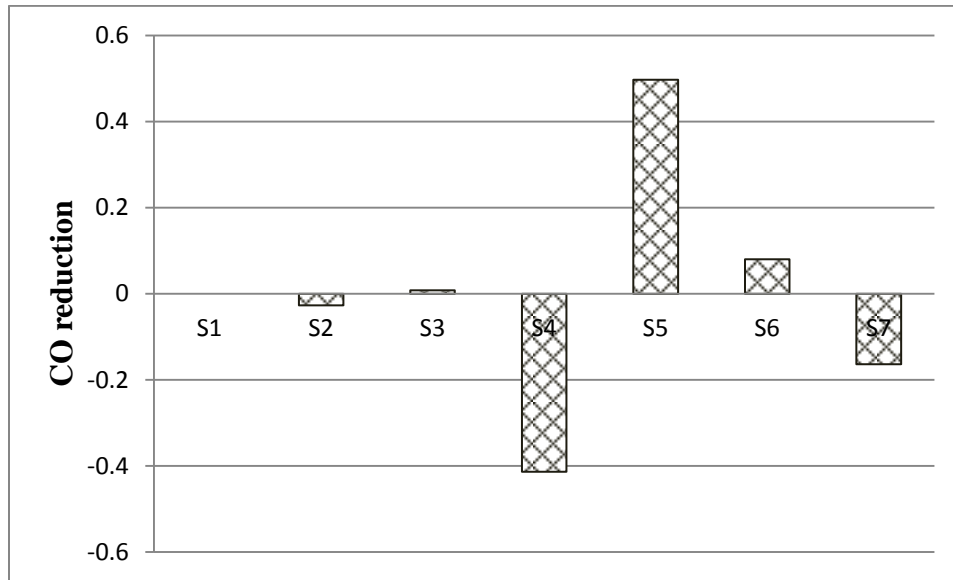
Figure 6.42: CO emissions reduction compare to the baseline system in terms of one duty cycle.

Figure 6.41 shows the amount of NOx reduction in one duty cycle compared with the baseline system that uses diesel only. System 2 has NOx reduction of 41% that uses both diesel and natural gas, with a considerable amount of diesel. System 3 has reduced the NOx emissions to reach 82% because of the use of natural gas as the primary fuel. However, the figure indicates that system 4 has high NOx reduction that achieves about 82% reduction due to the fuel combination of propane and methane. On the other hand, system 5 has about 47% reduction of NOx even with the use of hydrogen, but the mass flow rate of the fuel dominates the amount of NOx. Systems 6 and 7 each have a reduction of 90% and 87% respectively. That is due to the use of natural gas only as fuel, and the mass flow rate of the fuel is not high in system 6.
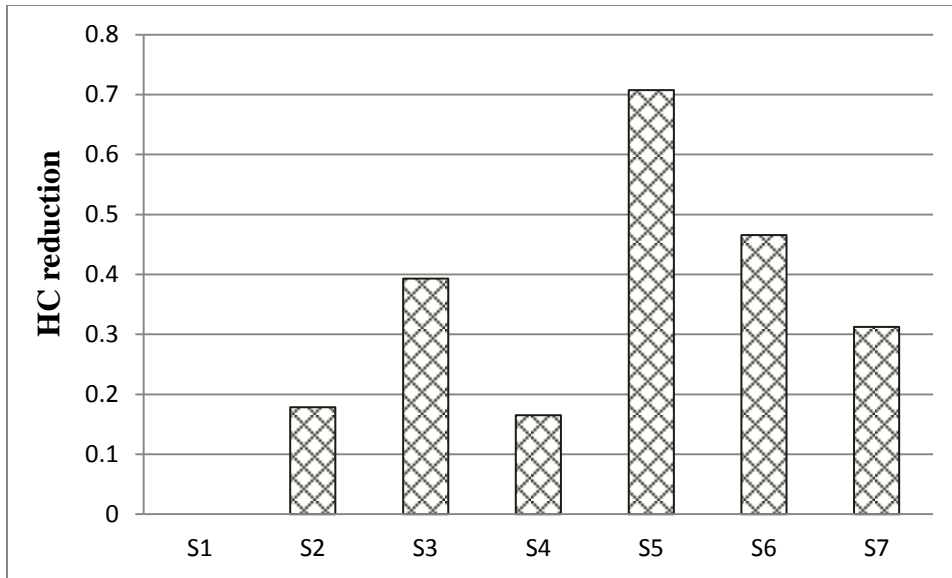
Figure 6.43: HC emissions reduction compare to the baseline system in terms of one duty cycle.
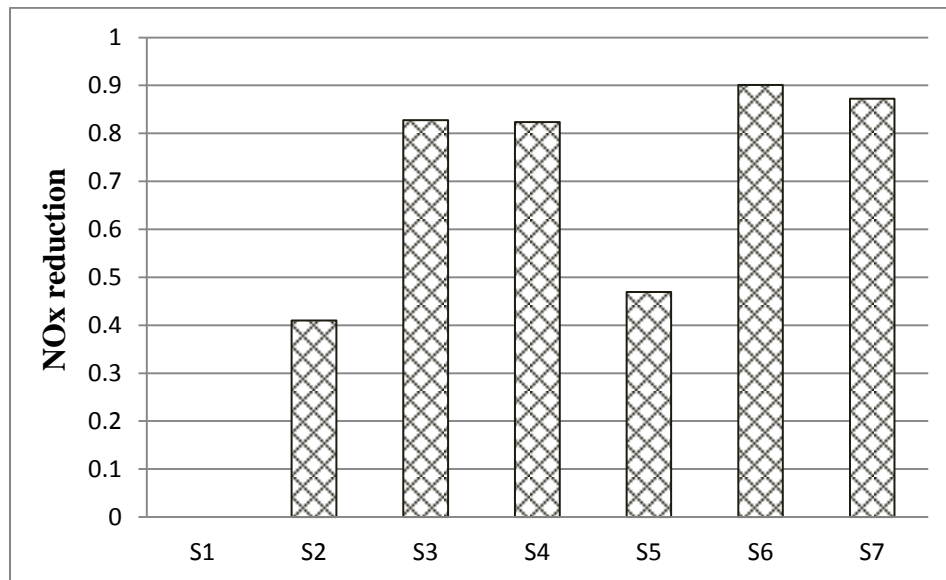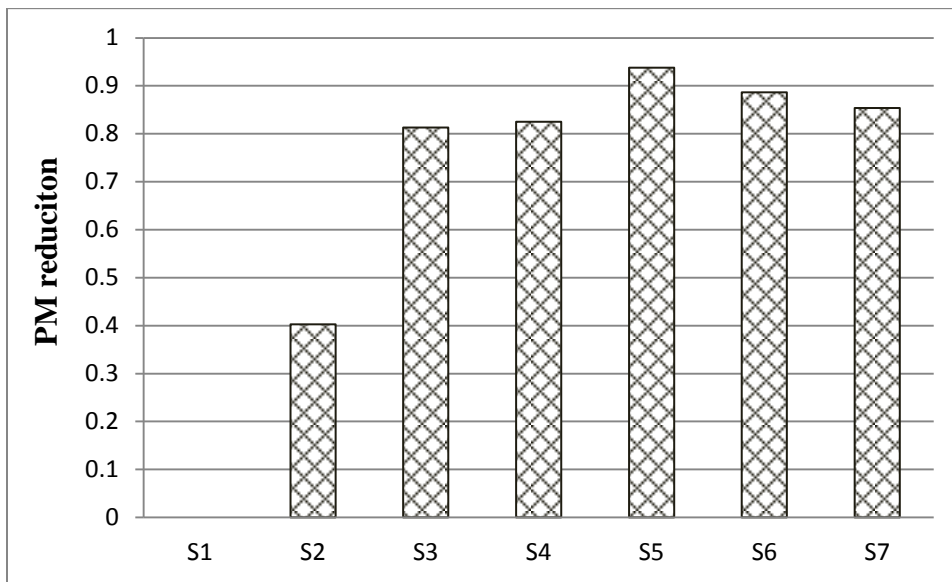

Figure 6.44: PM emissions reduction compare to the baseline system in terms of one duty cycle.

Figure 6.42 shows the reduction of CO of all systems compares to the baseline system per duty cycle. System 5 has the highest CO reduction that is about 49% due to the use of hydrogen which has carbon atoms. System 4 has 40% CO emission more than the baseline system due to the use of propane and its relation to the adiabatic flame temperature and CO formation that was discussed in the previous section. Systems 2 and 7 have CO emissions more than the baseline system which means there is no CO reduction in these systems in one duty cycle. .
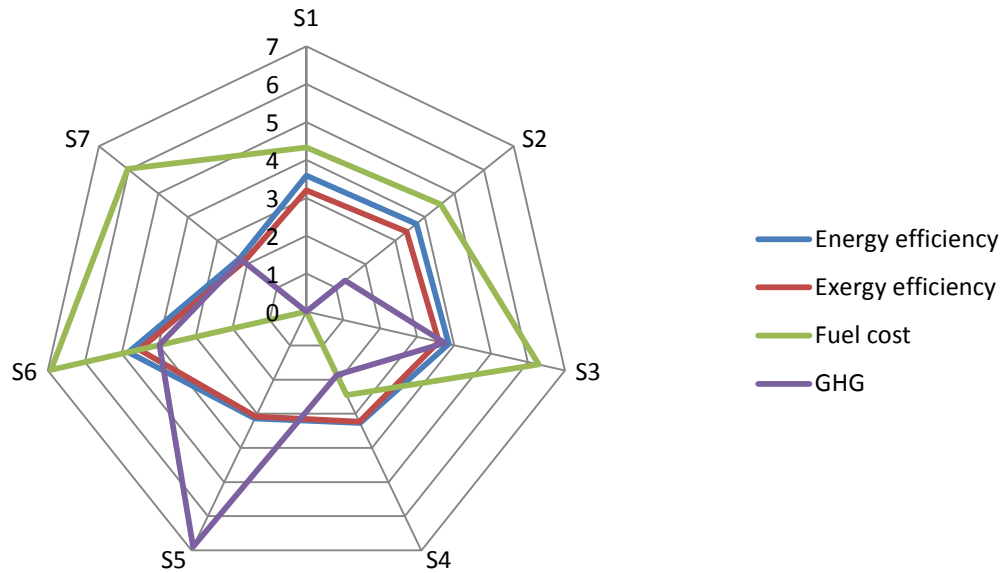
Figure 6.45: Comparison of the systems in terms of energy and exergy efficiencies, fuel cost and GHG emissions.

The reductions per duty cycle for HC of all systems compare to system 1 are shown in Figure 6.43. System 5 has the highest reduction with 70% fewer HC emissions compared to the baseline system. The sixth system has a reduction of 46% due to the use of the SOFC in the systems, which reduce the existence of unburned hydrocarbons. The third system has a considerable amount of HC reductions per duty cycle that reach 39% compare to the baseline system. Systems 2, 4, 7 have reasonable HC reduction of 17%, 16% and 31%, respectively.

Figure 6.44 shows the PM emissions reduction compare to the baseline system in terms of one duty cycle. System 2 has a PM emission reduction of 40% in one duty cycle because of the use of diesel. However, systems 3 to 7 have a PM emission reduction of more than 80%.

To compare all systems and identify the best system, a ranking methodology is applied. This ranking method is proposed by [112] where the selected factors for the comparison are normalized and plotted in a targeted plot. Figure 6.45 shows the systems ranking for different factors including energy efficiency, exergy efficiency, fuel cost, and GHG emissions. The higher the ranking number, the better is the system in that factor. In the figure, system 6 shows the best performance and fuel cost compare to all other systems, due to the high efficiency of the SOFC system and fuel volume need to run this system. In terms of GHG, system 5 shows the

advantages with the highest reduction of GHG compare to all systems. System 3, which uses mostly natural gas as fuel, has a moderate fuel cost and GHG benefits. Table 6.8 lists the pros and cons for all systems for clearer picture.

Table 6.8 Pros and cons for all systems

System	Advantages	Disadvantages
System 1	• Already established rail infrastructure • Not complicated system.	• High emissions. • High Fuel cost.
System 2	• It can run in diesel mode. • Fumigate engine as a solution for boil off gas problem. • Reduce the environmental impact.	• Increase the space. • More complicated system design. • Need for LNG supply stations.
System 3	• Low emissions. • High efficiency. • Fumigate engine for boil off gas problem.	• Can only run in LNG mode. • Need cryogenic system. • More complicated system design. • Need for LNG supply stations.
System 4	• Fumigate engine for boil off gas problem. • Can run in propane mode. • Low emissions.	• Need cryogenic system. • Low efficiency. • More complicated system design.
System 5	• Fumigate engine for boil off gas problem. • Low emissions.	• Need cryogenic system. • Low efficiency. • High fuel cost.
System 6	• High efficiency. • Low fuel cost. • Low emissions.	• Need cryogenic system. • Can only run in LNG mode. • Long time needed for the start up. • Need for LNG supply stations.
System 7	• Fast start up. • Low emissions. +Low fuel cost.	• Need cryogenic system. • More complicated system design. • Can only run in LNG mode.

6.11 Optimization

The newly developed systems are optimized to show the optimum values with the operational parameters. The objective function was defined in section 5.5, where it consists of the exergy efficiency of the system, the fuel consists in one duty cycle, and the emissions in one duty cycle. The values of these parameters are given in Table 6.9. The optimum operational parameters are tabulated in Table 6.10.

Table 6.9 Optimum exergy efficiency, fuel cost and emissions in one duty cycle.

System	Exergy efficiency	Fuel cost ($/duty cycle)	Emissions (g/duty cycle)				
			$CO_{2,eq}$	NOx	CO	HC	PM
1	0.3206	4,734	1.412×10^7	219,091	33,519	10,127	5,182
2	0.3678	3,922	1.227×10^7	134,939	35,922	8,687	3,233
3	0.3875	3,046	8.822×10^6	22,233	38,828	4,152	969
4	0.3362	5,878	1.149×10^7	22,361	33,519	8,456	906
5	0.3212	7,169	3.101×10^6	68,637	17,095	2962	321
6	0.4869	2,489	8.507×10^6	12,878	30,837	5417	590
7	0.328	3,252	1.103×10^7	16,803	28055	6967	761

Table 6.10 Optimum operational parameters.

Parameter	System1	System 2	System 3	System 4	System 5	System 6	System 7
$\eta_{isentropic}$	0.85	0.85	0.85	0.832	0.819	0.85	0.85
k	1.35	1.313	1.326	1.382	1.322	--	--
$T_{in,engin}$ (°C)	45	42.3	41.32	40	40.96	--	--
$P_{in,engin}$ (kPa)	217	187.2	207.6	218.6	189.3	101.3	--
T_{ref} (°C)	25	27.2	24.92	26.03	25.36	29.38	26.32
η_v	0.85	0.826	0.835	0.85	0.85	--	--
j (A/cm^2)	--	--	--	--	--	0.761	--
T_{SOFC} (°C)	--	--	--	--	--	839.6	--
r	--	--	--	--	--	--	18.01

Chapter 7 Conclusions and Recommendations

In this thesis, LNG locomotive has been investigated and compared to a diesel locomotive. The study included six systems in addition to the baseline system in which internal combustion engine, solid oxide fuel cell and gas turbine used as prime movers. Different combinations of fuels including ultra-low sulfur diesel, liquefied natural gas, liquefied petroleum gas, and hydrogen were used to study different fueling alternatives based on the locomotive infrastructure and fuel availability. The systems were compared in terms of their environmental impact and fuel economy.

7.1 Conclusions

The following conclusions can be derived from this thesis study:

- System 6 has the best energy and exergy efficiencies of all other systems.
- In terms of the GHG emissions, system 5 produces the least CO_2 emissions. However, the system has high fuel cost due to the use hydrogen.
- From the fuel cost point of view, system 6 has a significant fuel saving compared to the baseline system.
- In terms of emissions standards, which include Tire 3 and Tire 4, the proposed systems show signeficant reduction where some of the systems met Tire 4 standards for some emissions. Systems 5, 6, and 7 meet Tire 4 NOx emissions, where systems 3, 4, 5, and 6 meet the Tire 4 CO emissions. Additionally, system 5 meets the Tire 4 HC emissions and systems 5 and 6 meet the Tire 4 PM emissions.
- For the first 5 systems, the highest exergy destruction occurs in the internal combustion engines, which are the prime movers. In addition, for systems 6 and 7, the SOFC and the combustion chamber have the highest exergy destruction.
- System 2 fuel cost is slightly lower than the baseline, but it has a considerable advantage of the reduction in the environmental impact. This system is considered for the current locomotives and infrastructure that allows the locomotive to run on diesel only.

- System 4 uses the combination of LPG and LNG; it shows a small reduction in the GHG emissions but high reduction in the other emissions. However, the fuel cost of this system is higher than the baseline system.
- The LNG locomotives have shown a great reduction in the emissions and considerable saving in the fuel cost.

7.2 Recommendations

Further investigations are required to improve the efficiency of the systems, fuel cost, and environmental impact of the locomotives. Based on this thesis study, the following recommendations are made:

- Further research is required to compare the total cost and life cycle analysis of the locomotives for better comparison between the systems.
- Rail companies and locomotive manufacturers should consider LNG as potential fuel to build and run more cost effective and environmentally friendly locomotives.
- Further study should consider the use of more emissions control systems for further reduction in the emissions to meet Tire 4 standard for the systems that does not meet that requirement.
- Further research should be done to extend the current systems to be multigenerational systems that can supply more than one useful commodity, with the consideration of the cost and space limitations.

References

[1] Environment Canada, "Canada's Emissions Trends" Government of Canada, Ottawa, 2014.

[2] Railway Association of Canada, "Locomotive Emissions Monitoring Program 2012" www.railcan.ca, Ottawa, 2012.

[3] Federal Railroad Administration, "Broad Agency Announcement BAA-2013-1" U.S. Department of Transportation, 2013.

[4] S. Mokhatab, J Y Mak, J. V. Valappil, and D. A. Wood, "Handbook of liquefied natural gas" Gulf Professional Publishing, 2013.

[5] ILEX Consulting Limited, " Importing Gas into the UK- Gas Quality Issues" 2003.

[6] Y. A. Cengel, and M. A. Boles, " Thermodynamics: an engineering approach" New York: McGraw-Hill, 2006.

[7] J. L. Woodward, and R. Pitbaldo, "LNG risk based safety: modeling and consequence analysis" John Wiley & Sons, 2010.

[8] J. A. Alderman, "Introduction to LNG safety" Process Safety Progress 24, no. 3: 144-151, 2005.

[9] P. Cleaver, M. Johnson, and B. Ho, "A summary of some experimental data on LNG safety" Journal of Hazardous Materials 140, no. 3: 429-438, 2007.

[10] Westport Cummins, "Product Information Bulletin, Natural Gas Fuel System LNG" 2012.

[11] T. Flynn, "Cryogenic Engineering, Second Edition Revised and Expanded" CRC Press, 2004.

[12] A. J. Kidnay, W. R. Parrish, and D. G. McCartney, "Fundamentals of natural gas processing", Vol. 218, CRC Press, 2011.

[13] N. Yoshimura, "Vacuum technology: practice for scientific instruments" Springer Science & Business Media, 2007.

[14] J. C. Pacio, and C. A. Dorao,"A review on heat exchanger thermal hydraulic models for cryogenic applications" Cryogenics 51, no. 7: 366-379, 2011.

[15] K. Thulukkanam, "Heat Exchanger Design Handbook, Second Edition" CRC Press, 2013.

[16] Westport Power Inc., "Westport: Background on Dual Fuel Technology" www.westport.com, 2014. [Online]. Available: http://www.westport.com/is/core-technologies/combustion/dual-fuel. [Accessed 2014].

[17] Westport Power Inc., "Westport: First Generation Westport HPDI Technology" www.westport.com, 2014. [Online]. Available: http://www.westport.com/is/core-technologies/combustion/hpdi. [Accessed 2014].

[18] S. Garneu , "Canadian National Railways Tests Natural gas/diesel fuel powered locomotives between Edmonton and Fort McMurray", AB. CN Newsletter 33:1,2013.

[19] W. Vantuono, "Is LNG the next generation? ", Railway Age, ProQuest Business Collection pp. 28, 2014.

[20] BNSF, "BNSF to test liquefied natural gas in road locomotives" Available: http://www.bnsf.com/employees/communications/bnsf-news/2013/march/2013-03-06-a.html [Accessed 2014].

[21] M Lenz, "Natural gas goes on trial" International Railway Journal, pp 69, 2014.

[22] CSX, "CSX and GE Transportation Partner to Pilot Liquefied Natural Gas Locomotives" Available:http://www.csx.com/index.cfm/media/press-releases/csx-and-ge-transportation-partner-to-pilot-liquefied-natural-gas-locomotives/[Accessed 2014].

[23] Diesel Fuel News, "GE Inks Deal with Gasfin for LNG Truck Fuelling in Europe" Hart Energy, pp 9, 2013.

[24] K Smith, "Westport delivers LNG loco tenders to EMD" International Railway Journal, pp 8, 2014.

[25] Diesel Fuel News, "Indian Railways Eyes LNG Locomotive Test" Hart Energy, pp 15, 2014.

[26] Global Refining and Fuels Today, "Indian Railways Eyes LNG Locomotive Test" Hart Energy, pp 5, 2014.

[27] Diesel Fuel News, "Gazprom, Russian Railways to Test Natural Gas Turbine-Power Locomotives" Hart Energy, pp 17, 2013.

[28] K Barrow, "LNG locomotive technology on test in Russia" International Railway Journal, pp 74, 2014.

[29] Global Refining and Fuels Today, "Indiana Harbor Belt Railroad to Convert 31 Locomotives to CNG" Hart Energy, pp 6, 2014.

[30] NGV Global News, "Indiana Harbor Belt to Convert 31 Locomotives to CNG" Available:

http://www.ngvglobal.com/indiana-harbor-belt-to-convert-31-locomotives-to-cng-0102[Accessed 2014].

[31] Diesel Fuel News, "Norfolk Southern Testing CNG Switcher Locomotive" Hart Energy, pp 7, 2014.

[32] Marbek, "Study of Opportunities for Natural Gas in the Transportation Sector" Natural Resources Canada, 2010.

[33] M. E. Dunn, and V. N. LeBlanc, "Two engine system with a gaseous fuel stored in liquefied form" U.S. Patent 8,763,565, issued July 1, 2014.

[34] A. Foege, "Cryogenic pump system for converting fuel" U.S. Patent Application 13/715,456, filed December 14, 2012.

[35] J. Kipping, "Combined cycle powered railway locomotive" U.S. Patent 8,667,899, issued March 11, 2014.

[36] A. G. Foege, and E. J. Cryer, "Fuel distribution system for multi-locomotive consist" U.S. Patent Application 13/563,220, filed July 31, 2012.

[37] E. I. Nesterov, "Gas turbine arrangement for a locomotive" European Patent Application 12807474.7, filed February 2, 2012.

[38] J. H. Burkhart, "Method of converting diesel engine to natural gas engine" U.S. Patent 8,011,094, issued September 6, 2011.

[39] V. A. Peredelskii, Y. V. Lastovskii, R. V. Darbinyan, A. I. Savitskii, and A. A. Savitskii, "Analysis of the desirability of replacing petroleum-based vehicle fuel with liquefied natural gas" Chemical and Petroleum Engineering 41, no. 11-12: 590-595, 2005.

[40] Al. Arteconi, C. Brandoni, D. Evangelista, and F. Polonara, "Life-cycle greenhouse gas analysis of LNG as a heavy vehicle fuel in Europe" Applied Energy 87, no. 6: 2005-2013,2010.

[41] S. Kumar, H. T. Kwon, K. Ho. Choi, W. Lim, J. H. Cho, K. Tak, and I. Moon, "LNG: An eco-friendly cryogenic fuel for sustainable development" Applied Energy 88, no. 12: 4264-4273, 2011.

[42] T. Morosuk, and G. Tsatsaronis, "Comparative evaluation of LNG–based cogeneration systems using advanced exergetic analysis" Energy 36, no. 6: 3771-3778, 2011.

[43] A. Arteconi, and F. Polonara,"LNG as vehicle fuel and the problem of supply: The Italian case study" Energy Policy 62:503-512, 2013.

[44] S. Imran, D. R. Emberson, A. Diez, D. S. Wen, R. J. Crookes, and T. Korakianitis, "Natural gas fuelled compression ignition engine performance and emissions maps with diesel and RME pilot fuels" Applied Energy 124: 354-365, 2014

[45] K. Cheenkachorn, C. Poompipatpong, and C. G. Ho, "Performance and emissions of a heavy-duty diesel engine fuelled with diesel and LNG (liquid natural gas)" Energy 53: 52-57, 2013.

[46] M. R. Gómez, R. F. Garcia, J. R. Gómez, and J. C. Carril, "Review of thermal cycles exploiting the exergy of liquefied natural gas in the regasification process" Renewable and Sustainable Energy Reviews 38: 781-795, 2014.

[47] H. Sun, H. Zhu, F. Liu, and H. Ding, "Simulation and optimization of a novel Rankine power cycle for recovering cold energy from liquefied natural gas using a mixed working fluid" Energy ,2014.

[48] K. H. Kim, and K. C. Kim, "Thermodynamic performance analysis of a combined power cycle using low grade heat source and LNG cold energy" Applied Thermal Engineering 70, no. 1: 50-60, 2014.

[49] J. Szargut, and I. Szczygiel, "Utilization of the cryogenic exergy of liquid natural gas (LNG) for the production of electricity" Energy 34, no. 7: 827-837, 2009.

[50] H. Dong , L. Zhao, S. Zhang, A. Wang, and J. Cai, "Using cryogenic exergy of liquefied natural gas for electricity production with the Stirling cycle," Energy 63: 10-18, 2013.

[51] C. Poompipatpong, and K. Cheenkachorn, "A modified diesel engine for natural gas operation: Performance and emission tests" Energy 36, no. 12: 6862-6866, 2011.

[52] M. R. Gómez, R. F. Garcia, J. R. Gómez, and J. C. Carril, "Thermodynamic analysis of a Brayton cycle and Rankine cycle arranged in series exploiting the cold exergy of LNG (liquefied natural gas)" Energy 66: 927-937, 2014.

[53] H. M. Cho, and B. Q. He, "Spark ignition natural gas engines—A review" Energy Conversion and Management 48, no. 2: 608-618, 2007.

[54] Diesel Fuel News, " AMTRAK Launches B20 Biodiesel Test in Locomotive" Hart Energy, pp 7, 2010.

[55] News Release, "AMTRAK biodiesel heartland flyer results presented at railroad environmental conference" AMTRAK, 2011.

[56] AMTRAK, "2011 Environmental Health and Safety Report" 2011.

[57] L. David, "Biodiesel tested on 3 roads" Trains, 2010.

[58] Railway Gazette International, "Biofuel in the cold" 2010.

[59] R. Nelson, "Current Status of Biodiesel in Railroads and Technical Issues Moving Forward" National Biodiesel Board, 2012.

[60] S. Kanes, D Forster and L.Wilkinson, "Biofuels Outlook" Scotiabank, 2010.

[61] Norfolk Southern Corporation, "Alternative Fuels for the Future" Available: http://nssustainability.com/2014_sustainability_report/environmental_performance/alternative_fuels_for_the_future.html[Accessed 2014].

[62] Norfolk Southern Corporation, "Norfolk Southern Corporation 2010 sustainability report," 2010.

[63] Diesel Fuel News, "Norfolk Southern, EMD to Launch Locomotive Biodiesel-Blend Tests" Hart Energy, pp 5, 2010.

[64] L. David, "Rail Runner to feed on biodiesel" Trains, 2007.

[65] U.S Rail News, " Iowa" Capitol Press LLC, Sep 23, 2009.

[66] Railway Gazette International, "Biofuel self-sufficient" 2009.

[67] J. Schneyer, "Brazil's CVRD inks large Petrobras biodiesel contract" Platts Oilgram News, 2007.

[68] N. Lykova, and J. E. Gustafsson, "A survey of biofuel production potentials in Russia" Scientific Journal of Riga Technical University, Environmental and Climate Technologies 4, no. 1: 64-75, 2010.

[69] V. Mogila, , I. Vasyliev, and E. Nozhenko, "The use of biofuel on the railway transport" Transport Problems 7: 21-26, 2012.

[70] V. Prasad, "New Jersey firm supplying Indian oil companies with biodiesel" Renewable Fuel News, 2004.

[71] M. Whitaker, and G. Heath, "Life cycle assessment of the use of jatropha biodiesel in Indian locomotives" No. NREL-TP-6A2-44428. Golden, CO: National Renewable Energy Laboratory, 2009.

[72] I. Skinner, N. Hill, S. Kollamthodi, J. Mayhew, and B. Donnelly, "Railways and Biofuel First UIC Report" International Union of Railways, 2007.

[73] S. Lahane, and K. A. Subramanian, "Effect of different percentages of biodiesel–diesel blends on injection, spray, combustion, performance, and emission characteristics of a diesel engine" Fuel 139 : 537-545, 2015.

[74] B. Tesfa, F. Gu, R. Mishra, and A. Ball, "Emission Characteristics of a CI Engine Running with a Range of Biodiesel Feedstocks" Energies 7, no. 1: 334-350, 2014.

[75] N. Yilmaz, F. M. Vigil, K. Benalil, S. M. Davis, and A. Calva, "Effect of biodiesel–butanol fuel blends on emissions and performance characteristics of a diesel engine" Fuel 135: 46-50, 2014.

[76] D. Osborne, S. Fritz, and D. Glenn, "The Effects of Biodiesel Fuel Blends on Exhaust Emissions From a General Electric Tier 2 Line-Haul Locomotive" Journal of Engineering for Gas Turbines and Power 133, no. 10: 102803, 2011.

[77] BNSF, "Fuel Cell Locomotive" Available: https://www.bnsf.com/communities/environmental/fuel.html [Accessed 2014].

[78] BNSF, "BNSF Developing Fuel Cell Locomotive" Assembly, 2008.

[79] BNSF, "BNSF, Vehicle Projects demonstrate fuel cell switch locomotive" Fuel Cells Bulletin, 2009.

[80] International Railway Journal, "China develops hydrogen-fuel locomotive" 2011.

[81] Fuel Cells Bulletin, "US–SA partnership to produce five fuel cell mine locomotives" 2012.

[82] A. R. Miller, G. V. D. Berg, D. L. Barnes, R. I. Eisele, D. M. Tanner, J. M. Vallely, D. A. Lassiter, "Fuel cell technology in underground mining" The Southern African Institute of Mining and Metallurgy, 2012.

[83] T Fujii, N Teraya, and M Osawa, "Development of an NE train" JR EAST Technical Review-No.4, pp 62-70.

[84] H. Abiko, "Development of Hybrid Railcars and Catenary and Battery-powered Hybrid Railcar System" JR EAST Technical Review-No.23, pp 9-12.

[85] METROLIX, "Appendix 4 Rolling Stock Technology Assessment " 2010.

[86] R. M. Arnold, J. Peters, E. S. Brian, and A. V. Omourtag, "Analysis of fuel cell hybrid locomotives" Journal of Power Sources 157, no. 2: 855-861, 2006.

[87] D. Meegahawatte, S. Hillmansen, C. Roberts, M. Falco, A. McGordon, and P. Jennings, "Analysis of a fuel cell hybrid commuter railway vehicle" Journal of Power Sources 195, no. 23: 7829-7837, 2010.

[88] F. Peng, W. Chen, Z. Liu, Q. Li, and C. Dai, "System integration of China's first proton exchange membrane fuel cell locomotive" International Journal of Hydrogen Energy 39, no. 25: 13886-13893, 2014.

[89] J. S. David, and P. Majumdar, "Feasibility analysis for solid oxide fuel cells as a power source for railroad road locomotives" International Journal of Hydrogen Energy 35, no. 20: 11308-11314, 2010.

[90] S. M. Andrew, J. Brouwer, and G. S. Samuelsen, "Feasibility study for SOFC-GT hybrid locomotive power: Part I. Development of a dynamic 3.5 MW SOFC-GT FORTRAN model" Journal of Power Sources 213: 203-217, 2012.

[91] S. M. Andrew, J. Brouwer, and G. S. Samuelsen, "Feasibility study for SOFC-GT hybrid locomotive power part II. System packaging and operating route simulation" Journal of Power Sources 213: 358-374, 2012.

[92] A. Hoffrichter, P. Fisher, J. Tutcher, S. Hillmansen, and C. Roberts, "Performance evaluation of the hydrogen-powered prototype locomotive 'Hydrogen Pioneer" Journal of Power Sources 250: 120-127, 2014.

[93] G. D. Marin, G. F. Naterer, and K. Gabriel, "Rail transportation by hydrogen vs. electrification–case study for Ontario Canada, I: propulsion and storage" International Journal of Hydrogen Energy 35, no. 12: 6084-6096, 2010.

[94] G. D. Marin, G. F. Naterer, and K. Gabriel, "Rail transportation by hydrogen vs. electrification–Case study for Ontario, Canada, II: Energy supply and distribution" International Journal of Hydrogen Energy 35, no. 12: 6097-6107, 2010.

[95] Electro Motive, "EMD 16-710G3C-ES"Available: http://www.progressrail.com/cda/files/ 4564108/7/GT46AC_ENG_A4_Web.pdf [Accessed 2014].

[96] Caterpillar, "CG260-12" Available: http://www.cat.com/en_US/power-systems/electric-power-generation/gas-generator-sets/18487627.html [Accessed 2014].

[97] Cummins Westport, " ISX12 G" Available: http://www.cumminswestport.com/models/ isx12-g[Accessed 2014].

[98] I. Dincer, and M. A. Rosen, "Exergy: energy, environment and sustainable development" Newnes, 2012.

[99] C. R. Ferguson, and A. T. Kirkpatrick, "Internal Combustion Engines: Applied Thermosciences" John Wiley & Sons, 2001.

[100] K. L. Cashdollar , I. A. Zlochower, G. M. Green, R. A. Thomas, and M. Hertzberg, "Flammability of methane, propane, and hydrogen gases" Journal of Loss Prevention in the Process Industries 13, no. 3: 327-340, 2000.

[101] J. F. Griffiths, D. Coppersthwaite, C. H. Phillips, C. K. Westbrook, and W. J. Pitz, "Auto-ignition temperatures of binary mixtures of alkanes in a closed vessel: Comparisons between experimental measurements and numerical predictions" In Symposium (International) on Combustion, vol. 23, no. 1, pp. 1745-1752. Elsevier, 1991.

[102] F. Gharagheizi, P. I. Kashkouli, A. H. Mohammadi, and D. Ramjugernath, "A group contribution method for determination of the standard molar chemical exergy of organic compounds" Energy 70: 288-297, 2014.

[103] F. A. Al-Sulaiman, , I. Dincer, and F. Hamdullahpur, "Energy analysis of a trigeneration plant based on solid oxide fuel cell and organic Rankine cycle" International Journal of Hydrogen Energy 35, no. 10: 5104-5113, 2010.

[104] U. G. Bossel, "Final report on SOFC data facts and figures" Swiss Federal Office of Energy, Berne ,1992.

[105] British Colombia Ministry of Environment, "British Colombia Greenhouse Gas Inventory Report 2012" 2012.

[106] United States Environmental Protection Agency, "Emission Factors for Greenhouse Gas Inventories" 2014.

[107] U.S. Department of Energy, "Clean Cities Alternative Fuel Price Report" 2014.

[108] E. Talbi, "Metaheuristics: from design to implementation" Vol. 74, John Wiley & Sons, 2009.

[109] P. Ahmadi, and I. Dincer, "Thermodynamic and exergoenvironmental analyses, and multi-objective optimization of a gas turbine power plant." Applied Thermal Engineering 31, no. 14, 2529-2540, 2011.

[110] P. Ahmadi, and I. Dincer, "Exergoenvironmental analysis and optimization of a cogeneration plant system using Multimodal Genetic Algorithm (MGA)." Energy 35, no. 12, 5161-5172, 2010.

[111] Railway Association of Canada, "Locomotive Emissions Monitoring Program 2009" www.railcan.ca, Ottawa, 2009.

[112] C. Acar and I. Dincer, "Comparative Environmental Impact Evaluation of Hydrogen Production Methods from Renewable and Nonrenewable Sources" in Causes, Impacts and Solutions to Global Warming., New York, Springer, pp. 493-514, 2013.